Technische Universiteit
Eindhoven
University of Technology

Electrical Energy Systems
Department of Electrical Engineering

Den Dolech 2, 5612 AZ Eindhoven
P.O. Box 513, 5600 MB Eindhoven
The Netherlands
www.tue.nl

Author:
Ernauli Christine Aprilia

Coaches:
Prof. dr. ir. J. F. G. Cobben
Dr. P. F. Ribeiro
V. Ćuk, Msc

Reference:
EES.12.A.0012

Date:
August 2012

Modelling of Photovoltaic (PV) Inverter for Power Quality Studies

By: Ernauli Christine Aprilia

Where innovation starts

Modelling of Photovoltaic (PV) Inverter
for Power Quality Studies

a thesis submitted in fulfilment of the requirements

for the award of the degree

Masters of Sustainable Energy Technology

from

TECHNISCHE UNIVERSITEIT
EINDHOVEN
UNIVERSITY OF TECHNOLOGY

by

Ernauli Christine Aprilia
Bachelor of Engineering

DEPARTMENT OF ELECTRICAL ENGINEERING

2012

Abstract

With the growing awareness in sustainable environment, more electricity customers are becoming energy conscious. This leads to the increase of installation of grid-connected photovoltaic (PV) panels for small scale electricity generation. The nature of intermittent power generated by PV cells and the interconnection between PV panels and the network through DC-AC converter affect the quality of the electrical supply and these issues are as important as the environmental issues. Various studies observing the impact of (increasing) penetration of PV systems at distribution level and the methods to mitigate this impact have been conducted by many parties, including academia, network operators, even PV inverter manufacturers.

Very few of these studies are conducted on site by taking measurements of power quality aspects of electrical supply such as voltage level, harmonics, or dips. Computer modeling and simulations are used extensively to design PV plants and to study their interconnection and operation with the transmission and distribution systems. To get an accurate prediction, one has to employ a good representation of the inverters in these simulations.

An extensive literature review is conducted to investigate various models of PV inverters used in existing power quality studies. The two power quality aspects that this study focuses on are voltage dips and harmonics. To study PV systems contribution in short-circuit studies, PV inverters that have Fault Ride-Through (FRT) feature are mostly represented as a controlled current source which injects power to the network. The inverters employed in this study, however, do not have this feature because they disconnect immediately when they sense dips in the network voltage. This feature is found in newest inverters that follow recent requirements from several countries that distributed generators must be involved in improving voltage stability of utility lines upon disturbance. Harmonic current sources are also used to represent the harmonic current emissions of PV inverters for harmonic study. Since this study is usually concerned with resonance frequency(s) in the network, the output capacitors of the inverters are included in the model, in parallel to the harmonic current sources (Norton model).

A series of measurements are carried out to determine the values of the harmonic currents and the topology as well as the parameters of the output impedances of the inverters. These measurements are performed at the Point of Connection (PoC) and measure the harmonic voltages and currents at clean and distorted voltage supply. There are five inverters measured; four of them are single-phase inverters and the other one is a three-phase inverter that feeds the grid via one phase. The measurements are conducted at harmonic frequencies up to the 50th harmonic to obtain impedance-frequency characteristic of each inverter. Interharmonic measurements are also performed to observe if the inverter's harmonic current suppress the harmonic voltages injected from the source. The next step is to choose the elements constituting an inverter's output filter such as resistor, inductor, and/or capacitor. The topology and value of these elements are chosen in a way that the impedance profile of the model matches the impedance profile from the measurements.

The model created for each inverter is then validated in a simulation using Simulink® and DIgSILENT PowerFactory. Out of these models, a general model to represent inverters in power class 0-2kW and 2-5kW is presented to be used as reference for other inverters not measured in this study. An aggregation

of multiple inverters is modelled by paralleling the output impedances and summing in phasor the harmonic currents of the inverters. This is also verified with a network simulation and the result of both simulations in Simulink and Power Factory shows a good agreement with the measurements.

Table of Contents

1.   Introduction

1.1.   Thesis statement

Power quality issues in electrical power system are gaining more attention lately, especially those stemming from nonlinearity of power electronics used in certain grid connected equipments. Switching mechanisms implemented in converter-connected distributed generation units such as photovoltaic (PV) inverters are responsible for additional harmonics in the network and the output filters used to reduce these harmonics are also responsible for resonance frequencies in the network. Simulation models for PV inverters are essential for understanding the technical issues, developing solutions, and enabling future scenarios with high PV penetration. The model used to represent these inverters depends on the purpose of the study. This thesis presents alternative PV inverter models to be used in harmonic studies and investigates possible models to be used in voltage dip studies. The investigation on inverter behaviour during voltage dip, however, suggests that the models are to be developed for harmonic studies only. Following the experiment with voltage dip scenario, the models are verified in simulations and experiments in the laboratory that also observe the behaviour of an aggregation of inverters in harmonic study.

1.2.   Thesis objective

The objective of this thesis is to summarize and develop models of PV inverters which are appropriate for different types of Power Quality (PQ) studies, in particular harmonic and voltage dip studies. This main objective is broken down into small supporting objectives which are addressed individually and the outcomes are combined to address the main objective of this thesis. Because this thesis is a subsequent of traineeship project of related topic, some of the supporting objectives listed down here are already addressed in the traineeship report.

Supporting objectives:

-   Make an overview of PV inverter models used in existing power quality studies
-   Setup an experiment for measuring the output impedance and harmonic current of PV inverters
-   Determine output impedance model and harmonic current source model of the inverters
-   Examine inverter performance at voltage dip scenario
-   Implement the models in simulation harmonic studies of multiple inverters
-   Verify the simulation studies with laboratory experiments

1.3.   Methodology

This study begins with a literature review of existing PV inverter models which are then narrowed down to a Norton model for harmonic studies. Experiments in power quality laboratory are carried out to define the model topology and to measure the parameters of the circuit with the aid of numerical computing software MATLAB[1]. It is followed by an analysis to finalize the model for each inverter as well as aggregated inverters, using data analysis software OriginPro 8[2] and Microsoft Excel. The models are

---

[1] is a product of The MathWorks, Inc. www.mathworks.com
[2] is a product of OriginLab www.originlab.com

then implemented in a simple network simulation for harmonic studies by means of power system analysis software DIgSILENT PowerFactory[3] and simulation software Simulink®[4]. Finally, the network simulation is verified with an experiment in power quality laboratory. Additional studies contributing to the main objective are a study about the requirements for PV inverters during voltage dip and a measurement of the actual behaviour of PV inverters during voltage dip.

1.4.   Thesis layout

This section outlines a brief summary of the remaining chapters contributing to this thesis.

Chapter 2: This chapter explains the topology of grid-connected PV inverters including the output filter that is responsible for the harmonics emitted by the inverter to the grid and resonance frequencies in the grid. This chapter also explores existing power quality studies that use PV inverter models which serve as a reference for the model used later in this thesis. An aggregate model of multiple inverters is also investigated from several literatures.

Chapter 3: In this chapter, the set-up for the measurements of harmonic voltages and currents at the output terminal of the inverters is described. The basis of the measurement including the FFT analysis of the results is explained. The chapter also shows the measurement method and flow chart including the sourced harmonic voltages.

Chapter 4: The results of harmonic impedance measurements and the models derived from them are presented here along with the discussions on the discrepancies between the models and the measurement results, the influence of inverter's partial load to the measurement, and the cross-harmonic phenomenon.

Chapter 5: This chapter presents harmonic current measurement results and the consequent harmonic current source models at clean and distorted voltage supply as well as at partial load.

Chapter 6: The PV inverters behaviour during voltage dip is investigated in this chapter by discussing the sensitivity curves of the inverters in comparison to the curve of several recent standards related to voltage dip. Following this chapter's conclusion, the subsequent studies are focused on harmonic studies only.

Chapter 7: Out of individual models developed in Chapter 4 and 5, a general model that represents multiple inverters in the same power class is presented in this chapter. A model of an aggregation of multiple inverters is also shown along with the discussion on the consistency of individual models when they are combined. Verification using network simulation and experiments is also discussed.

Chapter 8: This chapter concludes the results and analysis presented in previous chapters and gives recommendation for future research in this area.

---

[3] is a product of DIgSILENT GmbH http://www.digsilent.de
[4] is a product of The MathWorks, Inc. www.mathworks.com

2. Literature review

Awareness of the influence of energy harnessing on environment instigate utilization of energy from renewable sources. Conversion of energy from sunlight to direct current (DC) through photovoltaic (PV) cells has become popular in recent year and the number of installed PV systems is increasing and will continue to grow. These systems can be either stand-alone or grid-connected. In both cases, the DC power generated by PV cells is converted to alternating current (AC) power using AC-DC inverter.

Conversion using power electronic components such as IGBT and diode results in non-sinusoidal voltage and current waveform at its output which injects harmonics into the network. The performance of PV systems in terms of power quality depends on the inverter structure and external conditions such as solar irradiance and temperature, type and amount of load, and the characteristics of the supply system.

There are international standards limiting the harmonic current and voltage emission by distributed generations to the grid, for example IEEE1547 and EN61000-3-2. However, some papers presented that the limit imposed by the standards may be exceeded by a large number of small inverters, even though the individual inverters meet the requirements of the standards. [1] [2] Unfortunately, these standards also do not limit the (additional) production of harmonic current due to harmonic distortion of the grid voltage. This might allow more harmonics in the network than expected.

2.1. Inverter topologies

Not only to invert DC current into a sinusoidal AC current, an inverter must also boost the array's voltage with a further element, if the PV array's voltage is lower than the grid voltage, in order to feed energy to utility grid. The electrical behaviour of PV systems connected to a network is determined by its inverter's topology. PV inverters are currently based on single-phase self-commutated voltage-source converters in the 1-5kW power range for individual households. These inverters utilize high-frequency or line-frequency transformers; some are even transformerless. [2]Figure 2-1 shows the topology of transformerless single-phase self-commutated inverters; DC source consists of PV panels and a DC-DC converter. [3]
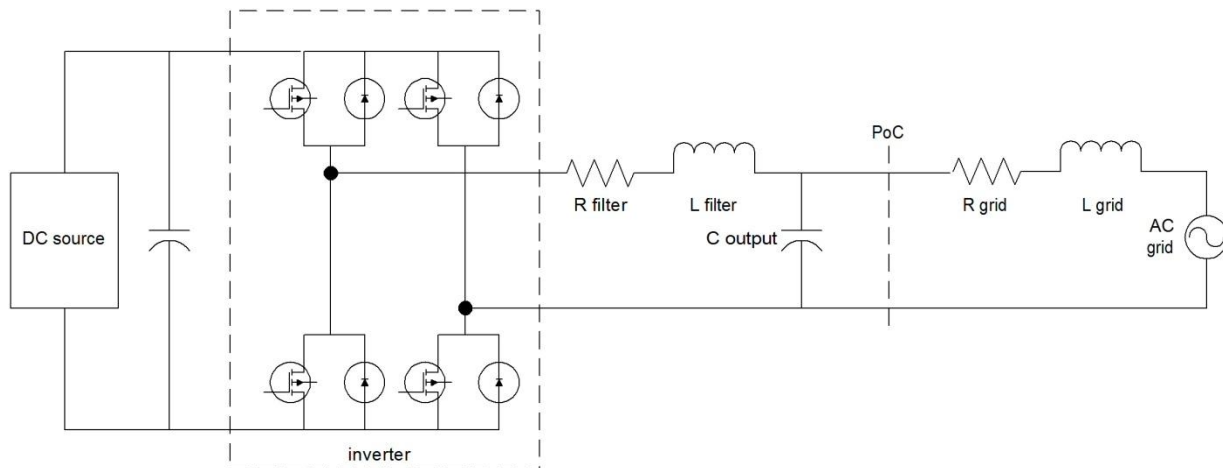
Figure 2-1 Topology of a single phase grid-connected inverter

An inverter generally emits harmonic current to the network in two ways: switching harmonic and its side bands, and the control algorithms fail to produce a perfectly sinusoidal current.

To comply with IEC 61000-3-2, inverters use Pulse Width Modulation (PWM) controllers to generate sinusoidal output current. PWM switching frequencies vary between 20-500 kHz. Due to this high-frequency switching, low-pass filter and damping networks are usually used to smooth the output waveform. Most filters consist of inductor(s), capacitor(s), and/or resistor(s). To reduce the cost, the combination of minimum reactance and maximum capacitance is preferable. The output capacitor, however, is mainly responsible for setting up a resonance circuit together with the network reactance (transformer and cable reactance). [2]

There are two types of resonance, series and parallel. Series resonance happens when the total system impedance is at the lowest; hence, small harmonic voltage distortion will result in high harmonic current which can harm components. When parallel resonance happens, the system impedance is at its highest and a small harmonic current will lead to high harmonic voltage distortion.
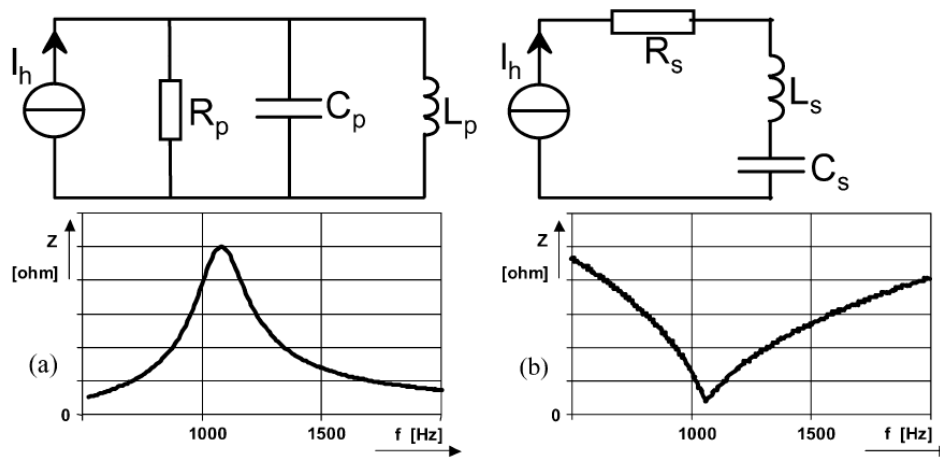
Figure 2-2 Mechanism of series and parallel resonance [2]

To ensure smooth sinusoidal output current, most inverters use inner current feedback loop that compares the output current waveform with a sinusoidal reference. This reference can be generated internally by the inverter itself (self-commutated) using a look-up table or using the network's voltage waveform (line-commutated). The problem with the latter is: when the grid's voltage contains harmonics, the reference signal will be distorted too and the current control with pollute its own current. While internally generated reference can prevent this problem, it cannot reduce the resonant effect caused by output capacitance. [1] [4]

Therefore, it is important to know the behaviour and interaction of PV inverters and the network in order to predict resonances. A proper model of PV inverters is required to get reliable results of the power quality studies. Various models of PV inverter have been used in many power quality studies and they are discussed in the following chapter.

2.2. Overview of PV inverter models used in power system studies

2.2.1. Power system studies

Power system studies include all studies related to the quality of supply, stability- and protection of components in the network. Quality of supply is mostly coupled to characteristics of the voltage, such as flicker, unbalance, harmonics, voltage dips, and voltage level. [5] Several power system studies measure the quality of supply on site; for example, harmonic measurements at Gardner Photovoltaic Project [6] and at Sidney Olympic Village [7]. Many other studies, however, are carried-out by computer simulation and modelling of electrical network and its component, including PV inverters [2], [6], [7], [8], [9]. These simulations are carried-out by PV inverter manufacturers, academia, or network operators to design PV plants and study their interconnection and operation with the transmission and distribution systems.

Power system studies are classified by the duration of the events whose effects are investigated in the studies and fall into three categories: steady state, dynamic, and transient, as shown in Figure 2-3. Steady-state studies have the longest duration while transient studies have the shortest duration. Each category of studies requires a different model of inverter determined by the technical issues associated with these studies and the components affected by these issues.
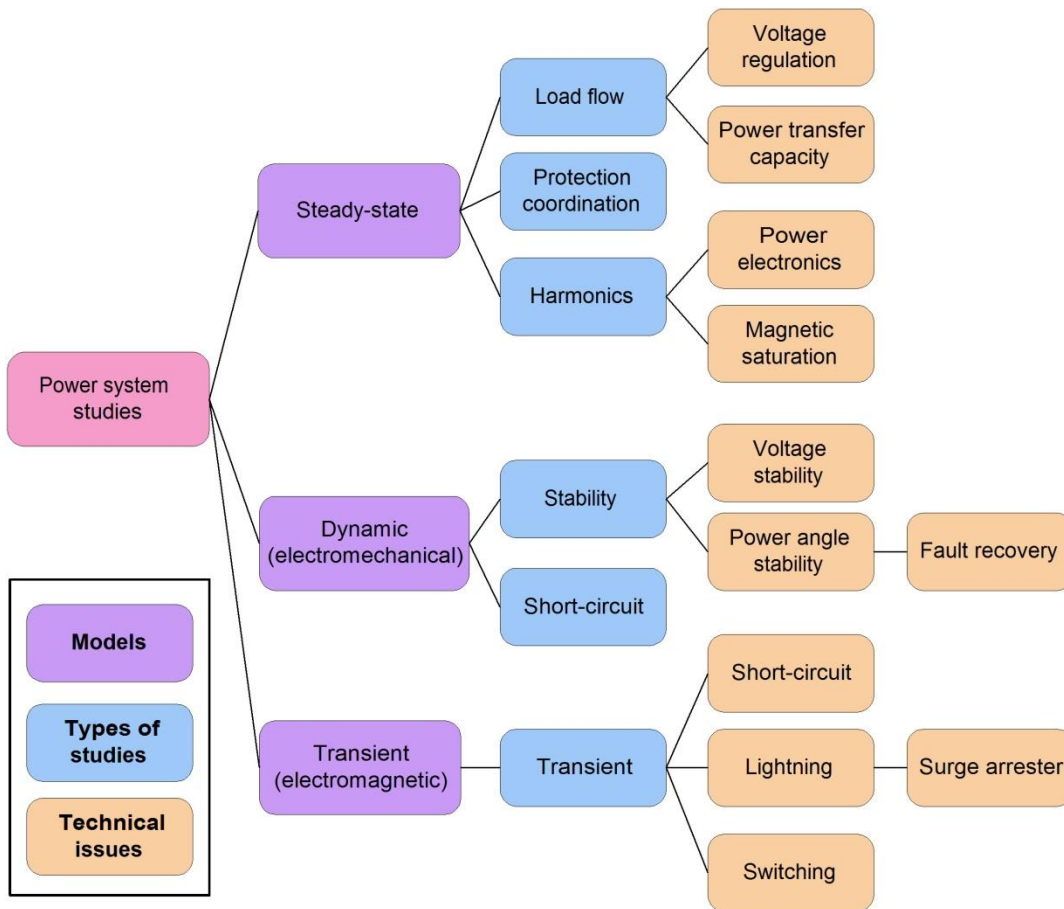
Figure 2-3 Power system study categories [10]
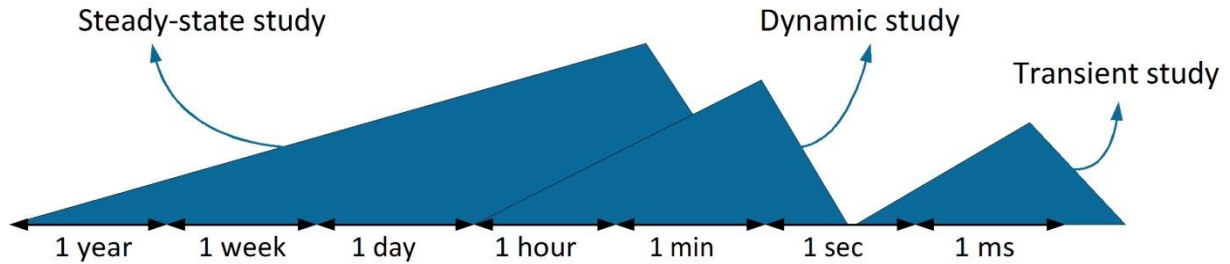
Steady-state

At distribution level, technical studies involve steady-state analysis such as voltage control and protection coordination. Power flow study is usually used to observe equipment loading, system losses, voltage drop/rise, transfer capability and conductor ampacity ratings. Short circuit study and protection coordination is used, for example, to determine the parameter used in protection settings. In a steady state study, a PV inverter may be modelled as a conventional power source –usually with constant power factor or reactive power. An example of steady-state study that observes PV inverter's ability to adjust its active and reactive power injection at PoC to maintain the overall system voltage within acceptable range. This study models the control system of the inverter that regulates the output power. [11]
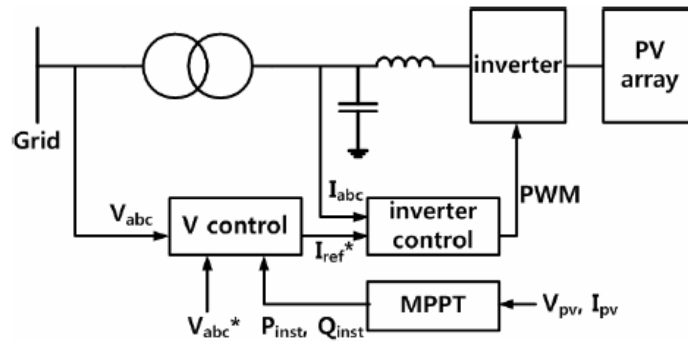
Figure 2-5 The proposed operation scheme of PV inverter that adjusts its active and reactive power to regulate the voltage of the network

If the voltage at the point of connection is assumed to be regulated from the distribution transformer, a PV inverter can be represented as a current source. The current (and thus, power) from multiple inverters are simply summed to make the aggregate model as shown in figure 2-6.
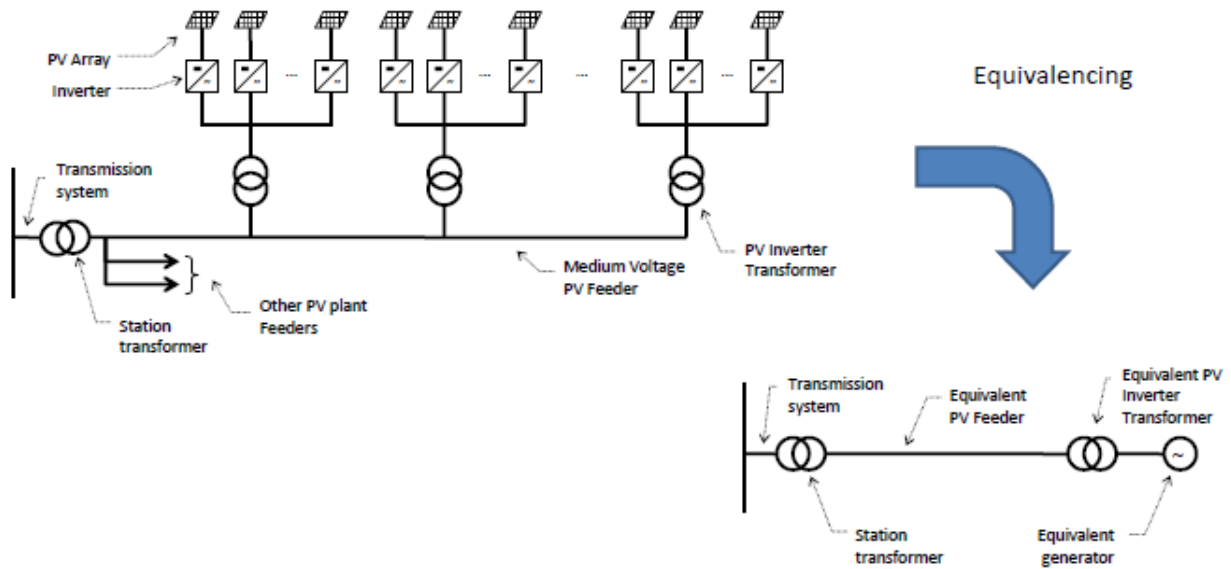
Figure 2-6 Equivalent circuit of utility-scale PV plants [12]

Dynamic (Electromechanical)

Dynamic studies focus on the power angle stability and fault recovery of (synchronous) machines. It is typically not used in distribution studies. Dynamic stability studies conducted at the transmission level use positive-sequence, reduced-order, or average model. This model represents not only central-station solar power plants but also the aggregated effect of a large number of distribution-connected PV systems on transmission network. Figure 2-7 shows an example of dynamic models for aggregated representation of distribution-connected PV. [13]
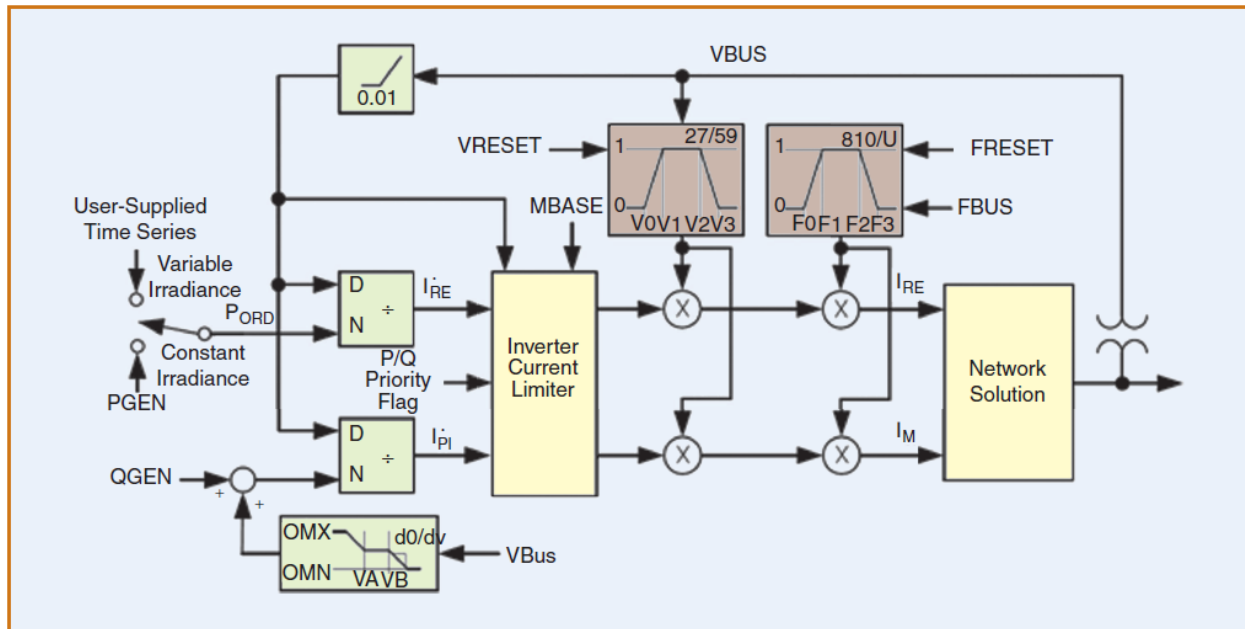
Figure 2-7 An example of dynamic model of PV system

14

Transient (Electromagnetic)

Transient studies are performed to determine if the system will remain in synchronism following major disturbances such as faults, sudden loss or gain of load, loss of generation, or line switching. Transient stability studies generally focus on 1 to 10 second period after a disturbance. Due to its fast nature, this type of study pays more attention on the control system of a PV inverter. Therefore, it uses detailed model of power electronics circuit with controls.
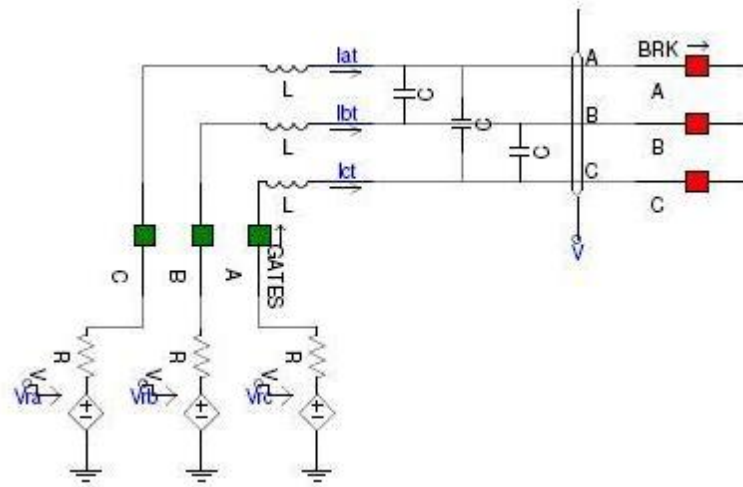
Figure 2-8 A transient model of PV inverter in a study on fault contribution of grid-connected inverters [14]

2.2.2. Voltage dip studies

Until around two years ago, all inverters had a common control feature called anti-islanding protection. It is a feature that strictly disconnects PV inverter from the grid when it detects a disturbance on the grid, following interconnection standards like IEEE 1547 or UL 1741. Recently, several countries are imposing regulations in their national code for distributed generators connected to high and medium voltage network to inject reactive power to the network upon fault condition to improve voltage stability. Since 1 January 2012, this requirement is also applied to PV inverters connected to Germany's low voltage network (VDE-AR-N 4105).

Many studies conducted so far examined and proposed control system that would enable PV inverters to increase voltage stability in the network. In these studies, the inverter is represented as a current source whose value is controlled by the proposed control system. [15] [16] The value of the current represents the (reactive) power injected by PV inverters to the network during the interruption. It is a controlled current source because the control system adjusts the injected reactive power according to the requirement of the grid.

2.2.3. Harmonic studies

All power-electronic devices produce distortion and inverters are no exception. The most common harmonic problems associated with PV inverters happen when the inverter topology has a low output-impedance as a function of frequency because a small harmonic present in the network's voltage will result in high harmonic current. The other problem is the non-ideal current source behaviour associated

with a high output-capacitance and small output-reactor. [2] The harmonic current source is non-ideal because its harmonic is influenced by the harmonic voltage present in the network and the output capacitance is responsible for setting up resonance circuit with network's transformer and cable reactance. Thus, this characteristic is necessary to be considered in the model when studying power quality phenomena associated with PV inverters.

The most common and simple model of a PV inverter in a harmonic study consists of a harmonic current source connected in parallel with an output impedance that represents the output filter's capacitance (Norton model). [2] [3] [17] Some other studies also include series impedance that represents the output filter's resistance and inductance. [18] [19] Another study present the output impedances of PV inverter as a combination of a parallel capacitance and conductance called "Complex Conductance". The capacitor of the inverter is calculated from measuring the imaginary part of the power at the output of the inverter while the conductor is calculated from measuring the real part. Figure 2-9 depicts the Complex Conductance model of the inverter along with the model of the grid and load. The capacitor and conductance of the inverter are symbolized with G and C, respectively. $Iinv$ represents the harmonic current emitted by the inverter without the influence of the harmonic distortion of the background voltage which is symbolized by Vb; Rb and Lb represent the resistance of (mostly) the LV cables and the inductance of the cable and MV/LV transformer, respectively. Gl and Cl denote the capacitance and conductance of the load. [20]
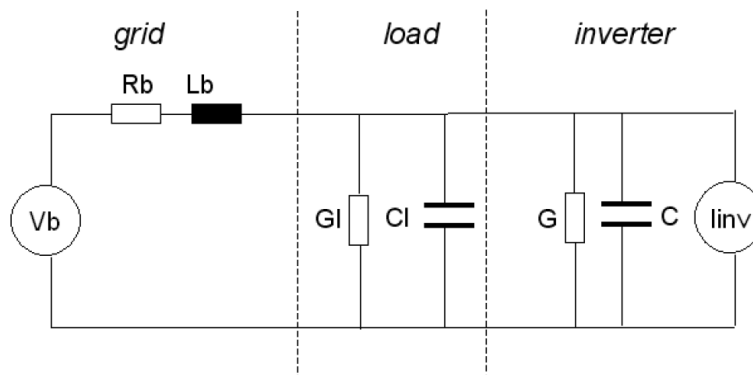
Figure 2-9 A model of grid-connected PV inverter using parallel capacitor and conductor

(a)   (b)
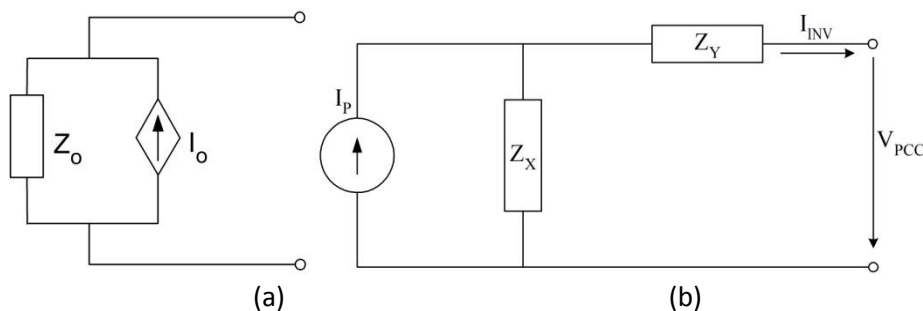
Figure 2-10 Norton model of PV inverter: (a) all output impedances are represented by Zo and (b) output capacitor is represented with Z_X while output resistor and/or inductor is represented by Z_Y

While other power system studies use the typical capacitance of residential single-phase inverter's output filter, the study [20] calculates the value of G and C from the power at the output terminal of the

inverter which is calculated from measured voltage and current at that connection point. Voltage and current measurement is also the basis for the calculation of Z_X and Z_Y in the study [19]. It measures the harmonic voltage across and the harmonic current at the terminal output of the inverter (see Figure 2-10b) for several particular frequencies. The parameter values for each frequency ($I_P(h)$, $Z_X(h)$, and $Z_Y(h)$) are then calculated iteratively using the Newton-Raphson algorithm:

$$[I_P(h)Z_X(h)] - [I_{INV}(h)Z_X(h)] - [I_{INV}(h)Z_Y(h)] = V_{PCC}(h) \qquad (1)$$

where I_P is the harmonic current emitted by the inverter, I_{INV} is the harmonic current at the output of the inverter, V_{PCC} is the voltage at the connection point between the inverter and the grid.

This approach uses a look-up table (there will be a different model for every frequency) which is not favorable because a large number of iterations are required to solve three unknown variables from only one equation. Moreover, since there are different models for different frequencies and the impedance value does not represent a particular element (capacitance/inductance), it is not possible to estimate the resonant frequency from this approach.

This paper presents an alternative circuit to model PV inverter's output impedances: the output impedances are not generalized as series or parallel impedance but are shown as physical elements such as capacitor, resistor, or inductor. The resultant impedance of these elements is shown as Z_{inv} in Figure 2-11. The topology and parameter values of each element are determined by measuring voltage $\overline{V_h}$ and current $\overline{I_h}$ at the connection point of the inverter and using Equation 2 to calculate the impedance $\overline{Z_h}$ at each frequency. The measurement and calculation method will be elaborated in Chapter 3.

$$\overline{Z_h} = \frac{\overline{\overline{V_h}}}{\overline{I_h}} \qquad (2)$$

Also, the harmonic currents generated by a PV inverter depend on many factors such as irradiation levels, temperature, types of PV module, power system impedance, or even orientation of the PV modules. It is also shown in a study that the harmonic currents generated by the inverter will increase with increases of background harmonic voltage. [7] Therefore, in general, the model uses a variable current source in the model as shown in Figure 2-11 as I_{inv}. This model is the basis for developing a more detailed model in Chapter 4 and 5.
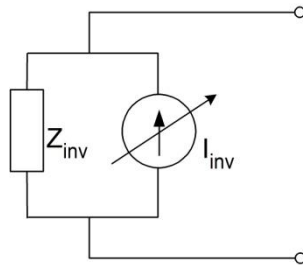
Figure 2-11 A model of PV inverter used harmonic study

2.2.4. Aggregate model

As harmonics increase, so do their negative impact on the network. It is therefore important that the interaction between inverters and their aggregate impact on the network are understood.

When multiple inverters are operating in parallel, two particular consequences arise which affect harmonic generation: attenuation and cancellation. Attenuation occurs because the generated currents cause voltage variations that in turn affect the other sources; the impact is such as to reduce the currents causing the disturbance. Cancellation is the result of the harmonic current components from different sources being -to some extent- out of phase, resulting in a reduction in that particular harmonic for the aggregate. [1] How the harmonic outputs of multiple inverters add up is rather complex because each inverter's harmonic output might have different phase for the same frequency. Thus, they have to be added using phasor calculation for each particular frequency.

On the other hand, when multiple impedances are connected in parallel, their resultant impedance will be lower than their individual impedance. It is undesirable that the resultant output impedance of aggregated inverters is low as a function of frequency, for the reason explained earlier. Paralleled output capacitance of several inverters is also suspected to shift the resonance frequency to lower frequencies.

If the impedance model in Figure 2-10a is used to represent an individual PV inverter, the corresponding model of multiple inverters connected in parallel is as shown in Figure 2-12. $I_{o,n}$ represents each inverter's current source, $Z_{o,n}$ represents each inverter's output impedance, while electrical loads are represented by a lumped impedance Z_{Ldn} and feeder impedances are represented by $Z_{f,dn}$. [3]
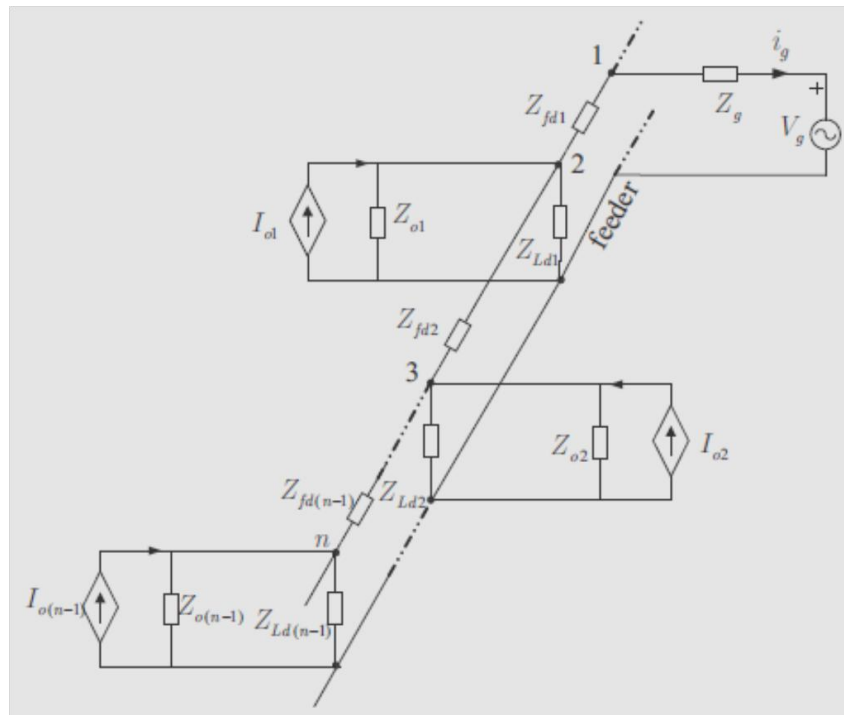
Figure 2-12 Impedance-model representation of a distribution grid with multiple inverter systems connected

3. Measurement Set-up

In this chapter, a measurement method of commercial PV inverters' impedance is proposed based on Fast Fourier Transformation (FFT) analysis of the voltage and current in time domain. This method measures the complex harmonic impedance spectrum for a range of harmonic frequencies up to the 50th. The commercial PV inverters used in the measurement are the ones typically installed in a residential house and connected to LV distribution network.

If the impedance profile against frequency is obtained, the impedance value can be estimated and a good model can be made.

3.1. Basis of measurement

The complex impedance measurement system is expected to measure harmonic impedance spectrums of up to 50th harmonic frequency. The system introduces voltage signals containing fundamental (V_{sf}) and a certain frequency component (V_{sh}) into the grid and measures the voltage (V_h) and current (I_h) of that frequency at the connection point of the inverter, as depicted in Figure 3-1. The impedance value of that particular frequency is then calculated simply using Equation 2.
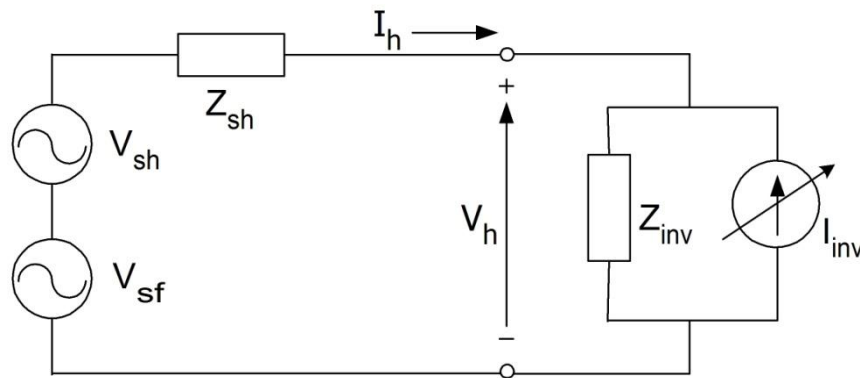
Figure 3-1 Measurement circuit

This method of measurement is based on many measurements of grid harmonic impedance that have been proven to be effective. Grid harmonic impedance measurement usually introduces voltage or current harmonics to the system and measures the current or voltage responds to calculate the impedance. Most of the time, current signal is chosen as the stimuli [21], [22], [23], [24] although a few employs voltage harmonics. [25], [26] The method of using current stimuli is effective because the current influences the whole network voltage through the network impedance. The voltage response is then dependent on the system impedance.

 In this measurement, however, the stimuli used are voltage signals because the inverter has only small influence on the system voltage. If a current signal is used, it will influence the voltage through the system impedance, and only indirectly the current of the inverter. In that way, it will have too much influence of the system impedance and little correlation with the inverter.

Some of the grid harmonic impedance measurement methods inject interharmonic signals to the system to obtain impedance-frequency (Z-f) plot to avoid interference of the injected signal with the grid

fundamental and its harmonics. [21] [24] [27] Interharmonics are non-harmonic frequency signals, for example, 15Hz or 37Hz for fundamental frequency 50Hz. The impedance values are then obtained from interpolation between two interharmonic impedances in the Z-f plot. In this measurement, however, both harmonic and interharmonic signals are injected to investigate whether the injected harmonics interfere with the harmonics emitted by the inverter.

The interharmonic frequencies used in the measurement are frequencies in between harmonics, i.e. 75Hz, 125Hz, 175Hz, and so on.
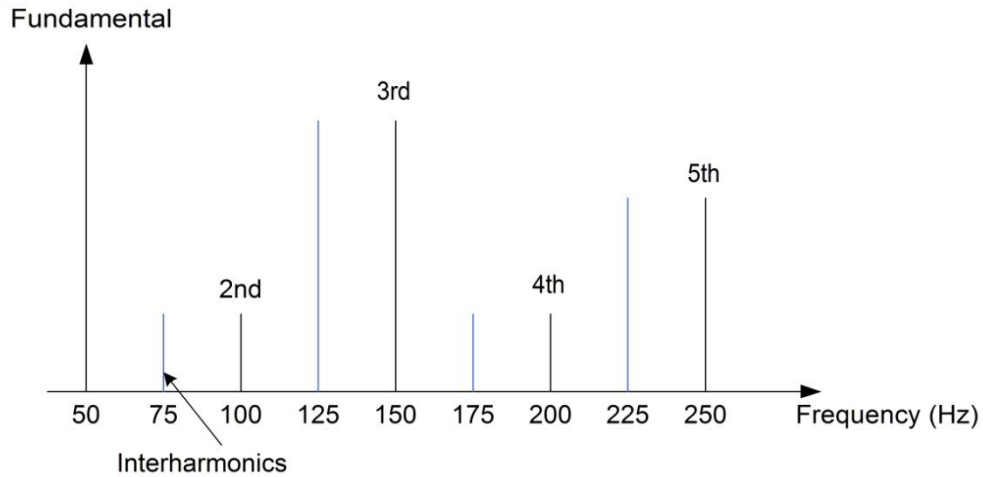
Figure 3-2 The interharmonic signals used for the measurement

3.2.   Choosing the stimuli

Since the PV inverter used in the measurement is a commercial PV inverter typically connected to LV distribution grid, the harmonic voltage stimuli should comply with the existing standard for harmonic voltage level in LV network. The two standards observed in the measurement are EN50160 and IEC61000-3-6. To comply with the standards, the injected amplitudes of harmonic components must descend with harmonic order. Figure 3-3 depicts the harmonic voltage limit by the standards and the corresponding harmonic voltage stimuli used in the impedance measurement of individual harmonics.

For aggregate measurement of parallel inverters, the maximum voltage stimuli are lower than that for individual measurements. The harmonic current responds of each inverter to the injected harmonic voltage add-up at PoC so the total current is much higher and if it is too high, the protection system at PoC is triggered.
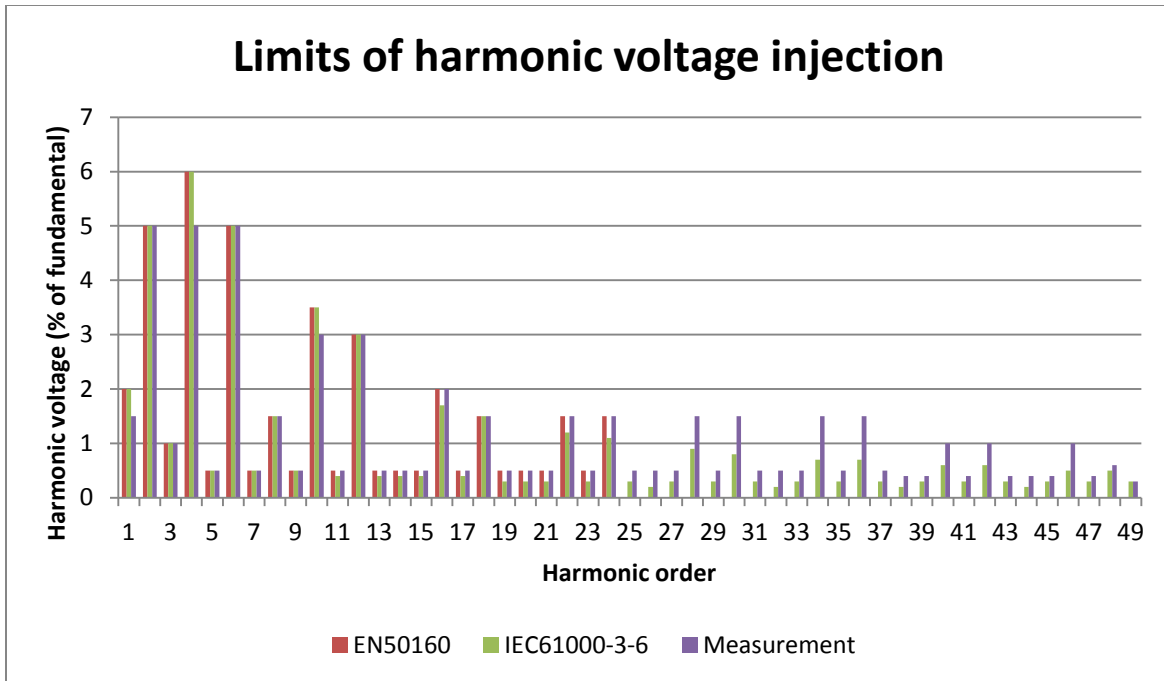
Figure 3-3 The stimuli amplitude spectrum compared to EN50160 and IEC61000-3-6 limits

For the interharmonics, there is no standard regulating the maximum amplitude of interharmonic components in the network. Thus, the stimuli follow the next harmonic closest to it. For example, the amplitude of interharmonic signal of 75Hz will be similar to that of 2nd harmonic (100Hz), 125Hz component's amplitude is similar to that of 3rd harmonic (150Hz) component and so on.

3.3. Injecting the stimuli

Unlike many other impedance measurement methods, the stimuli used in the measurement is not a signal containing multiple harmonic components. Instead, they are separate waveforms; each of them contains only fundamental and one harmonic component, for example, a fundamental and a 2nd harmonic (see Figure 3-1). Fundamental component is needed to get the inverter in operation. Thus, for 50 harmonic components, there should be 50 signals.

The same method is used for interharmonics. For each measurement, the injected signal will contain fundamental and one interharmonic component, for example, a fundamental and a 225Hz component. The current response is then measured right after injection of each signal.

Every harmonic and interharmonic component itself is injected with multiple amplitudes and phase angles to study the current response in different situation. Also, the current measured is more reliable if it varies in accordance to the voltage variation. For example, if the voltage amplitude increases, it is expected that the current amplitude also increases since the impedance is linear.

The amplitude varies according to the maximum amplitude specified by the standards and the amount of signals to be injected. For example, the 2nd harmonic voltage signal is limited to 2% of the fundamental voltage to comply with the standards mentioned above. Thus, the injected amplitudes of 2nd harmonic component are 0.5%, 1%, and 1.5%. The interval of the amplitude determines the amount

of different waveforms and measurements done for each harmonic. In the example above, there are three different amplitudes. The amplitude steps for all harmonic and interharmonic components can be seen in the Appendix A.

For interharmonics, there is no phase angle variation (i.e. all signals are injected with 0° phase angle) because the phase angle of interharmonic components rotates. For the harmonics, the phase angle varies from 0° to 300° (since 360° is the same with 0°). The phase angle step is 60°. Thus, there are 5 variations of waveform for every amplitude of each harmonic component.

In total, with phase angle and amplitude variations, there can be 12 to 30 different waveforms for each harmonic component. Since there is a large amount of waveforms to be injected every time, it is not practicable to inject them one by one manually. A group of MATLAB commands are utilized to upload the different waveforms for each frequency to the programmable voltage source.

Figure 3-4 shows the set-up of the measurement system.
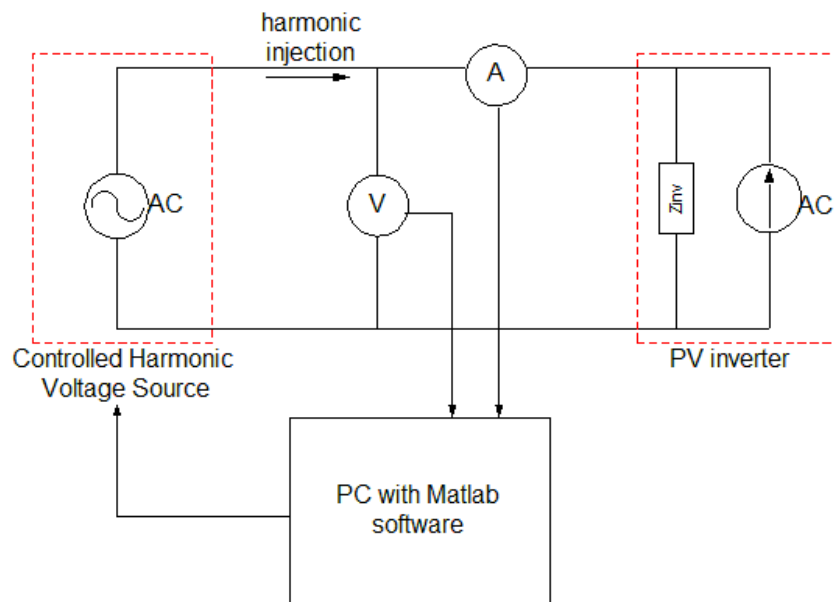
Figure 3-4 PV inverter impedance measurement set-up

3.4. Measuring the response

To get more valid data, every waveform is injected five times and after each injection the current is measured. Thus, for every different waveform, there are five different voltage and current measured. The value used in the calculation is the average of five measurements. The whole process is depicted in the flowchart below.

As can be seen from Figure 3-4, the voltage and current in time domain are measured using a PC-based scope which also converts the analogue signal to digital by taking samples of the voltage and current with sampling frequency f_s 50403Hz. A program in MATLAB acquires the data measured by the scope and save it in MATLAB files. Afterwards, the program will upload the next waveform following the algorithm shown in Figure 3-5. For the interharmonics, the phase angle loop is bypassed.
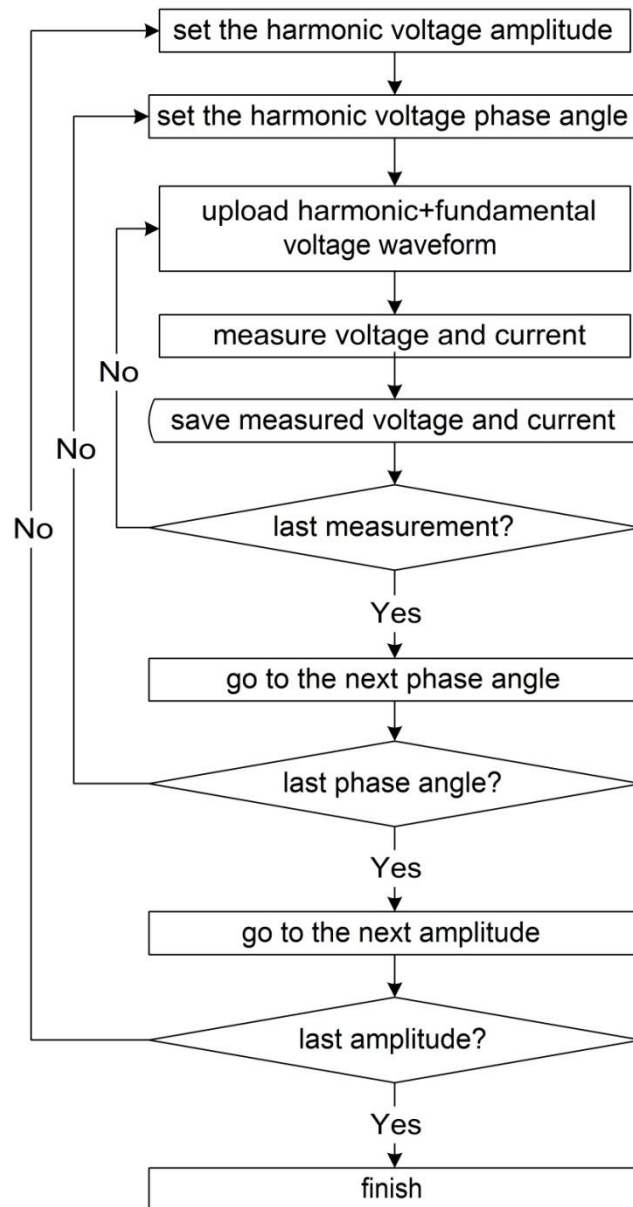
Figure 3-5 Process flow of the PV inverter impedance measurement system

Apart from the process depicted above, there is one more step during harmonic measurement. It is to inject a clean voltage signal containing only fundamental voltage and measure the current at the output terminal of the inverters. This is done to measure the actual harmonic current emission of the inverters without any influences of background harmonic voltages. The values of these harmonic currents are subtracted from the measured current so that the actual proportion between the injected harmonic voltage and the subsequent harmonic current can be obtained.

It is interesting to notice that even though the injected voltage is clean, the measured voltage is distorted. This happens because the programmable voltage source uses power electronics in generating its voltage, thus naturally switching harmonics are present in the output voltage. To eliminate its

influence in the impedance calculation, these harmonic voltages are also subtracted from the measured voltage, as shown in Equation 3. Now Equation 2 becomes

$$\overline{Z_h} = \frac{\overline{V_h} - \overline{V_{h,o}}}{\overline{I_h} - \overline{I_{h,o}}} \tag{3}$$

with $V_{h,o}$ and $I_{h,o}$ as the harmonic voltage and current for a particular frequency on a clean signal source.

3.5. Fast Fourier Transform (FFT) analysis

With Fourier series, a periodic time function *f(t)* can be expressed as the summation of a number of harmonically related complex rotating phasors $c_n e^{j\omega nt}$.

$$f(t) = \sum_{n=-\infty}^{\infty} c_n e^{j\omega nt} \tag{4}$$

If both sides of Equation 4 are multiplied with the conjugate of phasor $e^{j\omega nt}$, which is $e^{-j\omega nt}$, the phasor components in the signal *f(t)* that rotate at *ωn* will stop rotating and become constant components. All phasor components in the signal *f(t)* that rotate at speed different than *ωn* will still rotate at different speed.

$$f(t)e^{-j\omega nt} = \sum_{n=-\infty}^{\infty} c_n e^{j\omega nt} e^{-j\omega nt} = \underbrace{\sum_{n=-\infty}^{\infty} c_n}_{\text{integer harmonics}} + \underbrace{\sum_{n=-\infty}^{\infty} c_n e^{j\omega mt} e^{-j\omega nt}}_{\text{non-integer harmonics}} \tag{5}$$

If both sides are now integrated over a period of time, the non-integer harmonics will be averaged out and only the constants c_n remain.

$$\int_{-T/2}^{T/2} f(t)e^{-j\omega nt} dt = T \sum_{n=-\infty}^{\infty} c_n \tag{6}$$

Each phasor can now be found by calculating the complex factor c_n.

$$c_n = \frac{1}{T} \int_{-T/2}^{T/2} f(t)e^{-j\omega nt} dt \tag{7}$$

To do this digitally (for example in MATLAB), the continuous signal *f(t)* should be converted to a function of small discrete time steps *f(kT$_s$)* where *k* is the number of the sample and N is the total amount of the samples. The complex phasors are now expressed as shown in Equation 8.

$$c_n = \frac{1}{N} \sum_{k=0}^{N-1} f(kT_s) e^{-j\omega nkT_s} \tag{8}$$

Digital Fourier Transformation (DFT) is the process to obtain the coefficient c_n of certain frequencies that are integer multiple of fundamental frequency *F$_0$*. *F$_0$* is a measure of resolution of DFT and depends

on the total number of samples N used for the transformation. Fast Fourier Transformation (FFT) is a DFT with special calculation algorithm to reduce the number of complex multiplications of the DFT.

$$F_0 = \frac{1}{T_s N} = \frac{f_s}{N} \tag{9}$$

To find some particular frequency components from a time domain signal, F_0 should be chosen in a way that those particular frequencies are integer multiples of F_0.

In the measurement, the continuous voltage and current signal *v(t)* and *i(t)* are sampled by the PC-based scope with sampling frequency f_s 50403Hz. FFT analysis is performed afterwards to extract the harmonic and interharmonic spectra from the sampled voltage and current. The important step for this is to choose the frequency resolution of the transformation. As mentioned earlier, F_0 should be chosen in a way that the frequencies of interest are integer multiples of F_0. The frequencies of interest for harmonics are integer multiples of 50Hz; whereas for interharmonics, they are not integer multiples of any frequency (they can be said integer multiples of 25Hz but that includes the harmonic frequencies too). Thus, frequency resolution of 5Hz is chosen for the interharmonics.

From Equation 9, the number of samples (record length of the measurement) is determined by the sampling frequency and the frequency resolution. The chosen record length for harmonics and interharmonics are 100 and 10 periods, respectively. After the voltage and current spectra from all frequencies of interest are obtained, another program in MATLAB is used to calculate the impedance from these voltage and current spectra.

4. Harmonic Impedance Measurement and Model

The experiment is done on 5 commercial PV inverters: three single phase inverters, one single-phase power router, and one three phase inverter. Single-phase inverters (Inverter1, Inverter2, and Inverter3) have nominal output powers of 1000 W, 1500 W, and 1500 W, respectively. The single-phase power router has a nominal power of 5000 W, and the three-phase inverter 2500 W. Although the latter needs a 3-phase connection, it only feeds-in to the grid via 1 phase (hence it can be treated as a 1Φ inverter). The measured impedance values are explained for every inverter; each for the harmonic and interharmonic measurement. Further a general discussion about the measurement results is presented along with a conclusion.

4.1. Impedance measurement result

4.1.1. Single-phase (1Φ) inverters

Although the measured 1Φ inverters have different nominal power, they are all measured at the same DC-input power of 900Wdc to obtain better comparison. However, due to the differences in the inverter circuit, each of them has different output power: 825Wac, 814Wac, and 883Wac for Inverter1, Inverter2, and Inverter3, respectively.

As discussed in previous chapter, there are various phase angles and amplitudes of the harmonic voltage source thus there are several impedance values for every harmonic frequencies. It is expected that the values are convergent so that they can be averaged. Particularly for lower harmonics, convergent results are difficult to obtain because the current behaviour is not linear. As an example, Figure 4-1 compares the harmonic current fingerprint of Inverter3 for 5th harmonic and 25th harmonic. Despite this non-linear behaviour, all impedance values are averaged for every frequency to ensure the same treatment for all frequencies.
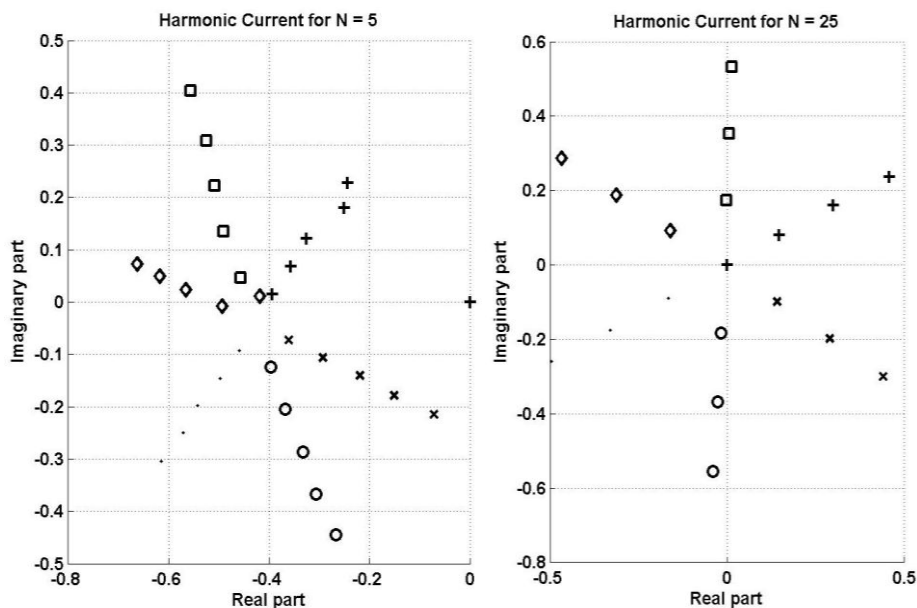
Figure 4-1 Comparison of current behaviour at 5th and 25th harmonic at single-phase inverter

Unlike the harmonic measurement, injected interharmonic voltages only vary in amplitudes and not in phase angles, but similar averaging method is utilized here. Similar scattered results are also found at lower interharmonic frequencies (75Hz, 125Hz, and 175Hz). The reason is not the non-linear current behaviour but the low signal-to-noise ratio. As the current raises with frequency increase, it is likely that current is smallest at lowest frequencies. In fact, the current is so small that it seems unaffected by the voltage variation. Another difference from harmonic measurement is the very low voltage source at highest interharmonic frequencies (2425Hz and 2475Hz). It is as if the voltage signals are noises and the average impedances at these frequencies do not follow the same trend with other interharmonic frequencies. Since the reason of these scattered results are not from the voltage or current behaviour but more from experiment limitations, the average impedances from these frequencies are omitted at the total impedance-frequency plot.

The harmonic and interharmonic results show good agreement, i.e. they make the same trend line and there is no harmonic suppression found. The trend line itself is similar to that of capacitor (the impedance is inversely proportional to the frequency). Therefore, a single capacitor is adequate to model the impedance. For Inverter2, however, a better fitting is obtained when the model includes a resistor in parallel with the capacitance. Fitting is done with a statistic program OriginPro 8 using Equation 10 for capacitor and Equation 11 for capacitor in parallel with resistor.

$$y = Ax^{-1} \tag{10}$$

where *y* is the impedance magnitudes (Ohm), *x* is the frequencies (Hz) and $A = \frac{1}{2\pi C}$ from which capacitance (F), *C*, is calculated.

$$y = \left(\sqrt{A^2 + (Bx)^2}\right)^{-1} \tag{11}$$

where *y* is the impedance magnitudes (Ohm), *x* is the frequencies (Hz), $A = \frac{1}{R}$ is the conductance (Siemens) and $B = 2\pi C$ from which the capacitance (F), *C*, is calculated.

The impedance profile for Inverter1, Inverter2, and Inverter3 are shown in Figure 4-2, Figure 4-3, and Figure 4-4, respectively while the impedance models of all three inverters are shown in Figure 4-5. The capacitance values of Inverter1 and Inverter2 are within the range of typical output capacitance of commercial inverters in 1-3kW power range –which is 0.5 to 10µF. The capacitance of Inverter3 is out of that range because it is one of the first generation inverters and that range of value is based on recent inverters.
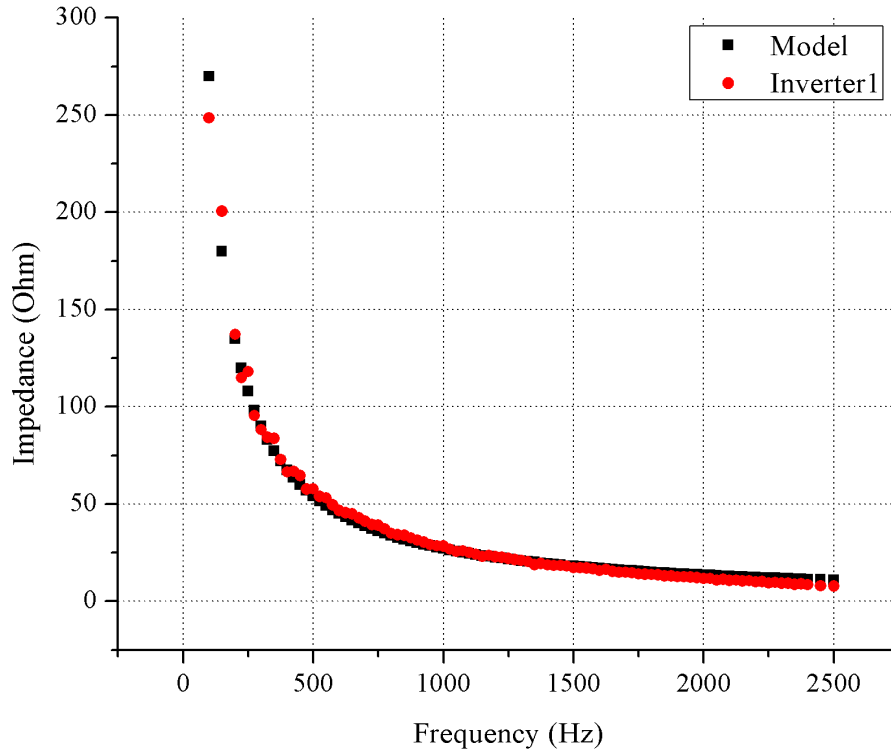
Figure 4-2 The impedance profile of Inverter1 and fitted curve
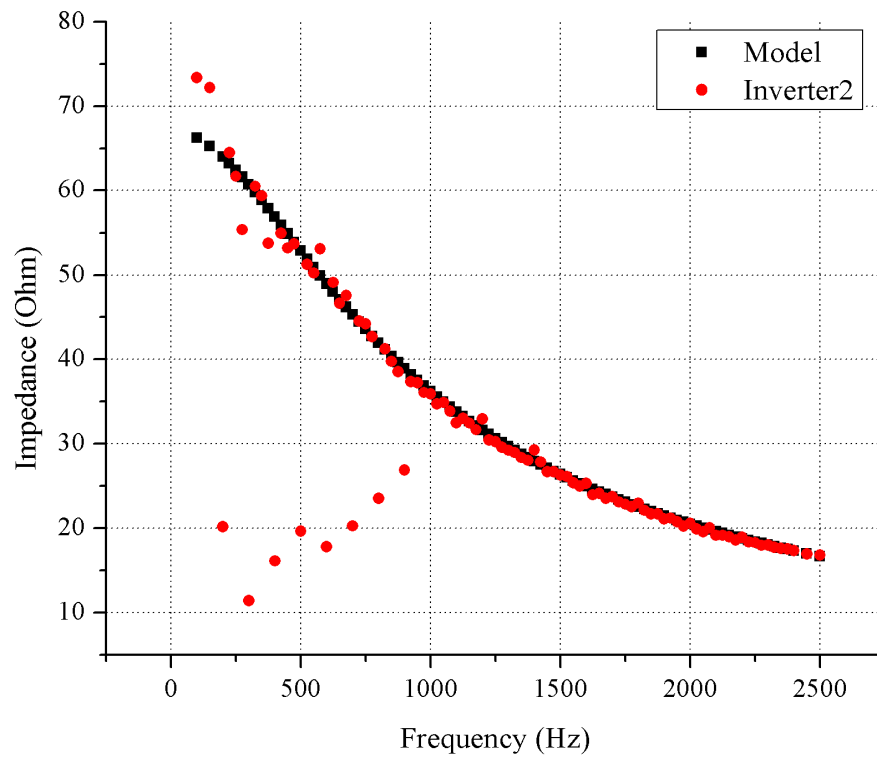
Figure 4-3 The impedance profile of Inverter2 and fitted curve
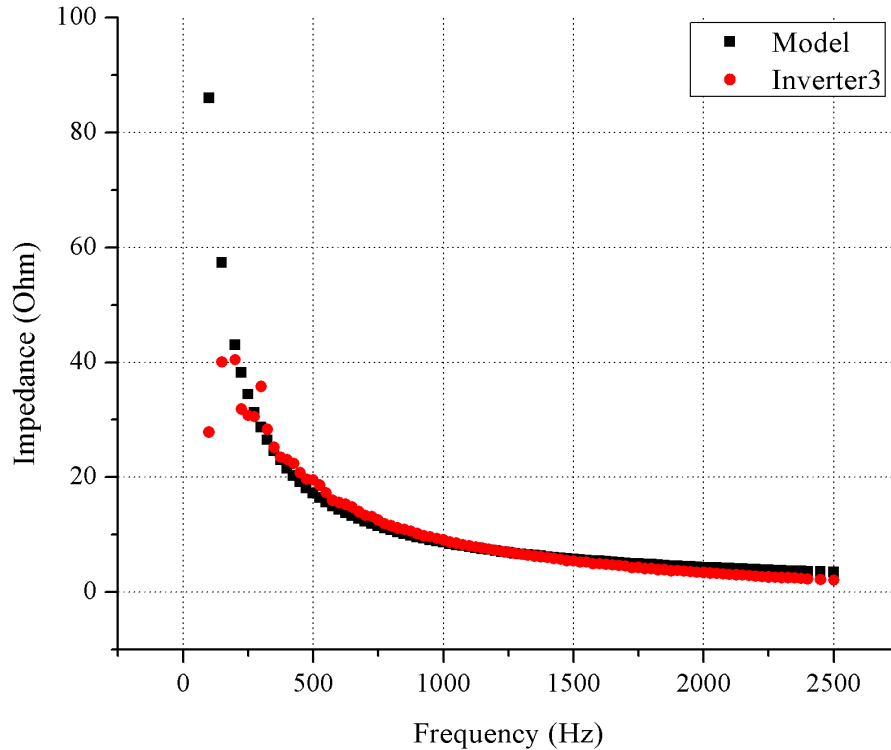
Figure 4-4 The impedance profile of Inverter3 and fitted curve
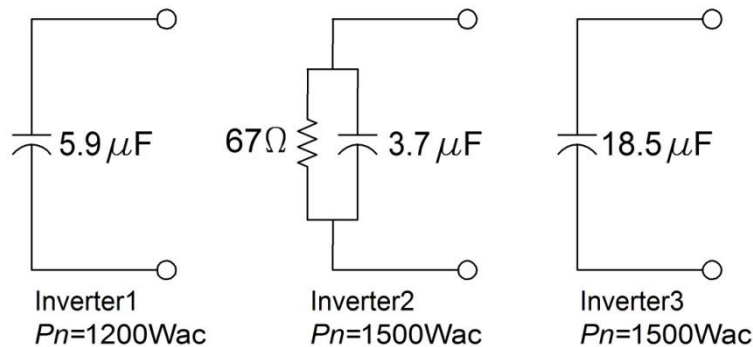
Figure 4-5 The impedance models of single phase PV inverters

4.1.2. Single-phase power router

A power router operates in a slightly different way from most commercial PV inverters complying with "anti-islanding" regulation. It can be connected to a DC storage that supplies backup power in the event of a grid failure. Unlike other inverters, the power router switches to "island mode" when the grid fails. After a short delay, it resumes operation to supply a stable 230Vac power signal to the connected loads. This backup works as long as there is sufficient solar power or energy in storage.

Although in principal it works as a 1Φ inverter, the impedance profile differs from the other 1Φ inverters; there is a parallel resonance at 33rd harmonic (see Figure 4-6). This happens due to the different topology of the filter inside the inverter. Only harmonic measurement results are presented

here because it is not possible to do interharmonic measurements on this inverter. Interharmonic components of the voltage trigger the protection system of the power router.
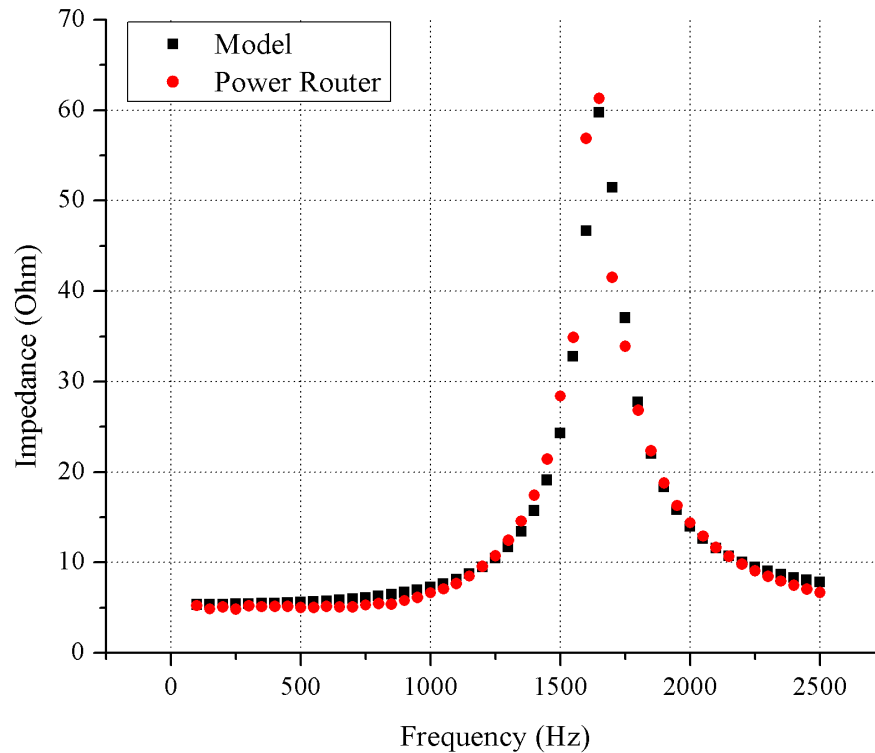
Due to its unique impedance profile, it is difficult to create the impedance model that fits very well. A good estimation, however, was obtained based on below considerations.

a. The resonance is parallel, at f=1650Hz. This is the starting point to make the topology of the circuit which is an inductor in series with a capacitor (see Figure 4-7). At first, the capacitor value is chosen to be in the range of 5-18.5µF which is the value of output capacitors of single phase inverters measured earlier. After the capacitance is chosen, the parallel inductance is calculated from the resonant frequency using Equation 12 where L is the parallel inductance, C is the capacitance, and f is the resonant frequency 1650Hz.

$$L = \frac{1}{\omega^2 C} = \frac{1}{(2\pi f)^2 C} \tag{12}$$

b. A damping resistor determines the peak value. Without damping resistors (R1 and R2), the peak resonance value of the model is much higher than the measured value. Not only reduces the peak value, damping resistors also decrease the Q factor which is a widespread measure used to characterise resonators. Here the damping resistors determine the slope of the mountain. Since the curve is quite flat up to 750Hz, smaller damping resistors are chosen to make the mountain steeper but it results in high peak value. Thus, the capacitor needs to be bigger to reduce the peak point. Optimum values of damping resistors and capacitor are chosen in such a way as to minimize the discrepancy between the measurement results and the model.

c.   A series resistor determines the magnitudes at lower harmonics. The impedance magnitudes at lower harmonics (up to 750Hz) seem to be quite flat at 5 Ohm and it can be modelled by a series resistor (R3) of 5 Ohm.
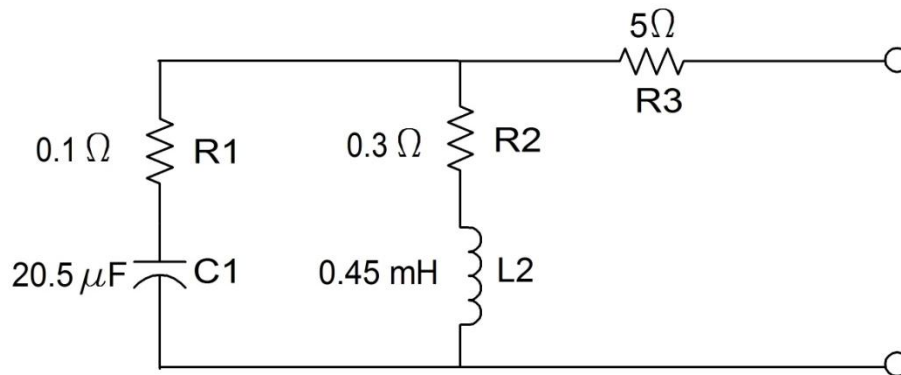
Figure 4-7 The impedance model of single-phase power router

4.1.3. Three-phase (3Φ) inverter

Although this 3Φ inverter needs 3-phase connection, it feeds-in to only one phase. Therefore, the harmonic and interharmonic voltage signals are only injected to one phase (the feed-in phase) and consequently, the harmonic current responses are also measured at this phase. Notwithstanding its one phase feed-in, the impedance profile looks different from other 1Φ inverters (see Figure 4-8). It still has the negative characteristic of a capacitor (i.e. the impedance decreases when the frequency increases) but the slope is not as steep. Therefore, a simple capacitor-resistor model as that of other 1Φ inverters cannot be applied here. In fact, the complex impedance topology of the power router is used as the template here, only the parameters are changed accordingly.

a.   At lower frequencies (up to 600Hz), the curve is quite flat and it can be fitted using parallel resonance at low frequency with wide bandwidth. Figure 4-8 shows the influence of damping resistor R2 in flattening the curve at low frequencies. The capacitance value is again chosen as the starting point and chosen to be in the range of 0.5-10μF because the nominal power of this inverter is 2.6kW (which is in the range of 1-3kW). Then, the parallel inductance is calculated from the resonant frequency using Equation 12.

b.   A series resistor (R3) determines the magnitudes at lower harmonics. The impedance magnitudes at lower harmonics (up to 500Hz) seem to be quite flat at 6Ohm and the series resistor chosen to fit it is 16Ohm.

c.   A series inductor determines the magnitude at highest frequencies. A capacitor's impedance profile tends to be flat at high frequencies but the measured data does not show this tendency. Therefore, an inductor is connected in series to reduce the influence of the capacitor and to match the magnitude at highest frequencies. The impedance model is shown in Figure 4-9.
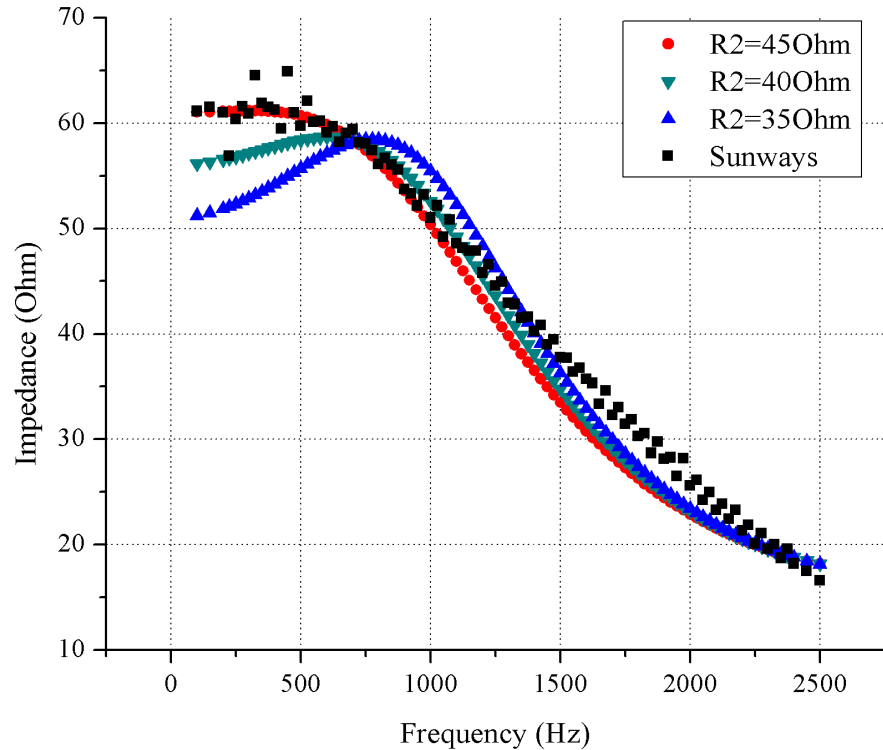
Figure 4-8 The impedance profile of three phase inverter and the fitted curve for different damping resistor values
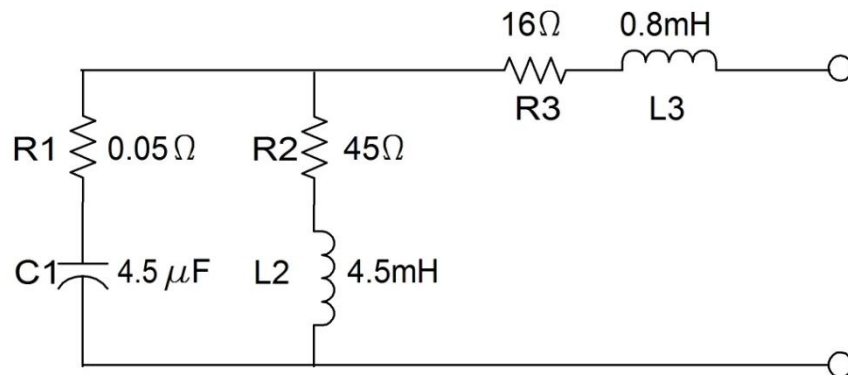
Figure 4-9 The impedance model of 3Φ inverter

As with other 1Φ inverters, both harmonic and interharmonic measurements can be performed on this inverter. At low (75Hz, 125Hz, and 175Hz) and high (2425Hz and 2475Hz) interharmonic frequencies, scattered results due to small signals are also encountered. Therefore, the average impedances from these frequencies are omitted at the total impedance-frequency plot. However, there are also some differences with other 1Φ inverters. There is some oscillation in the impedance profile at lower frequencies but they are not caused by non-linearity, unlike the case in 1Φ inverters. At lower harmonics, the current behaviour of the 3Φ inverter is linear as shown in Figure 4-10.
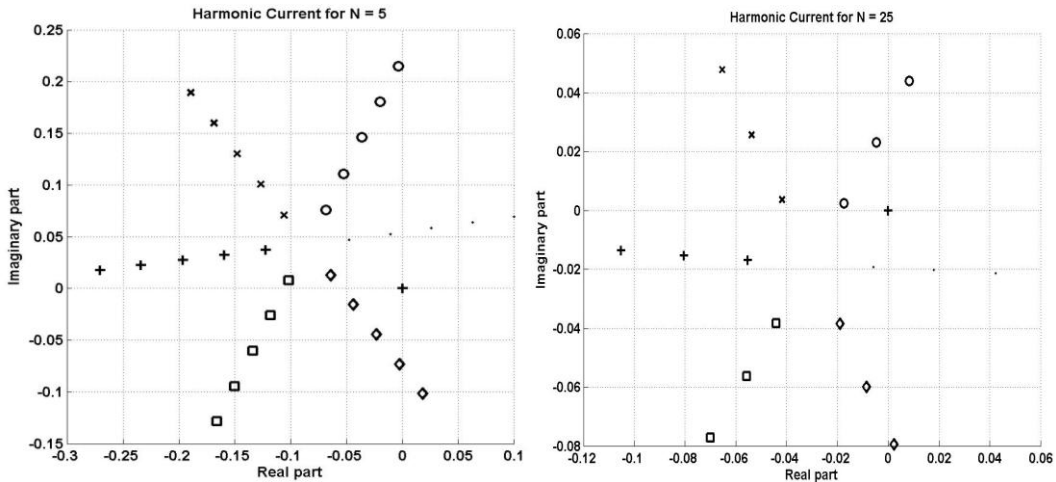
Figure 4-10 Comparison of current behaviour at 5th and 25th harmonic of 3Φ inverter

4.2. Results analysis

As the nature of a model is to mimic the characteristic of something, there are some differences in the behaviour between the model and the original. With the impedance circuits presented above to model the frequency response of PV inverters, there are also some discrepancies between the model and measured data. A comparison between the model current and the measured current show the reliability of the model. Only the significant harmonics are compared, they are 3rd, 5th, 7th, 9th, and 11th harmonics. Comparison at different output powers are also carried out to investigate the influence of output power on the consistency of the impedance models.

4.2.1. Discrepancies between measured and model current

Mostly, discrepancies between measured and model current are caused by phase angle differences instead of magnitudes. As shown in previous chapters, models are built by fitting the impedance magnitudes plot against frequency. As it turns out, although the magnitudes of the model match well the magnitudes of measured impedance, the phase angles do not. Some measures have been taken to match the phase angles, for example by adjusting the series inductance value for the 3Φ inverter, as shown in Figure 4-11. However, this yields disagreement in the magnitude profile. Thus, the fitting of magnitude profile is chosen at the expense of phase angle profile. Also, better matching will be obtained if the model is more complex but too complex model will have limited use due to its specific characteristic. A simpler model with broader use is desirable.
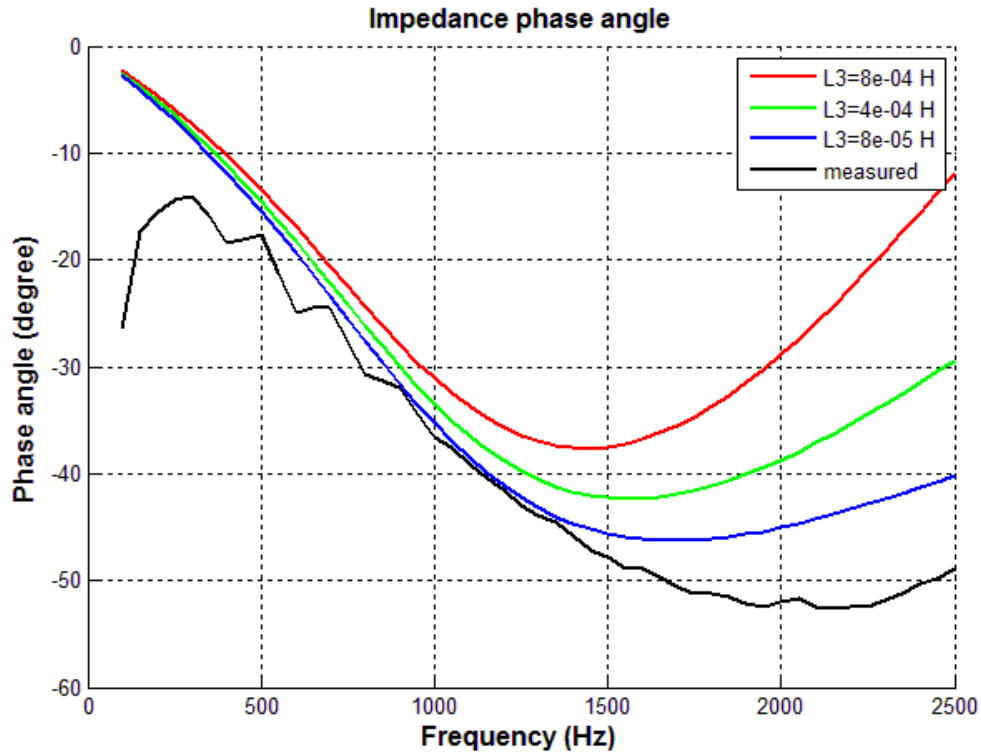
Figure 4-11 Three-phase inverter model phase angle profiles when the series inductance is changed, compared to measured phase angle profiles

Single-phase inverters

Out of three 1Φ inverters, Inverter2 has the biggest phase angle discrepancy between the model and measured data. The phase angle of the measured data itself oscillates at lower harmonic –as also seen in the magnitude profile which makes it difficult to fit. As a result, the model lags the measured data 60° as shown in Figure 4-13. As with Inverter1 and Inverter3, the phase angle profile is constant at -90°, see Figure 4-12 and Figure 4-14. The harmonic current fingerprints shown are for 7th harmonic at 0.8kWac.

Despite the phase angle difference, the current discrepancies of Inverter1 and Inverter3 are still reasonable; they are at the maximum 40%. On the contrary, phase angle difference and non-linear current behaviour of Inverter2 cause the current discrepancy to be more than 100%. The harmonic frequency itself does not seem to play a role in the current discrepancy as the percentages do not increase nor decrease at higher harmonic orders. Figure 4-15 shows the 7th, 9th, and 11th harmonic current discrepancies of Inverter1.
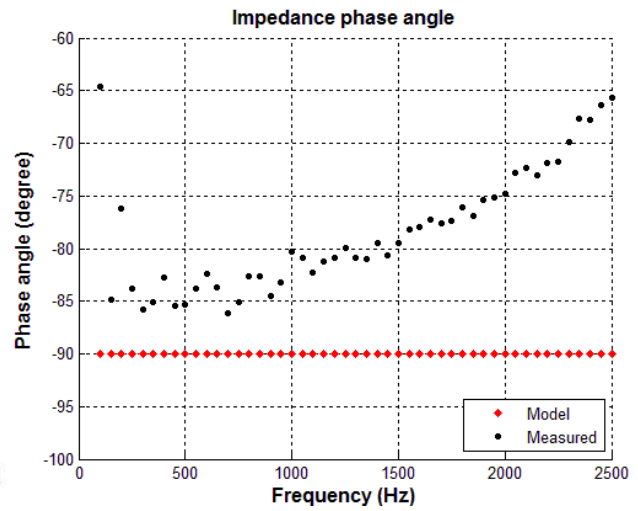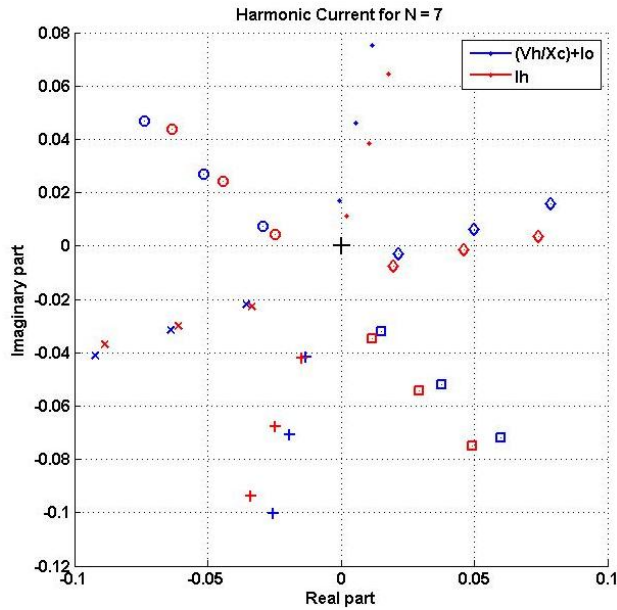
Figure 4-12 7th harmonic fingerprint of measured and model current with phase angle profile of measured data and model of Inverter1, there is about 5° phase angle difference
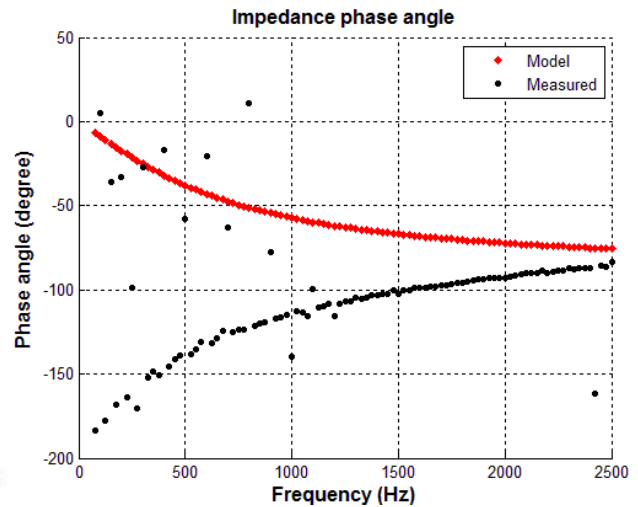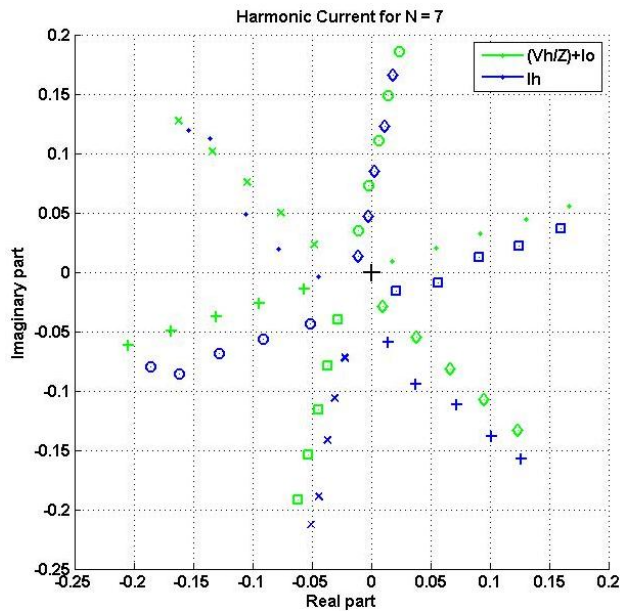
Figure 4-13 7th harmonic fingerprint of measured and model current with phase angle profile of measured data and model of Inverter2, there is about 120° phase angle difference
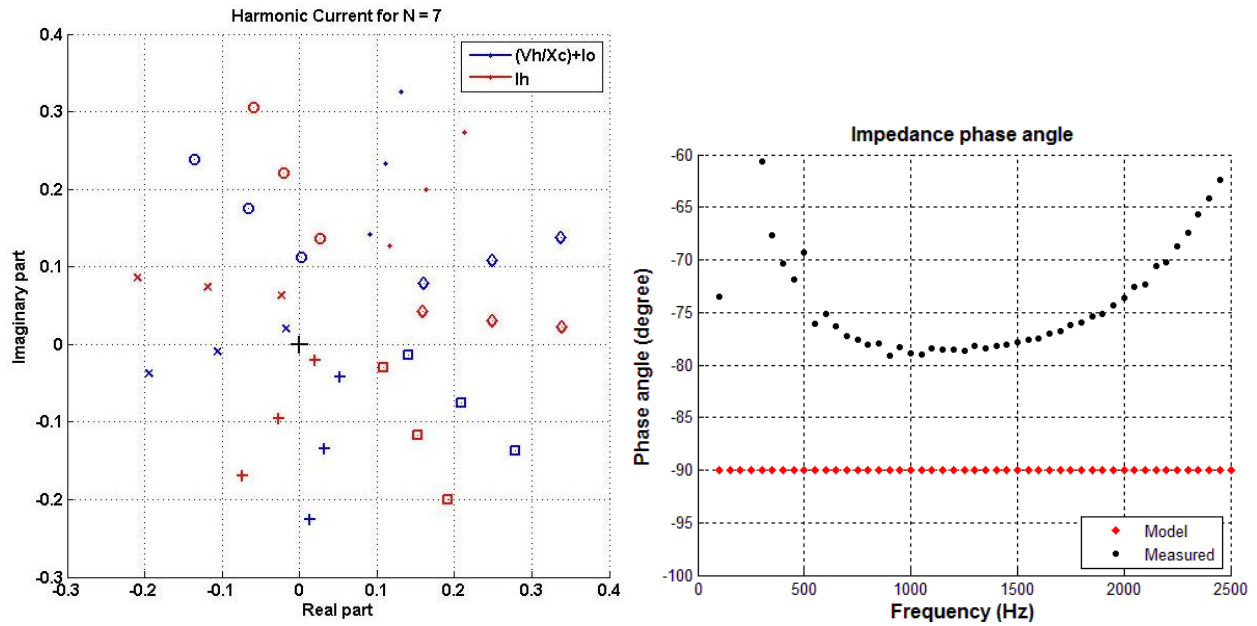
Figure 4-14 7th harmonic fingerprint of measured and model current with phase angle profile of measured data and model of Inverter3, there is about 20° phase angle difference
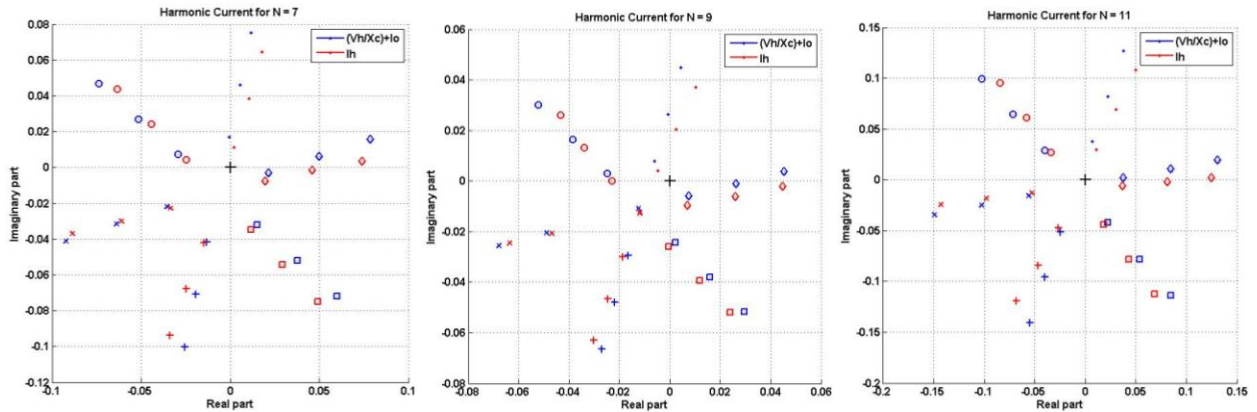
Figure 4-15 7th, 9th, and 11th harmonic fingerprint of measured and model current of Inverter1

Three-phase inverter and power router

Because the impedance profile of 3Φ inverter and power router are fitted with more complex models, the current discrepancies between measured and model current are much lower than those of 1Φ inverters, up to maximum 35%. For lower harmonics (up to 11th), the phase angle discrepancies are also much lower than those for 1Φ inverters. The phase angle profile of power router is shown in Figure 4-16. It is apparent that the phase angles of power router match better than that of 3Φ inverter thus the discrepancies between model and measured 5th harmonic current of 3Φ inverter are more noticeable than that of power router (see Figure 4-17).
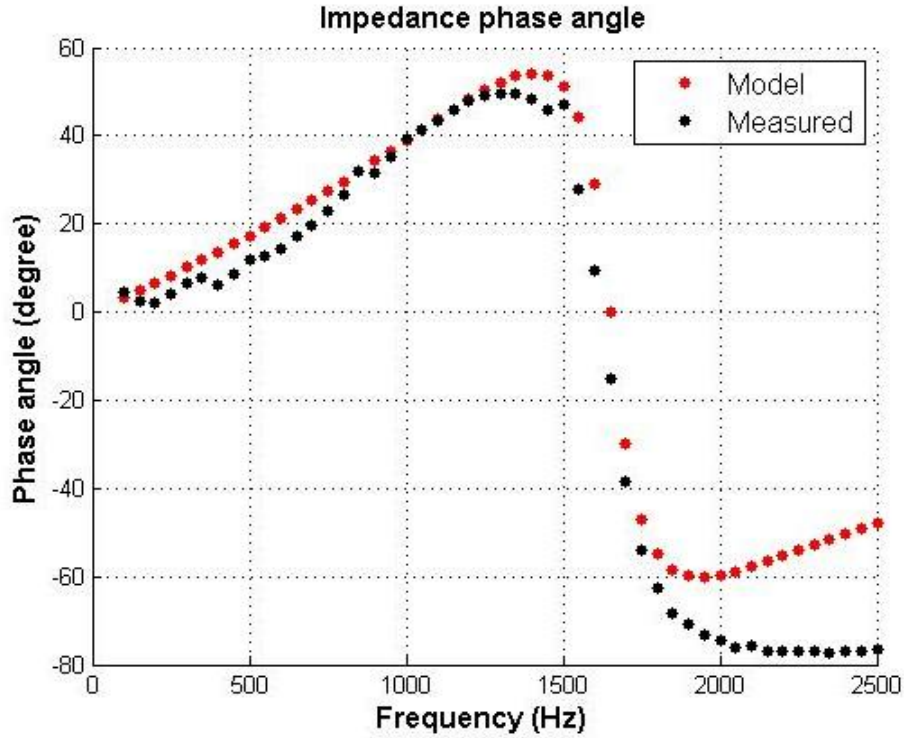
Figure 4-16 Power router model phase angle profiles compared to measured phase angle profiles
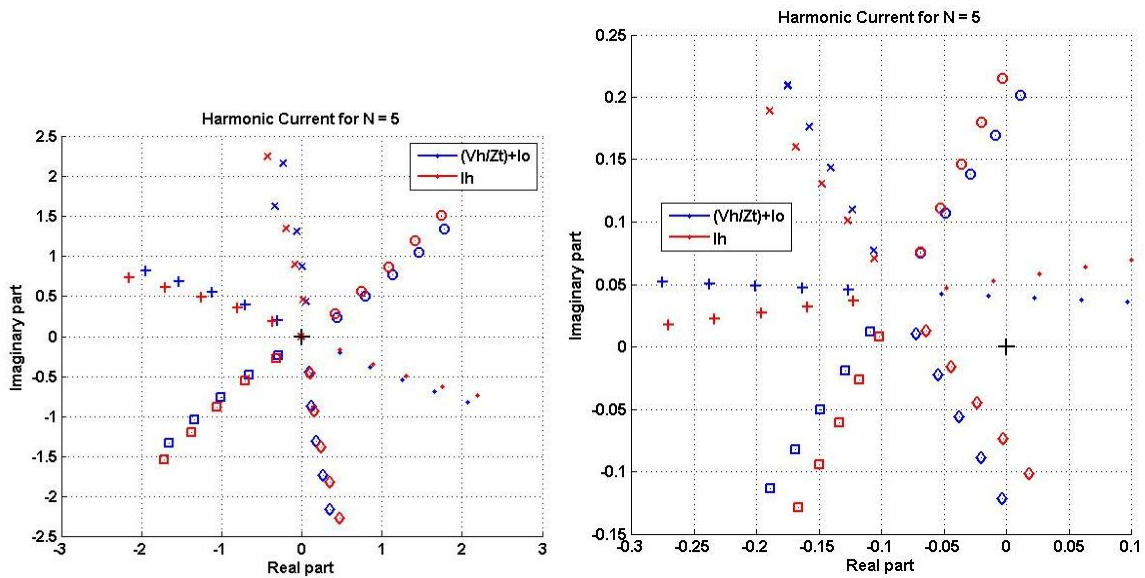
Figure 4-17 The 5th harmonic current fingerprint of measured and model current of power router and 3Φ inverter, respectively

4.2.2. Influence of output power on current discrepancies

It is known that the output power of PV inverter influences its efficiency and harmonic current emission which presents a question whether it also influences the reliability of the impedance measurement. It is

investigated by comparing the current discrepancies between measured current and model current at different output powers –both at 3rd and 5th harmonic because they are the most prominent harmonics.

The comparison is carried out for three single-phase inverters (0.6kWdc, 0.9kWdc, 1.2kWdc) and 3Φ inverter (0.9kWdc, 1.2kWdc, 2kWdc). The 1Φ inverters are fed from PV simulator which has maximum open-circuit voltage (V_{OC}) of 256V and short-circuit current (I_{SC}) of 4.74, hence, maximum input power for 1Φ inverters is 1200W. To compare the 3Φ inverter with the 1Φ inverters, it is also fed with 1200W. However, due to the differences in topology and efficiency, the output power generated differs from one inverter to the others. For some reason, during impedance measurement, although the nominal power of power router is 5000W, the protection system was triggered when the PV simulator is set at 1.2kWdc –which makes it only able to be measured at 0.65kWdc or 0.4kWac.

For the 3Φ inverter, the current discrepancies are not influenced by the inverter's output power. For Inverter1, the discrepancies are bigger at lower output power but in contrast the discrepancies are smaller at lower output power for Inverter2. For Inverter3, the 3rd harmonic discrepancies are smaller at lower output power while the 5th harmonic discrepancies are bigger at lower output power. Thus, a general conclusion that output power influences the consistency and quality of the impedance measurement cannot be drawn.

4.2.3. Cross-frequency (influence of 5th harmonic on 3rd and 7th harmonic)

A simple way to model the frequency response of non-linear load is proposed in [28] which can also be used for PV inverter's considering an inverter can be perceived as non-linear load with negative power flow. It represents the frequency response by a "crossed-frequency" admittance matrix which takes into account the harmonic current of order (k) produced by harmonic voltage of different order (j). In this case, the 3rd and 7th harmonic current produced by 5th harmonic voltage will be investigated.

Most prominent cross-frequency phenomenon is found at Inverter3 and 3Φ inverter, as shown in Figure 4-18 and 4-19, respectively. The 3rd and 7th harmonic currents produced by 5th harmonic voltage at 3Φ inverter are more linear at lower output power while those at Inverter3 are not influenced by the output power. On the other hand, no cross-frequency phenomenon is found at Inverter 2 and power router. While at Inverter1, this phenomenon occurs at low output power (0.4kWac) but not noticeable at higher output power (0.6kWac and 0.8kWac). Therefore, this phenomenon is not influential to the output impedance modelling and thus not incorporated in the models described earlier.
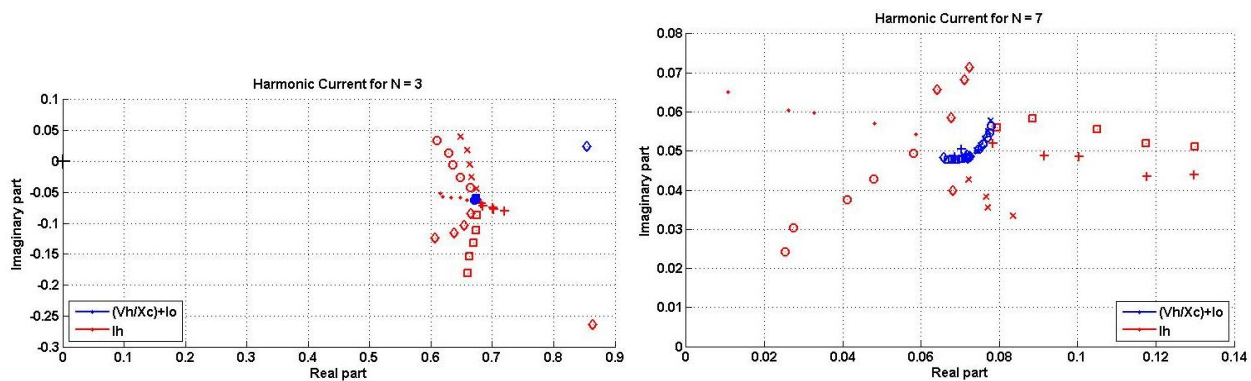
Figure 4-18 Inverter3's 3rd and 7th harmonic currents produced by 5th harmonic voltage at output power 0.8kWac
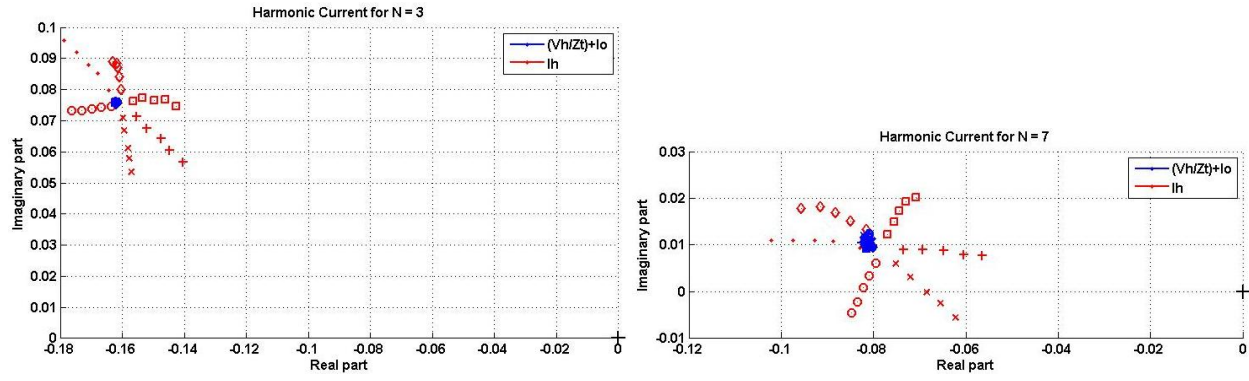
Figure 4-19 3Φ inverter's 3rd and 7th harmonic currents produced by 5th harmonic voltage at output power 0.8kWac

5.   Harmonic Current Model

As explained in Chapter 3, the PV inverter model that serves as basis for the models developed in this thesis for harmonic studies consists of a capacitance to represent the output capacitance of the inverter which might cause additional resonance in the grid and a harmonic current source(s) to represent the inverter's harmonic current emission to the grid without the influence of background harmonic voltage. A PV inverter is generally assumed to be a constant harmonic current source. In reality, however, the harmonic currents generated by a PV inverter depend on many factors such as irradiation levels, temperature, inverter's output power (part/full load), and background harmonic voltage in the grid. [7]

 Therefore, after the finalising the impedance circuit of the model, the next step is to measure the harmonic current emissions of the inverters under different conditions (in this case, at partial load, with and without background harmonic voltage). These measurements are actually conducted during the impedance measurement when the harmonic currents are measured at the connection point of the inverters at clean and distorted voltage source. Partial load operation analysis is done by measuring the harmonic current emission at different inverter's output power.

5.1.   Harmonic current at clean background voltage

At clean voltage supply, harmonics emitted by inverters arise from the switching harmonics. Its values are not determined by the voltage supply but by the input from solar cells, such as power (irradiation level), temperature, orientation of PV modules, type of PV modules, etc. These harmonic currents will be modelled with variable current sources. Due to the low-pass filter, the harmonic currents at higher frequency are small; small enough to be neglected. From the measurement, it is seen that frequencies with significant harmonic current are the 3rd, 5th, 7th and 9th harmonic. Thus, in the model, there will be four harmonic current sources for the four frequencies mentioned above. As an example, Figure 5-1 shows the 5th and 7th harmonic current emission of Inverter1 at clean background voltage, shown by the red '+' mark on the harmonic fingerprint –which are [-0.005,-0.024i] and [-0.006,-0.015i], respectively.
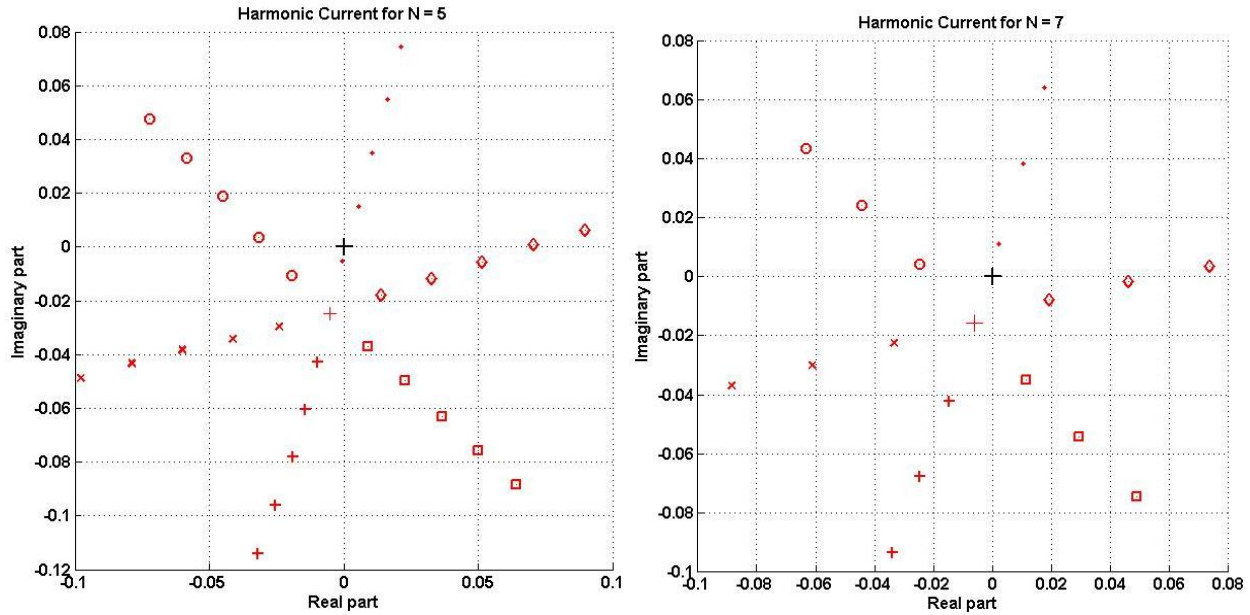
Figure 5-1 Harmonic fingerprints of Inverter1 for 5th and 7th harmonic showing the harmonic current with and without harmonic background voltage

5.2. Harmonic current at distorted background voltages

As previously explained, background harmonic voltage plays a role in escalating the harmonic current emission of PV inverters. With line-commutated inverters, grid's distorted voltage serves as the reference signal in output current control, hence the output current will have two causes of distortion: the switching harmonic and the harmonic presents in the grid. This is a phenomenon that can be prevented using internally generated reference signal. Almost all inverters used in the experiment are self-commutated except Inverter1.

The relationship between increase of harmonic in voltage supply and in current emission is linear and the ratio is the output impedance. Thus, the output impedance model is not only needed for predicting resonant frequency but also to model this effect. Harmonic current emission at polluted background voltage is actually already measured during impedance measurement.

5.3. Harmonic current at partial load

As solar irradiation is an intermittent quantity, a PV inverter is not always operating in its nominal power. Even with Maximum Power Point Tracker (MPPT) feature built in almost all PV inverters, there are more situations where a PV inverter delivers power below its rating than at full power. It is, therefore, important to analyse and understand a PV inverter's behaviour during partial load operation, including its harmonic current emission.

Obviously, when the DC power decreases, the converted AC power will also decrease and since power is the product of time and voltage, when the voltage is kept constant, the current decreases. Thus, it is logical to expect that the absolute harmonic current emitted by the inverter decreases at partial load. However, at partial load, the inverter control does not perform as accurately as at nominal power due to low measurement resolution. [1] This results in higher harmonic distortion at the output of the inverter.

41

During impedance measurement, all 1Φ inverters are individually measured with PV simulator at partial load due to PV simulator's limitation in maximum open-circuit voltage (V_{OC}) and short-circuit current (I_{SC}). Later on, however, the PV simulator is not used during measurement of aggregation of inverters due to equipment limitation and the 1Φ inverters are fed directly from DC power supply. Figure XX shows that the supplied power from PV simulator is smaller than from DC supply although the V_{OC} and I_{SC} are the same. In this chapter, the inverter harmonic current emissions are shown both for measurements using PV simulator and DC supply. Notice that those of DC supply are the ones that will be referred to later in the chapter of aggregation of inverters.
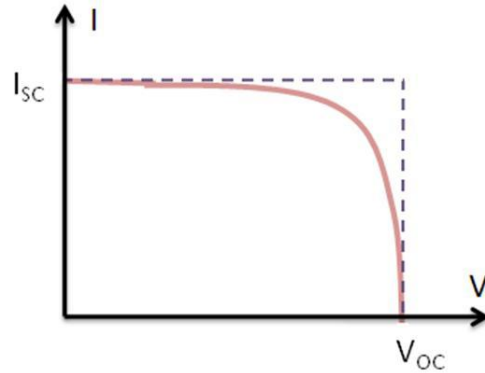
Figure 5-2 IV curve of solar cell as mimicked by PV simulator, the outer line shows the IV curve of DC supply

It can be observed from Figure 5-3 to Figure 5-7 below that some individual harmonic distortions decrease while others increase at partial load.
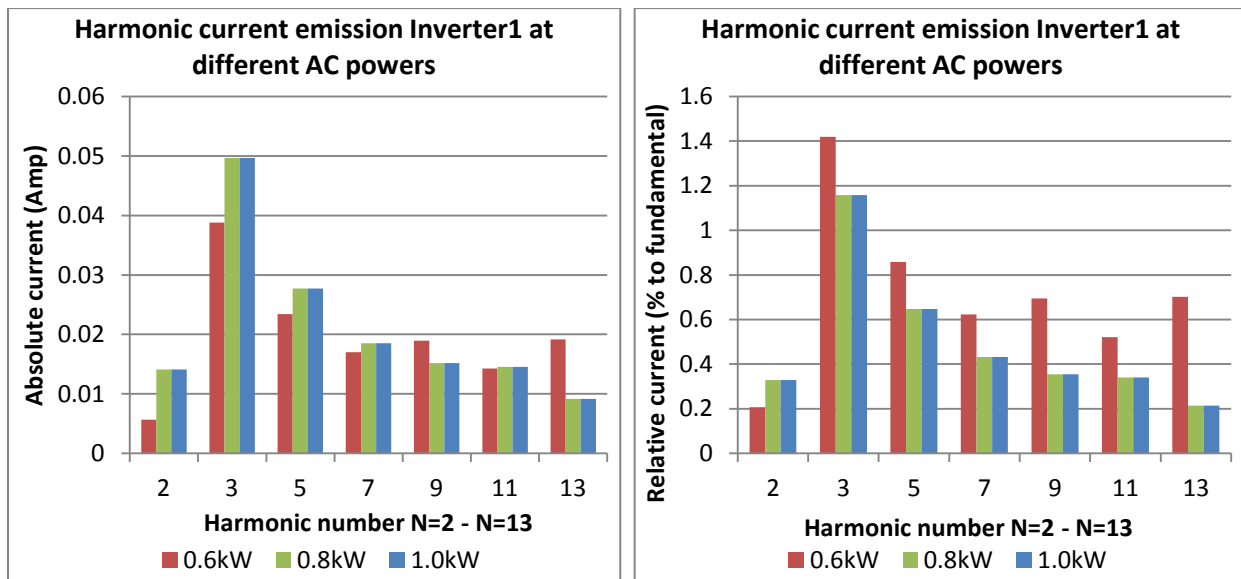
Figure 5-3 Harmonic current emission of Inverter1 at various AC output power, shown in absolute value (Amp) and relative to fundamental (%)
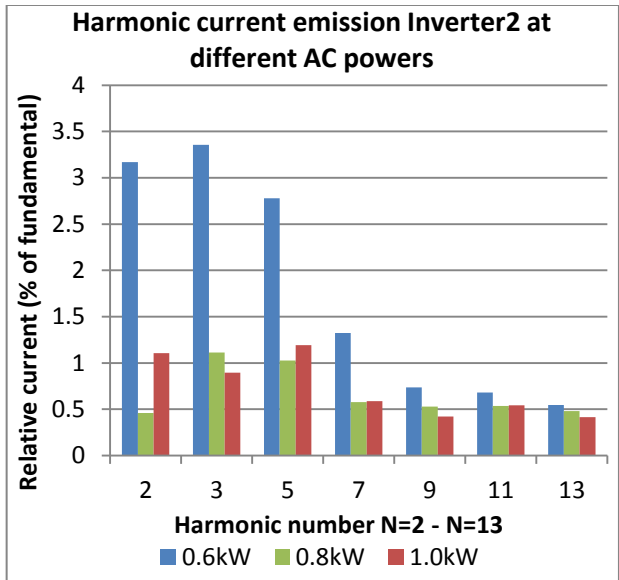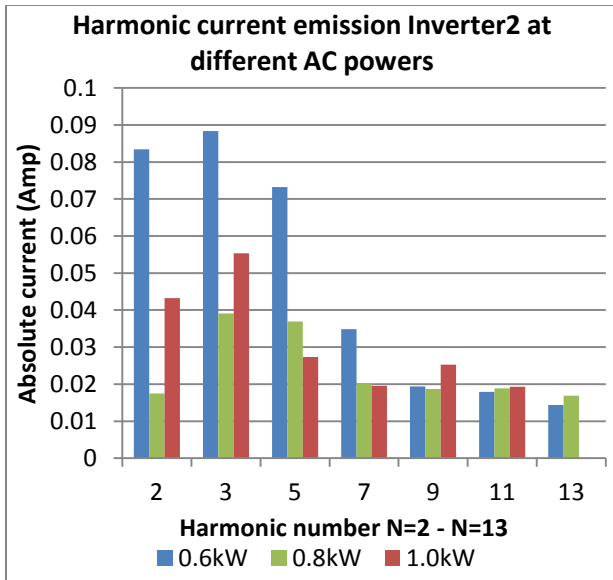
Figure 5-4 Harmonic current emission of Inverter2 at various AC output power, shown in absolute value (Amp) and relative to fundamental (%)
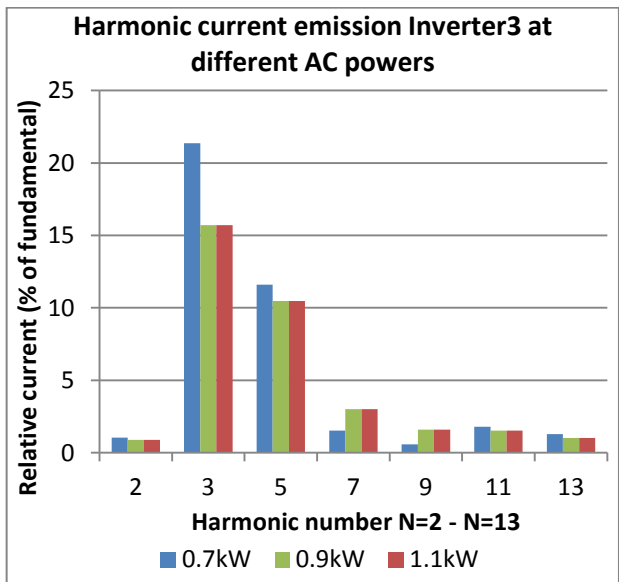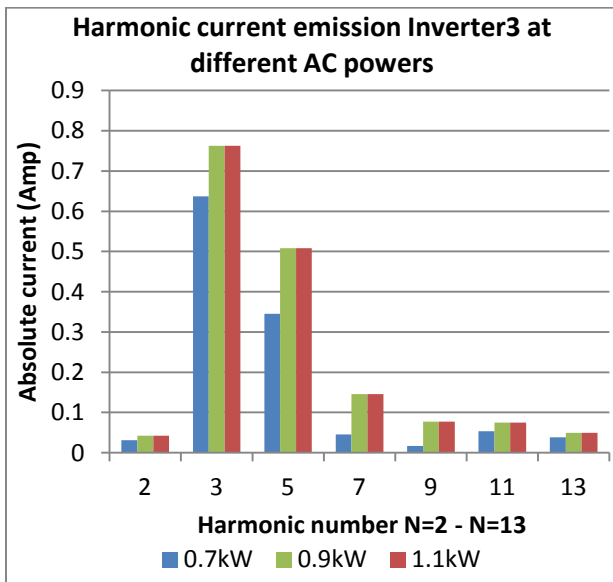
Figure 5-5 Harmonic current emission of Inverter3 at various AC output power, shown in absolute value (Amp) and relative to fundamental (%)
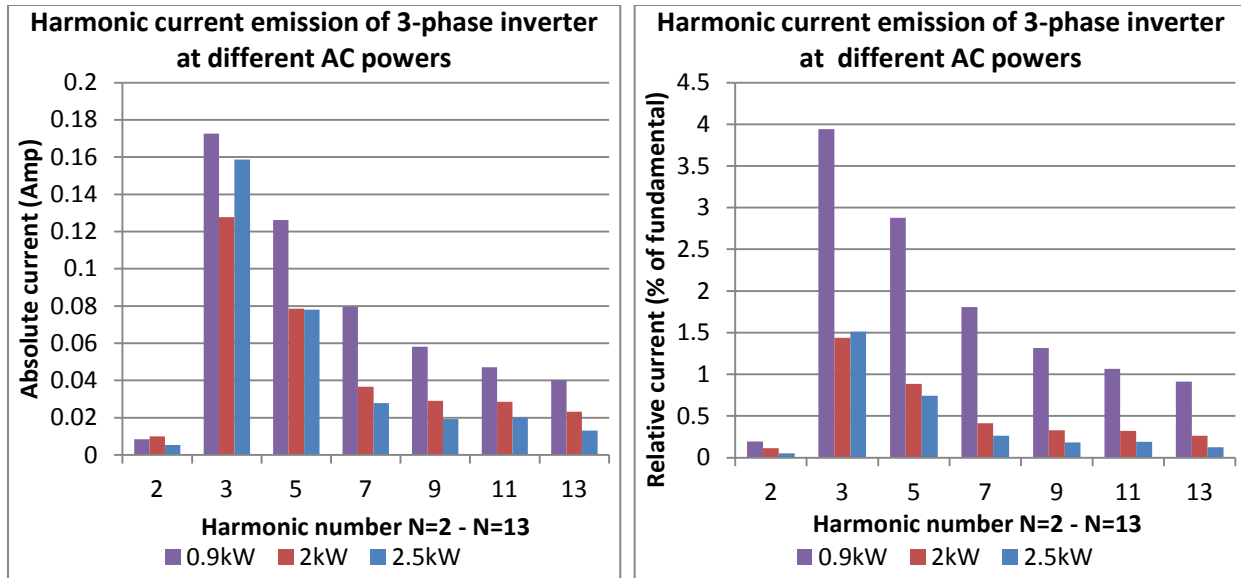
Figure 5-6 Harmonic current emission of 3Φ inverter at various AC output power, shown in absolute value (Amp) and relative to fundamental (%)
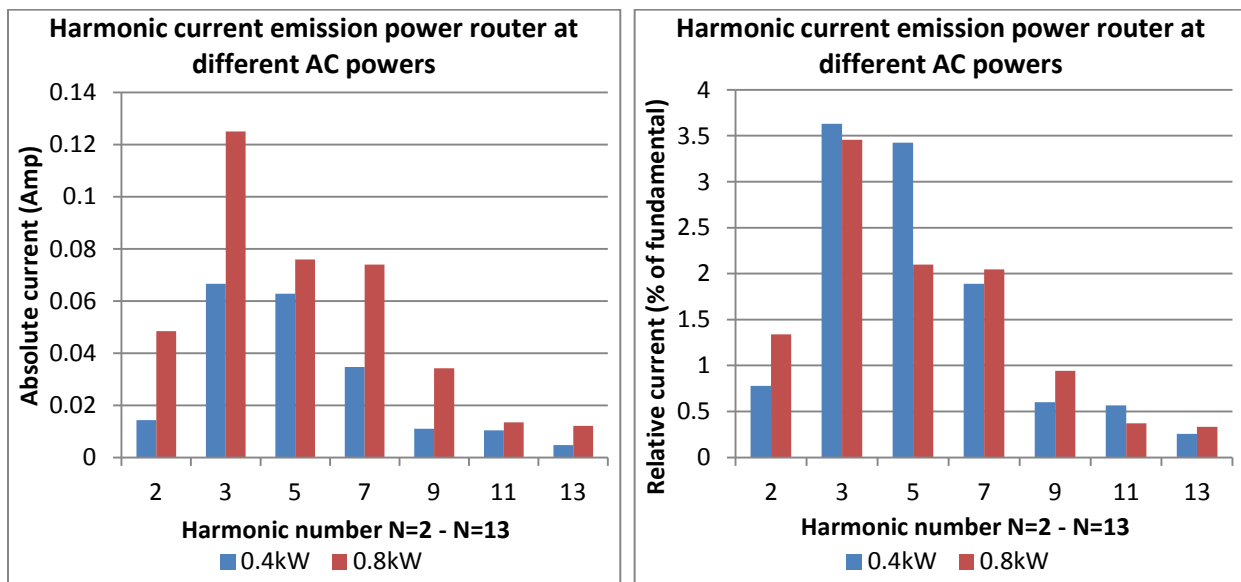
Figure 5-7 Harmonic current emission of power router at various AC output power, shown in absolute value (Amp) and relative to fundamental (%)

While generally the 2nd harmonic current is very small compared to other harmonics, it is almost as big as 5th harmonic current for Inverter3. Similarly, the harmonic current distribution between different harmonic orders is quite uniform for Inverter1; while for other inverters, higher harmonic orders have lower harmonic current emission. Furthermore, the year of production and sales of each inverter is also evident here. Inverter3 has very high current emissions which is not possible with current regulations because it was produced and sold before such regulations were made. Other inverters' harmonic currents are within the limit set by the regulations at their nominal power. However, at partial load,

Inverter1 maintains its harmonics within the limit specified for nominal conditions. The values of harmonic current magnitudes and phase angles emitted by all inverters are listed in Appendix B.

6. Voltage Dip Sensitivity Measurement

One of many aspects of power quality is voltage dip. Voltage dips are defined as sudden reduction in voltage to lower voltages for a short period of time, followed by recovery to the original voltage. They occur due to faults, motor starting, energizing of transformers, etc. A voltage drop is defined as voltage dip when the drop ranges from 1% to 90% of its nominal level and lasts for 10 milliseconds to 1 minute. [5] At 230V nominal level, the range is from 2.3V to 207V.
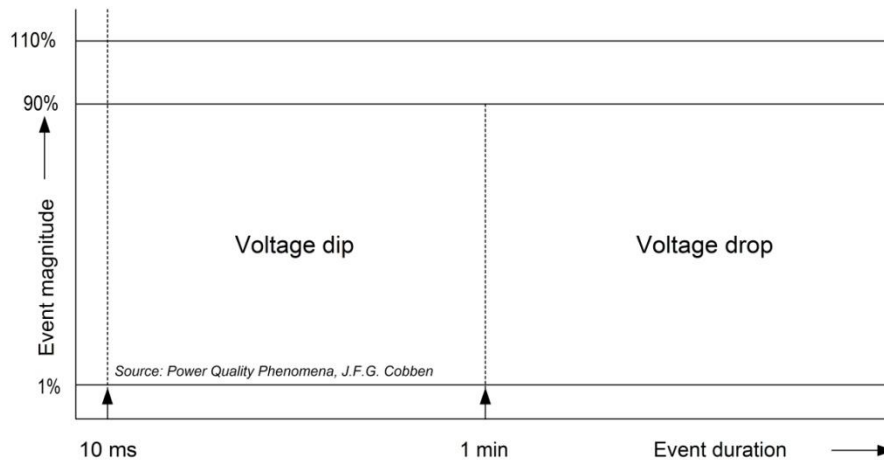
Figure 6-1 Voltage dip

One of the safety requirements of PV inverters concerns the anti-islanding protection which ensures that the inverters stop feeding power when the grid properties are not within the given range [29]. For example, in IEEE Std 929-2000, PV inverters are recommended to stop energizing the network whenever the voltage at PoC is not within 88% and 110% of its nominal voltage. This requirement varies from one country or standard to the other. German standard DIN/VDE 0126 requires inverters to disconnect from the grid within 0.2s when the voltage is not within 80% and 115% of its nominal voltage.

In voltage dip scenario, the actual behaviour of the PV inverters used in the experiment during voltage dip will be analyzed.

6.1. Inverter sensitivity to voltage dip

All tested inverters disconnect from the grid during voltage dip. However, the depth and duration of the dip required are different from one inverter to the other.

Figure 6-2 shows how sensitive each inverter is to voltage drop in the grid; duration of dip is only shown until 1s to highlight the diversity of the curves, especially between 10ms to 300ms. For the 3Φ inverters, sensitivity is measured towards 3 phase and 1 phase voltage dip (in this case phase A because the inverter feeds in to the grid via phase A). From the curve it is apparent that all inverters comply with the standards, UL 1741 (harmonized with IEEE 1547) and VDE 0126.
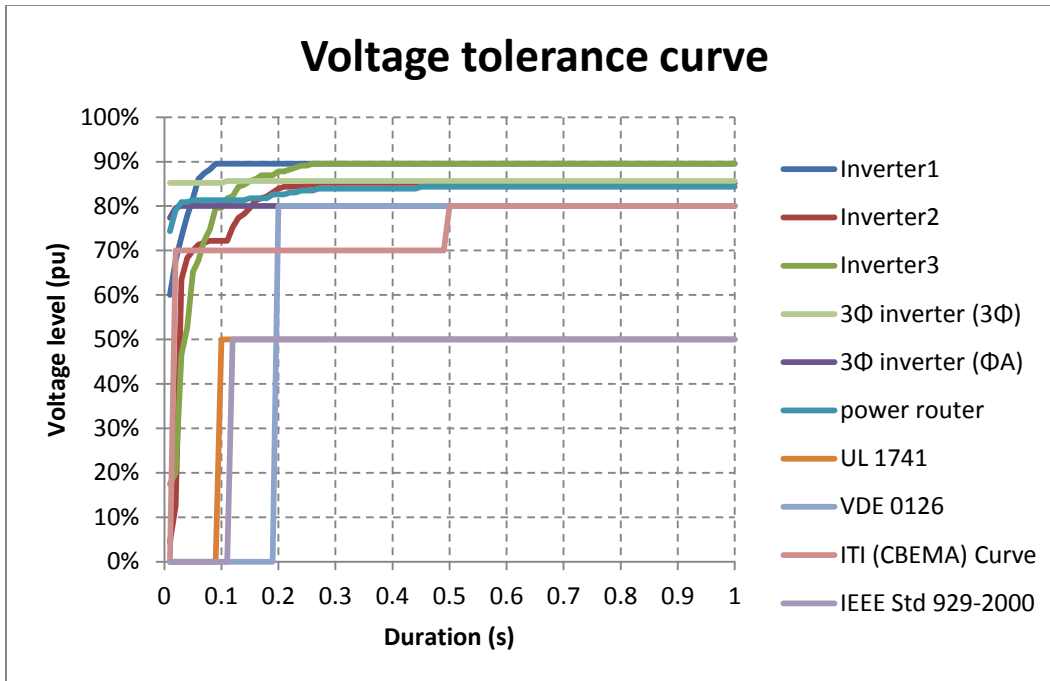
Figure 6-2 Voltage tolerance curve for all inverters, compared to several known requirements

The differences in disconnection time between one inverter and the others are determined by many factors. The first factor is the resolution of the inverter's measurement on the voltage level at PoC, i.e. how often and for how long the inverter measures the voltage level. The second factor is the amount of information needed by each inverter to decide whether a situation is a disturbance and it needs to disconnect. One inverter might decide to disconnect after first reading while others need more reading to be "sure" that a situation is indeed a disturbance. Lastly, each inverter needs a different amount of time from deciding to disconnect to actually disconnecting from the grid. This factor is determined by the speed of the microcontrollers inside the inverter.

6.2.   Regulations on voltage dip

The question is whether the regulations to disconnect PV inverters in case of grid disturbances is really necessary because distributed generation (DG) can actually increase the voltage level at PoC. Anti-islanding protection is designed to protect the utility system, loads, and DG units from safety and power quality problems that arise due to islanding scenario. For example, the DG units (in this case, PV systems) might drive the island to out-of-range voltage and frequency due to its inability to energize the island without the support of the grid. It can also pose utility workers to energized circuits that should be de-energized. [30] However, as power generated from DG units increases, disconnection of DG units on grid disturbances might cause power unbalance which in turn causes instability.

In order to increase power stability in combination with large penetration of DG, some grid operators require PV inverters to remain connected during a certain period of low/high voltage situation and inject (reactive) power to the network, known as Low Voltage Ride-Through (LVRT) or Fault Ride-Through (FRT). Figure 6-3 shows the Germany's Grid Code requirement for generating plants, including PV systems, connected to medium voltage network. In this standard, for voltage above Limit 1, inverters

must continue operation while for voltages between Limit 1 and Limit 2, inverters may disconnect in accordance with grid operator. Inverters may disconnect when the voltage is below Limit 2 or below 30% of nominal voltage. [31]
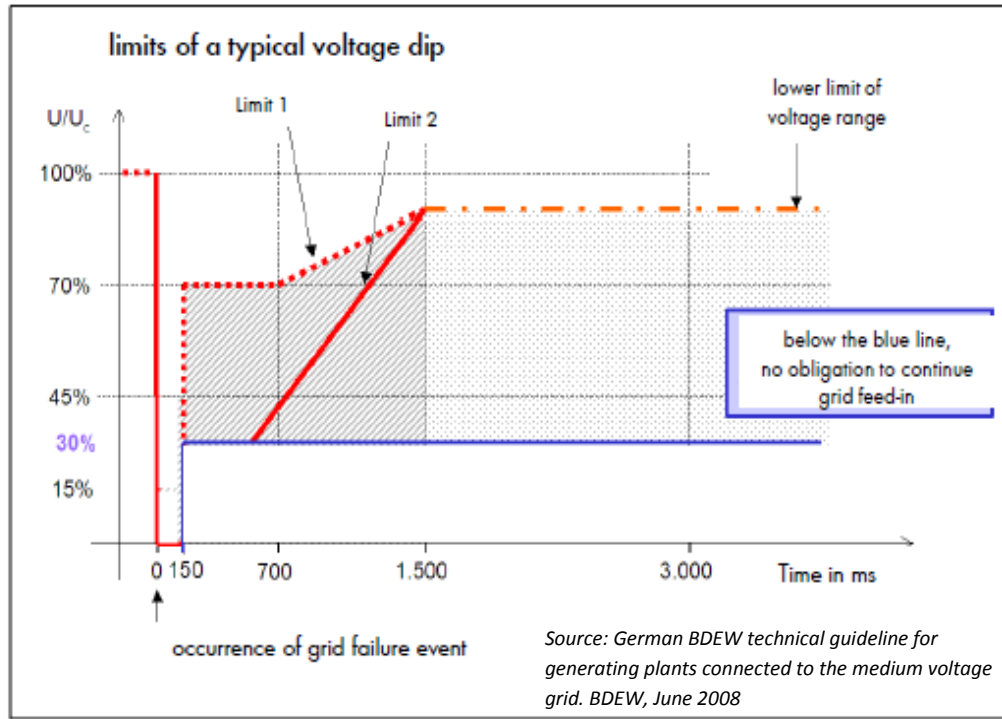
Figure 6-3 Voltage support that must be given by generating plants connected to medium voltage network

Many investigations have been carried-out to study the influence of LVRT on the grid itself. A study [32] reported that while in weak grid LVRT might prevent instabilities, in strong grid it is somewhat unrealistic and costly. Converter-connected DG (such as PV modules) has high influence in mitigating voltage dip in high voltage networks. However, its effect on low voltage network –which is where PV modules are mostly installed- is rather minimal. [33] However, PV inverter manufacturers are increasingly providing LVRT feature in their inverters, especially for countries whose national grid code requires LVRT.

In Figure 6-2, half of the inverter curves are above the ITI (CBEMA) curve –which describe an AC input voltage envelope which typically can be tolerated (no interruption in function) by most Information Technology equipment (ITE). When inverter's voltage immunity curve is above the ITIC curve, it means the inverter is more sensitive than most ITE. Every time an inverter ceases to feed power to the network, it brings less profit for the owner so it might not be desirable for the owner to have a too sensitive inverter.

Since all inverters switch off at grid disturbance, there will not be many things to observe from computer simulation and modelling of the inverters in voltage dip scenario. Thus, the models developed previously are only going to be used in harmonic scenario in Chapter 7.

7. Photovoltaic (PV) Inverter Model

After the output impedance and harmonic current emission of the PV inverters are measured, a complete model consisting of harmonic current sources and impedances can be built for each inverter. For the 1Φ inverters, the models are based on the measurement done on highest power to imitate their behaviour at their nominal power as close as possible. Similarly, the model for 3Φ inverter is based on the measurement at its rating. All complete models are shown in Appendix C.

7.1. General model

Admittedly, there are only five inverters tested in this experiment. This triggers a question about what the models of other PV inverters are like. Therefore, a general model is suggested in this chapter to represent not only the five inverters tested in this experiment but also other inverters commonly installed in the low voltage network. Single phase inverters usually have nominal power not more than 5000W because higher power will draw too much current in one-phase. To represent different power classes, the tested inverters are divided in two groups: 0-2kW and 2-5kW. The first group consists of three 1Φ inverters and the latter consists of 3Φ inverter and power router.

7.1.1. General impedance model

Looking at the similarity between the 1Φ inverters output impedances, a simple general model for 0-2kW power class can be deduced. It is a single capacitor with values ranging between 4.8-18.5µF. A single capacitor is chosen because two of the inverters are modelled adequately with a single capacitor and even though Inverter2 has a resistor in its model, its impedance profile shows a strong characteristic of a capacitor. Typical values of output capacitor of commercial 1-3kW PV inverters are between 0.5-10µF, as reported in [4]. A single capacitance value cannot represent every inverter but using several values from the range is adequate. Note that the 3Φ inverter in this experiment cannot be taken as a general case of 1Φ inverter in 1-3kW power class because although it feeds in via 1 phase, it still needs 3-phase connection.

(a)   (b)
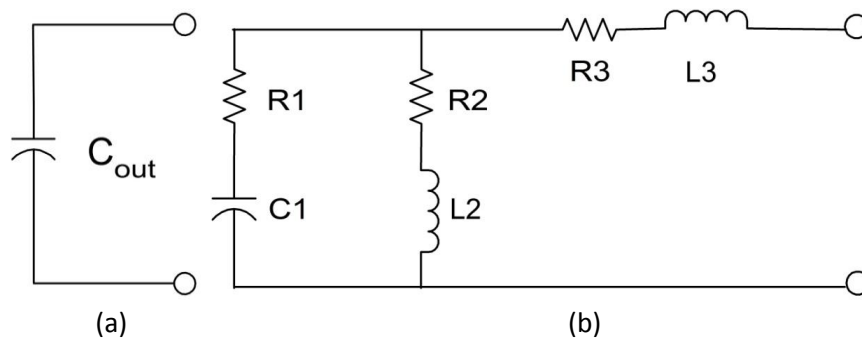
Figure 7-1 Simple model for 1Φ inverters in the class 0-2kW and more complex model for 1Φ inverters in the class 2-5kW

As for higher power class inverters, the model shown for the 3Φ inverter and power router can serve as a general representation of the output impedance. The parameter values will surely be different from

one inverter to the others and the exact parameter values can only be obtained from measurement. However, a look-up table of parameters for different power class (e.g. 2-3kW, 4-5kW) can be build which speaks for all inverters in that particular power class. If one wants to make a network simulation using this model, one can use the impedance circuit depicted in Figure 7-1b with parameters from the look-up table. An example of look-up table based on this experiment is shown below for two power class: 2-3kW and 4-5kW.

Table 1 Parameter values for general model of 1Φ inverters in the class 2-5kW

Nominal power	Parameter values					
	R1	C1	R2	L2	R3	L3
2-3kW	0.05 Ω	4.5 μF	45 Ω	4.5 mH	16 Ω	0.8 mH
4-5kW	0.1 Ω	20.5 μF	0.3 Ω	0.45 mH	5 Ω	0 mH

7.1.2. General current source model

It is difficult to make a general model of the harmonic current sources because harmonic current emission is a very dependent quantity. As mentioned in the background theory, it depends on many factors, such as operating power, solar irradiation, type of PV modules, type of inverter, and even manufacturer of the inverter. The second power class (2-5kW) has noticeably a big range, especially for a quantity as sensitive as harmonic current emission. Furthermore, this group is represented by power router which was not measured on its power rating due to its protection system and PV simulator limitation. Therefore, the harmonic current emission of power router cannot be used to represent this power class and hence only that of 3Φ inverter will be included in the look-up table.

As for 0-2kW class, Inverter3's harmonic currents are way higher than allowed by current standard. Assuming that most inverters installed to the grid nowadays follow the standard, involving Inverter's harmonic current will result in overestimation of harmonics. Therefore, the general current source model of this class is formed by averaging the harmonic current emission of Inverter1 and Inverter2. The phase angles are also the average of them.

Figure 7-2 shows the general harmonic current source model and Table 2 lists the parameter values of the 3rd harmonic current (I_3), 5th harmonic current (I_5), 7th harmonic current (I_7) and 9th harmonic current (I_9).
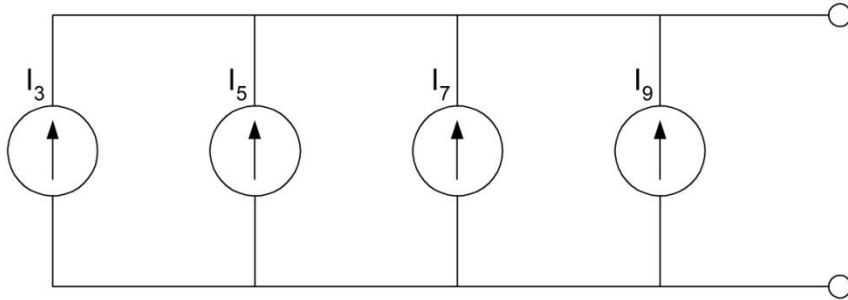
Figure 7-2 General harmonic current model

Table 2 Parameter values for general model of the class 0-2kW and 2-5kW

Harmonic order	General 0-2kW model		2kW model from a literature [33]		General 2-5kW model		IEEE Std 519-1992
	Absolute current at 0.9kW	Relative current to fundamental	Absolute current at 2kW	Relative current to fundamental	Absolute current at 2.5kW	Relative current to fundamental	Relative current to fundamental
3	0.04A	1.20%	0.25A	2.82%	0.16A	1.51%	4%
5	0.03A	0.88%	0.25A	2.82%	0.08A	0.74%	4%
7	0.02A	0.51%	0.12A	1.39%	0.03A	0.26%	4%
9	0.02A	0.51%	0.11A	1.22%	0.02A	0.18%	4%

It is obvious from Table 2 that the general current model parameters for 0-2kW class are far below the standard in term of relative current. Using very low values of harmonic current can lead to harmonic underestimation. There is another simulation with harmonic current modelling of commercial 2kW PV inverters whose values are closer to the standard. [34] It is shown here as comparison and alternative parameters.

7.2. Aggregated model

When simulating a network for power quality studies, it is desired that the simulation reflects the network's condition as close as possible to reality. In reality, there are many inverters connected to the grid, either in one phase or in different phases. This experiment investigates a possible model of aggregation of inverters connected in parallel in one phase to the grid. Both the impedance and current source models are investigated.

7.2.1. Aggregated impedance model

When multiple inverters are connected in parallel, the parallel capacitance value will be higher and it might yield a lower resonant frequency. To observe the consistency of each inverter's individual model, experiments with multiple inverters were carried out. These inverters are connected in parallel to the

voltage source and at PoC, harmonic voltages and currents are measured in the same way they were measured for individual measurements. In this chapter, the measurement results of aggregation of all 1Φ inverters and of all inverters are shown and discussed.
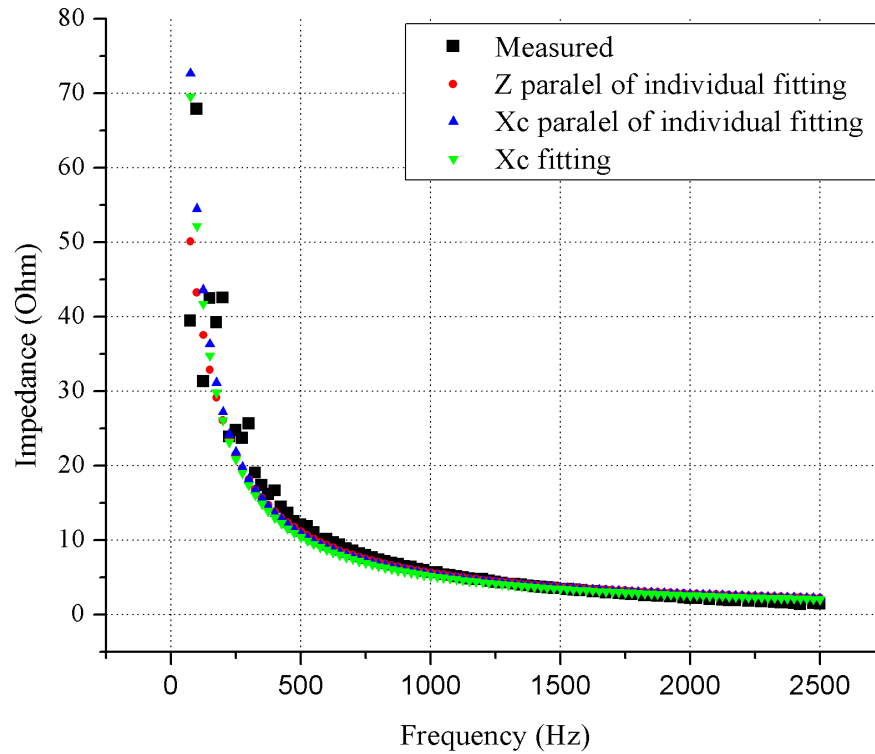
Figure 7-3 The impedance profile of an aggregation of three 1Φ inverters

Figure 7-3 shows harmonic and interharmonic impedances of aggregation of all 1Φ inverters. Also shown here is the resultant impedance from the inverter's individual impedances connected in parallel, calculated by Equation 13, where Z_P is the resultant impedance, $X_{C,1}$ is Inverter1's capacitive reactance, $Z_{S,2}$ is the series of resistor and capacitor of Inverter2, and $X_{C,3}$ is Inverter3's capacitive reactance. As with individual measurement of 1Φ inverters, a curve fitting was also applied to the impedance and the curve of a single capacitor fits the measurement curve the best (see Equation 10). The capacitance found from curve fitting is 30.5μF, which is close to the resultant capacitance of paralleled inverters 29.2μF (summation of 5.9μF, 4.8μF, and 18.5μF). The impedance profile from both capacitance values are shown in blue and green marker, respectively.

$$\frac{1}{Z_P} = \frac{1}{X_{C,1}} + \frac{1}{Z_{S,2}} + \frac{1}{X_{C,3}} \tag{13}$$

The influence of each individual inverter is also seen in the aggregated model. Figure 4-3 shows significant discrepancies between measured and model impedance of Inverter2, particularly at lower frequencies. It translates to discrepancies between measured and calculated impedance of the aggregated model at lower frequencies, only much less because the other two inverters damp this phenomenon.

Each inverter's discrepancies between its model and measurement combine and intensify with each other in an aggregation of multiple inverters. In the case of 1Φ inverters above, although the impedance profile of the model matches that of measurements, the impedance value at every frequency differs between one and the other. This phenomenon is also apparent for the aggregation of all inverters, including the 3Φ inverter and power router. Since both the 3Φ inverter and power router have a parallel resonance in the frequency range lower than 2500Hz, it is bound to happen that an aggregation of these inverters will also yield a parallel resonance and it is shown in the impedance profile of all inverters below.
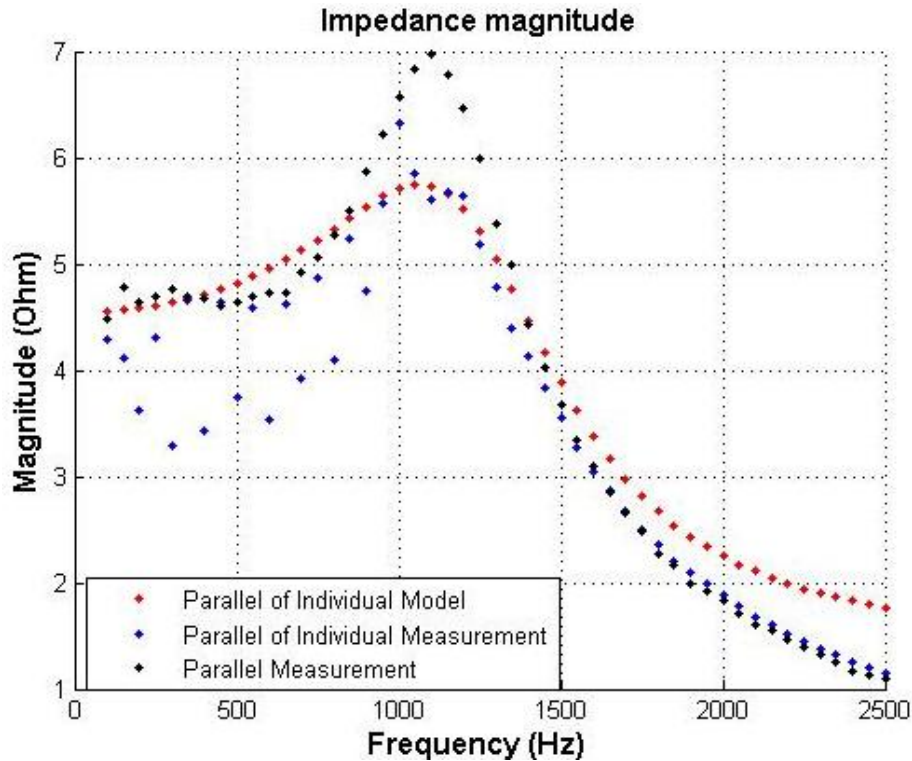
Figure 7-4 Impedance profile of the aggregation of all inverters

From the model and measurement results, it can be expected that when all these inverters are connected in parallel, there will be a parallel resonance at the 21st or 22nd harmonic. Although the expected value of the voltage or current might be different due to the different value of impedance, a network operator can already forecast this phenomenon and thus better prevent 21st harmonic current from flowing in the network. For comparison purpose, the measurement results of individual inverters are also summed using Equation 14 where Z_{IN1}, Z_{IN2}, Z_{IN3}, $Z_{3\Phi}$, and Z_{PR} are the measured impedances of Inverter1, Inverter2, Inverter3, the 3Φ inverter, and power router, respectively.

$$\frac{1}{Z_P} = \frac{1}{Z_{IN1}} + \frac{1}{Z_{IN2}} + \frac{1}{Z_{IN3}} + \frac{1}{Z_{3\Phi}} + \frac{1}{Z_{PR}} \qquad (14)$$

The impedance profile derived from this equation shows the characteristic of Inverter2 clearly (i.e. the curve oscillates at frequencies lower than 1000Hz) but the impedance profile of the model and measurement do not show this characteristic anymore. At higher frequencies, the discrepancy between

the model and measurement is obvious in both impedance magnitude and phase angle profiles. This happens because the models were built with more attention paid to fit lower frequencies than higher frequencies as lower harmonics occur more in the network. Figure 7-5 demonstrates how the phase angle of lower harmonics fit better then higher harmonics.
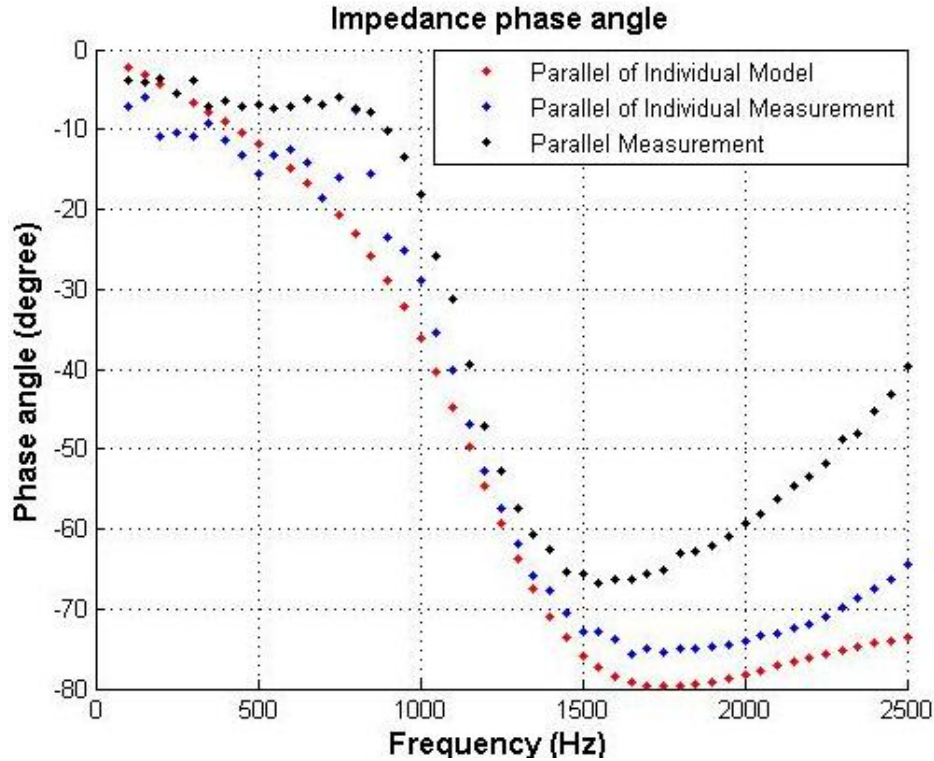
Figure 7-5 Impedance phase angle profile of the aggregation of all inverters

7.2.2. Aggregated current source model

When current sources are connected in parallel, according to Kirchoff's Law, the resultant current is the summation of individual currents. Nevertheless, when multiple inverters are connected to the grid, the harmonic interaction does not automatically result in higher current THD but it may also yield lower current THD. Lower THD is possible because the harmonic currents and voltages in the grid are phasor quantity which means they have magnitudes and phase angle. When two harmonic currents or voltages of the same frequency have the same magnitude and 180° apart, they cancel each other. Comparing Table B-1 and Table E-1 in the Appendix gives an idea how some harmonic currents of individual inverters add up in case of aggregated inverters and how other harmonic currents subtract each other. For example, the 5th harmonic current of Inverter3, $I_{3,Inv3}$ is 0.51A ∠-175.2° and that of Inverter1 $I_{3,Inv1}$ is 0.03A ∠69.4° and the resultant 5th harmonic current when the two inverters are connected in parallel is 0.49A ∠182.6°. Here, the aggregated current is smaller in amplitude than the individual Inverter3's current.

7.3. Implementation of Models

The purpose of modelling PV inverters is to be able to observe its behaviours in a network and its possible implications on the network's power quality and one way to study it is by a simulation of a network containing PV inverters. This chapter shows and discusses the implementation of PV inverter models developed in previous chapters in a harmonic study. Only harmonic study is conducted because all inverters disconnect during voltage dip thus a simulation with voltage dip scenario will not give much remarkable information.

This harmonic study observes how the harmonic currents and impedances from the inverters interact with the grid and with each other. The simulation is carried-out with the aid of two graphical simulation programs: Simulink® and DIgSILENT PowerFactory. For each simulation program, the inverters are modelled individually and later on, multiple (and all) inverters are connected in parallel to the grid. The complete models for all inverters are shown in Appendix C.

It is desirable that the models developed in Chapter 4 and 5 represent the real situation as much as possible. In Chapter 4, the validity of the individual impedance models is tested by comparing the models with the measurement. In this simulation, the validity of the harmonic current models and their combination with the impedance models are observed.

PowerFactory is one of the major network modelling programs widely used by network operators thus it is a natural choice to simulate the PV inverters. However, due to its nature of modelling generation-, transmission-, distribution- and industrial grids, it is not very convenient to model the measurements performed in a laboratory. For example, the single phase inverters are modelled as a balanced three-phase system in PowerFactory. Simulink is chosen as an alternative simulation because it is relatively convenient for detailed, single-phase, low voltage simulation –which is also the reason why the individual models are built with Simulink.

7.3.1. Network modelling

Since this harmonic study is intended for assessing the validity of the model, both the simulation and measurement do not include loads or other network components like transformers than the grid and the cables connecting the inverters with the grid. The measurement itself is carried out in the Power Quality Lab with a big busbar and a short distance from the source to the inverters thus the grid's impedance is modelled with a very low resistance of 1mΩ. The cables connecting the inverters with the grid to PoC are also very small (since the currents are also very small) hence their resistance and reactance are negligible. In Simulink, the cables are not represented at all but the grid impedance is set at 3mΩ to include the cable's resistance while in PowerFactory they are represented by cables with a very low resistance and short length.

7.3.2. Grid modelling

The programmable voltage source is modelled in Simulink as an AC voltage source with only fundamental component of 230Vrms and 0° phase angle. In PowerFactory, it is represented with a grid, as a slack bus of voltage 1 pu and phase angle 0°. Since the source's resistance is assumed to be 1mΩ, the short-circuit capacity of the grid in Power Factory is set to be 160MVA.

7.3.3. Inverter current modelling

In PowerFactory, harmonic current sources can be modelled with current sources or general loads. General load is chosen in this simulation to represent the currents generated by PV inverters because of its versatility.

In Simulink, the fundamental current measured at PoC is modelled with a fundamental current source to represent the fundamental current injected by the inverter. This method is fairly valid because the inverter's impedance is much bigger than the grid's impedance. This is not possible, however, for the power router because its impedance is rather low at low harmonics and it is modelled with a series resistance of 5Ω. With this resistance, the grid's fundamental voltage of 230V yields a rather big current of around 46A, contrary to the measured fundamental current of 4A. Note that the harmonic impedances are only measured at harmonic frequencies with small harmonic voltages (maximum 5% of fundamental) thus it is possible to have small harmonic impedance.

This creates a problem to model the output impedance of the inverters; additional impedance will make up for the big fundamental current but it will also influence the harmonic currents. It is also not possible to eliminate the grid fundamental voltage because in reality, PV inverters cannot operate without being connected to the grid. Since all measurements are done at PoC, more attention will be given to the model the current and voltage at PoC. This means adjustments in the internal model of the inverters and in this simulation, the fundamental current of the inverter is chosen in a way as to reduce the current from the grid to fit the measured current. The consequence of this method is that the simulation does not represent the actual power produced by the power router.

7.3.4. Inverter impedance modelling

The models built in Simulink are already presented in Chapter 3. In PowerFactory, the elements of capacitor, inductor, and resistor are integrated in blocks of shunt/filter and series reactor/capacitor. When the correct parameters are entered, however, these blocks behave similarly to the simulation in Simulink.

7.3.5. Simulation result

Before the simulations with multiple inverters are conducted, each inverter's model in PowerFactory is first measured up to the measurement result. Afterwards, several combinations of inverters are connected in parallel to the grid and the simulation measures the harmonic voltage and current as well as the impedance-frequency characteristic at PoC. The same schemes are set at the laboratory and the same harmonic voltage and current measurements are conducted. Figure C-1 and C-2 depict the simulation scheme in Simulink and PowerFactory, respectively. The harmonic currents from the aggregation of inverters are compared in absolute and relative magnitude with phase angles. Unfortunately, the harmonic analysis in PowerFactory does not show the phase angle of each current component thus the comparison for phase angle is only done between Simulink and measurement. In Figure 7-6 and 7-7, the absolute magnitude and phase angle of the aggregated harmonic currents from phasor summation, laboratory measurements and Simulink simulations are shown. It is apparent that

although the phase angles differ from one another, the magnitudes are in good agreement (including the magnitudes resulting from PowerFactory simulation). Full comparison is shown in Table E-1.
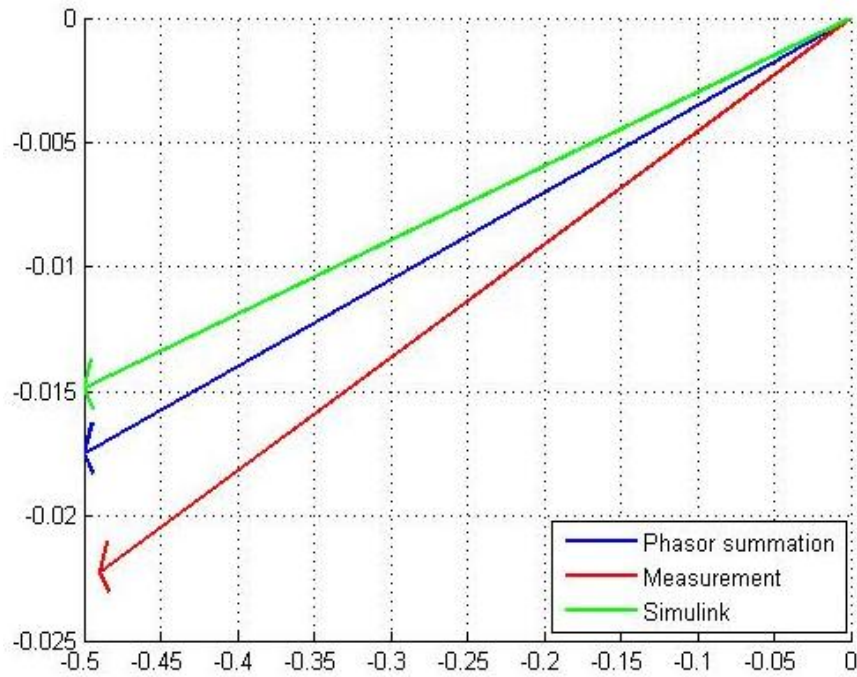
Figure 7-6 Comparison of aggregated 5th harmonic current from Inverter1 and Inverter3
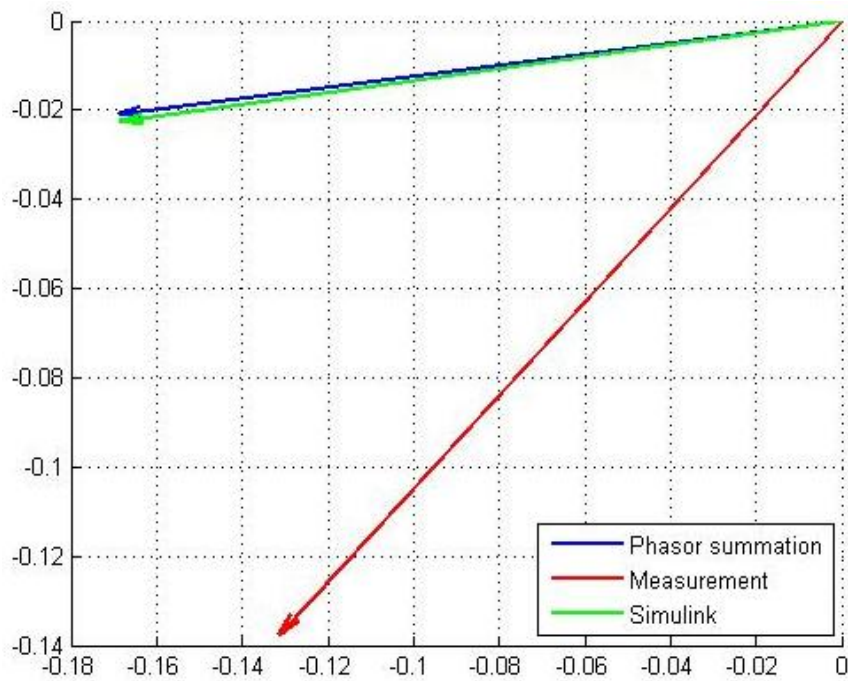
Figure 7-7 Comparison of aggregated 7th harmonic current from all inverters

The differences come from many factors. First, the harmonic impedances are modelled with the approach of mimicking the magnitude-frequency characteristic. As a result, there are discrepancies on the impedance phase angle, most prominently for the 3Φ inverter. Some of the harmonic currents from the current sources flow to these impedances and some to the grid. Therefore, the harmonic current measured at the PoC is not (always) the total of harmonic currents produced by the current sources. The amount of current flowing to the inverter impedances or to the grid is also determined by the grid impedance itself. It is assumed that the grid impedance is very low but in reality, there are many things connected to the grid, for example the wattmeter, which also provide additional impedances and draw current. Furthermore, the individual models themselves already have some discrepancies with the measurements and these discrepancies combine and intensify in an aggregation of multiple models.

8. Conclusions and recommendations

From all the measurements and analysis explained in this thesis, several conclusions can be deducted from this study and based on the results and issues faced in this study, some recommendations are given below for future research.

8.1. Conclusions

In this thesis, several models to represent commercial single-phase grid-connected PV inverters in power quality studies has been developed and verified with laboratory experiments and computer simulation. The models are developed from voltage and current measurements at the output of the inverter. Measurements are done on harmonic and interharmonic frequencies –the latter is to estimate the influence of inverters harmonic suppression. Out of the measured voltages and currents, impedances are calculated for every frequency to create impedance-frequency characteristic from which elements like capacitor, resistor, and inductor are chosen and put together to model the output impedance of the inverters. From the same measurements, harmonic current emissions of the inverters are also modelled with harmonic current sources.

This study is intended to model single-phase inverters and four single-phase inverters with different nominal powers are employed. One three-phase inverter is also involved because it feeds in to the grid with one phase thus it behaves, concerning harmonics, like a single-phase inverter. The model built for each inverter is verified by utilizing it in a simulation and comparing the simulation results with measurement results, both individually and as an aggregation of multiple inverters. Out of individual models, a general model is also developed to represent inverters of other power classes.

The first thing that can be concluded from this experiment is the measurements on harmonic and interharmonic frequencies are in good agreement. This is evident especially at higher harmonics. At lower harmonic measurements of Inverter2, the even-harmonic suppression is prominent as it causes the even-harmonic current behaviour to be highly non-linear. It can be seen from the non-linearity of even harmonics in the impedance profile of Inverter2 that translates to the impedance profile of multiple single-phase inverters. At higher harmonics, the suppression from inverter's harmonics is not apparent because they are so small, even smaller than the injected harmonics. A problem with interharmonic frequencies is encountered when measuring power router because it caused internal frequency error.

From the impedance-frequency plot, the models represent the inverters characteristic satisfactorily at most of the frequency range observed. The discrepancies come from several assumptions made before the measurement. First, the line impedance is zero; this is not completely true although it is indeed really small. Second, there are two harmonic sources (voltage source and inverter current). Theoretically, this problem can be solved using the superposition theorem by eliminating one harmonic source each time but it is not applicable because it is not possible to operate the inverter without its harmonic current source. Moreover, the priority when choosing the elements, their parameters and their configuration is to match the magnitude of the impedance profile rather than the phase angle.

The discrepancies in phase angle yield small disagreements in the simulation of individual models compared to measurement results. These small disagreements intensify when multiple inverter models are combined to represent a case of aggregation of inverters. Fortunately, the discrepancies are still within reasonable limit and thus the models are verified through the simulations.

Thirdly, during voltage dip measurement, all inverters disconnect during voltage dip. It means they follow the safety requirements of current standards but it also means their contribution to the network's stability under low voltage condition is zero. One way to model these inverters in a short-circuit study is as an open circuit to represent their lack of contribution at grid disturbance.

Another thing evident from this study is that while harmonic current emission is dependent on the output power of the inverter, there is no correlation between harmonic output impedances and partial generation of the inverter. The power rating of the inverter, however, does determine the output impedances as bigger power needs bigger output capacitor.

Lastly, a model of aggregated inverters is possible to build by simply calculate the resultant impedance of paralleled output impedances of each inverter as shown in Equation 13 or 14. As proven by the simulation and measurement, this calculation is sufficient to create the model for aggregation of inverters.

8.2. Recommendations for future work

8.2.1. Modelling of other power classes

With five inverters employed in this study, the models presented relatively represent various commercially available PV inverters. However, three of them have similar power rating and the other two inverters are unique cases (a power router and a three-phase inverter) thus they do not represent every power class of available PV inverters in the market. It is interesting, therefore, to conduct this experiment with other power classes (that have not been measured here) in order to have a look-up table of models for different power classes that can be generally used by anyone wishing to simulate an electrical network involving PV inverters.

8.2.2. Modelling of more recent inverters

During harmonic current measurement, it is noticeable that the harmonic current emission of Inverter3 is really high, much higher than allowed by current standard IEEE Std 519-1992. Its output capacitance is also the highest among the three single-phase inverters. This is possible because this inverter is the one of the oldest inverters in the laboratory. It is desirable to study and model more recent inverters as they are more likely to be found in the network nowadays then the modelling can be more applicable to the recent situation.

For voltage dip study, a case study utilizing the models is not performed because all inverters disconnect immediately during voltage dip. Recent inverters are designed to stay connected for a specified period upon disturbance on the grid to inject reactive power to increase the voltage level at PoC. It would be useful l to measure the behaviour of these inverters during grid disturbance and to model that behaviour in order to study PV inverters contribution in a short-circuit study.

8.2.3. Modelling with PV emulator

As described in Chapter 5, due to the limitation in the amount of PV emulator available in the laboratory, only power router is supplied with a PV emulator during the measurement of multiple inverters while the others are fed directly from DC sources. The power supplied by DC sources is obviously different from that of PV emulator thus it will be better if all inverters can be fed from PV emulator during the measurements. Then, a more realistic measurement taking into account the actual generation of PV cells including their dependency on temperature, cloud cover, inclination, etc can be performed.

8.2.4. Implementation of the model in a real case study

The models developed in this study are implemented in a network simulation that is validated with an experiment in the laboratory. This simulation, however, does not reflect the actual present and expected future penetration of PV inverters in the network because it is not possible to create that situation in the laboratory. It is interesting to implement the models in a bigger network simulation and verify the result with measurement on site. Measurements of the inverters actually present on site and a thorough modelling of the network are required in order to do this.

Bibliography

[1] D. G. Infield, P. Onions, A. D. Simmons and G. A. Smith, "Power Quality From Multiple Grid-Connected Single-Phase Inverters," *IEEE Transactions on Power Delivery,* vol. 19, no. 4, pp. 1983 - 1989, 2004.

[2] J. H. R. Enslin and P. J. M. Heskes, "Harmonic Interaction Between a Large Number of Distributed Power Inverters and the Distribution Network," *IEEE Transactions on Power Electronics,* vol. 19, no. 6, pp. 1586 - 1593, 2004.

[3] F. Wang, J. L. Duarte and M. A. M. Hendrix, "Analysis of Harmonic Interactions Between DG Inverters and Polluted Grids," in *IEEE International Energy Conference*, Manama, 2010.

[4] P. J. M. Heskes and J. H. R. Enslin, "Power Quality Behaviour of Different Photovoltaic Inverter Topologies," in *PCIM-2003 24th International Conference* , Nürnberg, 2003.

[5] J. F. G. Cobben, Power Quality: Implications at the Point of Connection, Eindhoven: Technische Universiteit Eindhoven, 2007.

[6] D. Cyganski, J. A. Orr, A. K. Chakravorti, A. E. Emanuel, E. M. Gulachenski, C. E. Root and R. C. Bellemare, "Current and Voltage Harmonic Measurements and Modelling at the Gardner Photovoltaic Project," *IEEE Transactions on Power Delivery,* vol. 4, no. 1, pp. 800 - 809, 1989.

[7] E. Vasanasong and E. D. Spooner, "The Prediction of Net Harmonic Current Produced by Large Numbers of Residential PV Inverters: Sydney Olympic Village Case Study," in *International Conference on Harmonics and Quality of Power*, 2000.

[8] E. Demirok, D. Sera, R. Teodorescu, P. Rodriguez and U. Borup, "Clustered PV inverters in LV networks: An overview of impacts and comparison of voltage control strategies," in *IEEE Electrical Power & Energy Conference (EPEC)*, Montreal, 2009.

[9] N. Jayasekara and P. Wolfs, "Analysis of power quality impact of high penetration PV in residential feeders," in *20th Australasian Universities Power Engineering Conference (AUPEC)*, Christchurch, 2010.

[10] B. Kroposki, "Distribution System Models - Power System Studies and Modeling PV Inverters," in *Utility/Lab Workshop on PV Technology and Systems*, Tempe, 2010.

[11] G. C. Pyo, H. W. Kang and S. I. Moon, "A new operation method for grid-connected PV system considering voltage regulation in distribution system," in *IEEE Power and Energy Society General*

Meeting - Conversion and Delivery of Electrical Energy in the 21st Century, 2008.

[12] A. Ellis, "PV System Models for System Planning and Interconnection Studies," Sandia National Laboratories, Cedar Rapids, 2009.

[13] A. Ellis, "Simulating PV Systems in Transmission and Distribution Planning," *IEEE Power and Energy Magazine,* Vols. 1540-7977, no. 11, pp. 55-61, 2011.

[14] D. Turcotte and F. Katiraei, "Fault Contribution of Grid-Connected Inverters," in *IEEE Electrical Power Conference*, Montreal, 2009.

[15] I. J. Gabe, F. F. Kunzel Palha and H. Pinheiro, "Grid connected voltage source inverter control during voltage dips," pp. 4571-4576, 2009.

[16] I. J. Gabe and H. Pinheiro, "Impact of Unbalance Voltage Dips on the Behavior of Voltage Source Inverters," in *Brasilian Power Electronics Congress COBEP-09*, 2009.

[17] J. L. Agorreta, M. Borrega, J. Lopez and L. Marroyo, "Modeling and Control of N-Paralleled Grid-Connected Inverters With LCL Filter Coupled Due to Grid Impedance in PV Plants," *IEEE Transactions on Power Electronics,* vol. 26, no. 3, pp. 770 - 785, 2011.

[18] Y. Li, P. Jing, Y. Luo, B. Zhang, C. Mao and X. Ruan, "A Study on Dynamic Power Flow Caused by the Grid-Connected PV Systems," in *2nd IEEE International Symposium on Power Electronics for Distributed Generation Systems*, Hefei, 2010.

[19] C. Limsakul, A. Sangswang, D. Chenvidhya, M. Seapan, B. Meunpinij, N. Chayavanich and C. Jivacate, "An Impedance Model of a PV Grid-Connected System," in *33rd IEEE Photovoltaic Specialists Conference*, San Diego, 2008.

[20] P. J. M. Heskes, P. M. Rooij, J. F. G. Cobben and H. E. Oldenkamp, "Estimation of the potential to pollute electricity network with harmonics due to the use of small micro generators with inverters - Measurement of the Complex Conductance, an additional test method for inverters," Energieonderzoek Centrum Nederland (ECN), Petten, 2004.

[21] L. Asiminoaei, R. Teodorescu, F. Blaabjerg and U. Borup, "A new method of on-line grid impedance estimation for PV inverter," in *Nineteenth Annual IEEE Applied Power Electronics Conference and Exposition*, Anaheim, 2004.

[22] M. B. Harris, A. W. Kelley, J. P. Rhode and M. E. Baran, "Instrumentation for measurement of line impedance," in *Ninth Annual Applied Power Electronics Conference and Exposition*, Orlando, 1994.

[23] A. de Oliveira, J. C. de Oliveira and J. W. Resende, "Practical Approach for AC System Harmonic Impedance Measurements," *IEEE Transactions on Power Delivery,* vol. 6, no. 4, pp. 1721 - 1726, 1991.

[24] J. P. Rhode, A. W. Kelley and M. E. Baran, "Complete Characterization of Utilization-Voltage Power System Impedance Using Wideband Measurement," *IEEE Transactions on Industry Applications,* vol. 33, no. 6, pp. 1472 - 1479, 1997.

[25] M. Ciobotaru, R. Teodorescu and F. Blaabjerg, "On-line grid impedance estimation based on harmonic injection for grid-connected PV inverter," in *IEEE International Symposium on Industrial Electronics*, Vigo, 2007.

[26] M. Sumner, B. Palethorpe, D. W. P. Thomas, P. Zanchetta and M. C. di Piazza, "A Technique for Power Supply Harmonic Impedance Estimation Using a Controlled Voltage Disturbance," *IEEE Transactions on Power Electronics,* vol. 17, no. 2, pp. 207 - 215, 2002.

[27] P. J. M. Heskes, "Impedance Measurement for PQ Indication," in *Minimizing the Impact of Resonances in Low Voltage Grids by Power Electronics based Distributed Generators*, Eindhoven, Technische Universiteit Eindhoven, 2011, pp. 39 - 40.

[28] M. Fauri, "Harmonic Modelling of Non-Linear Load by means of Crossed-Frequency Admittance Matrix," *IEEE Transactions on Power Systems,* vol. 12, no. 4, pp. 1632-1638, 1997.

[29] B. Bletterie, R. Bründlinger and H. Fechner, "Sensitivity of Photovoltaic Inverters to Voltage Sags – Test Results for a Set of Commerical Products," in *18th International Conference on Electricity Distribution*, Turin, 2005.

[30] P. P. Barker and R. W. De Mello, "Determining the impact of distributed generation on power systems. I. Radial distribution systems," *IEEE Power Engineering Society Summer Meeting,* vol. 3, pp. 1645 - 1656, 2000.

[31] H. Knopf, "The 4th International Conference on Integration of Renewable and Distributed Energy Resources," 6-10 December 2010. [Online]. Available: http://www.4thintegrationconference.com/downloads/Distribution%20Grid%20Codes%20Tutorial _SMA_Knopf.pdf. [Accessed 23 July 2012].

[32] C. Abbey and G. Joos, "Effect of low voltage ride through (LVRT) characteristic on voltage stability," in *IEEE Power Engineering Society General Meeting*, 12-16 June 2005.

[33] B. Renders, K. De Gusseme, W. R. Ryckaert, K. Stockman, L. Vandevelde and M. H. J. Bollen, "Distributed Generation for Mitigating Voltage Dips in Low-Voltage Distribution Grids," *IEEE*

Transactions on Power Delivery, vol. 23, no. 3, pp. 1581 - 1588, July 2008.

[34] A. A. Latheef, Harmonic impact of photovoltaic inverter systems on low and medium voltage distribution systems, Wollongong: University of Wollongong Thesis Collection, 2006.

[35] M. McGranaghan and G. Beaulieu, "Update on IEC 61000-3-6: Harmonic Emission Limits for Customers Connected to MV, HV, and EHV," in *Transmission and Distribution Conference and Exhibition, 2005/2006 IEEE PES*, 2006.

Appendix A: Maximum harmonic voltage allowed by standards and subsequent voltage stimuli

Table A-1 Maximum harmonic voltage allowed by EN-50160 [5]

Odd harmonics				Even harmonics	
Not multiples of 3		Multiples of 3			
h	Relative Volt (%)	h	Relative Volt (%)	h	Relative Volt (%)
5	6	3	5	2	2
7	5	9	1.5	4	1
11	3.5	15	0.5	6 ≤ h ≤ 24	0.5
13	3	21	0.5		
17	2				
19	1.5				
23	1.5				
25	1.5				

Table A-2 Maximum harmonic voltage allowed by IEC-61000-3-6 [34]

Odd harmonics				Even harmonics	
Not multiples of 3		Multiples of 3			
h	Relative Volt (%)	h	Relative Volt (%)	h	Relative Volt (%)
5	6	3	5	2	2
7	5	9	1.5	4	1
11	3.5	15	0.4	6	0.5
13	3	21	0.3	8	0.5
17 ≤ h ≤ 49	$\left(1.9 \cdot \dfrac{17}{h}\right) - 0.2$	27 ≤ h ≤ 45	0.2	10 ≤ h ≤ 50	$\left(0.25 \cdot \dfrac{10}{h}\right) + 0.22$

Table A-3 Harmonic voltage amplitudes used for individual impedance measurement

Odd harmonics				Even harmonics	
Not multiples of 3		Multiples of 3			
h	Relative Volt (%)	h	Relative Volt (%)	h	Relative Volt (%)
5	1:1:5	3	1:1:5	2	0.5:0.5:1.5
7	1:1:5	9	0.5:0.5:1.5	4	0.5:0.5:1
11	1:1:3	15	0.3:0.1:0.5	6 ≤ h ≤ 38	0.3:0.1:0.5
13	1:1:3	21 ≤ h ≤ 33	0.3:0.1:0.5	40 ≤ h ≤ 48	0.1:0.1:0.4
17	1:1:2	39 ≤ h ≤ 45	0.2:0.1:0.4	50	0.1:0.1:0.3
19 ≤ h ≤ 37	0.5:0.5:1.5				
41 ≤ h ≤ 47	0.5:0.5:1				
49	0.2:0.2:0.6				

Table A-4 Harmonic voltage amplitudes used for aggregate impedance measurement

Odd harmonics				Even harmonics	
Not multiples of 3		Multiples of 3			
h	Relative Volt (%)	h	Relative Volt (%)	h	Relative Volt (%)
5	1:1:4	3	1:1:4	2	0.5:0.5:1.5
7	1:1:4	9	0.5:0.5:1.5	4	0.5:0.25:1
11	0.5:0.5:2	15	0.2:0.1:0.4	6 ≤ h ≤ 26	0.1:0.1:0.4
13 ≤ h ≤ 17	1:1:2	21 ≤ h ≤ 33	0.2:0.1:0.4	28 ≤ h ≤ 46	0.1:0.1:0.3
19 ≤ h ≤ 25	0.75:0.25:1.25	39 ≤ h ≤ 45	0.1:0.1:0.3	48 ≤ h ≤ 50	0.1:0.1:0.2
29	0.3:0.3:0.9				
31	0.4:0.2:0.8				
35 ≤ h ≤ 43	0.25:0.25:0.75				
47	0.3:0.1:0.5				

49	0.2:0.2:0.4				

Table A-5 Interharmonic voltage amplitudes used for the measurement

Frequency (Hz)	Voltage Amplitude compared to fundamental (%)	
	Individual measurement	Aggregate measurement
75	0.5:0.5:2	0.75:0.25:1.5
125	2:1:5	1:1:4
175	0.25:0.25:1	0.2:0.2:0.8
225	2:1:5	1:1:4
275	0.3:0.1:0.6	0.2:0.1:0.5
325	2:1:5	1:1:4
375	0.3:0.1:0.6	0.2:0.2:0.5
425	0.5:0.5:2	0.75:0.25:1.5
475	0.3:0.1:0.6	0.2:0.2:0.5
525	1:1:4	1:0.5:2.5
575	0.3:0.1:0.6	0.2:0.2:0.5
625	1:1:4	1:0.5:2.5
675	0.3:0.1:0.6	0.2:0.2:0.5
725	0.3:0.1:0.6	0.2:0.2:0.5
775	0.3:0.1:0.6	0.2:0.2:0.5
825	0.5:0.5:2	0.75:0.25:1.5
875	0.3:0.1:0.6	0.2:0.2:0.5
925	0.5:0.5:2	0.75:0.25:1.5
975	0.3:0.1:0.6	0.2:0.2:0.5
1025	0.3:0.1:0.6	0.2:0.2:0.5

1075	0.3:0.1:0.6	0.2:0.2:0.5
1125	0.5:0.5:2	0.75:0.25:1.5
1175	0.3:0.1:0.6	0.2:0.2:0.5
1225	0.5:0.5:2	0.75:0.25:1.5
1275	0.3:0.1:0.6	0.2:0.2:0.5
1325	0.3:0.1:0.6	0.2:0.2:0.5
1375	0.3:0.1:0.6	0.2:0.2:0.5
1425	0.5:0.5:2	0.75:0.25:1.5
1475	0.3:0.1:0.6	0.2:0.2:0.5
1525	0.5:0.5:2	0.75:0.25:1.5
1575	0.3:0.1:0.6	0.2:0.2:0.5
1625	0.3:0.1:0.6	0.2:0.2:0.5
1675	0.3:0.1:0.6	0.2:0.2:0.5
1725	0.5:0.5:2	0.75:0.25:1.5
1775	0.3:0.1:0.6	0.2:0.2:0.5
1825	0.5:0.5:2	0.75:0.25:1.5
1875	0.3:0.1:0.6	0.2:0.2:0.5
1925	0.2:0.1:0.5	0.1:0.1:0.4
1975	0.2:0.1:0.5	0.1:0.1:0.4
2025	0.25:0.25:1	0.2:0.2:0.8
2075	0.2:0.1:0.5	0.1:0.1:0.4
2125	0.25:0.25:1	0.2:0.2:0.8
2175	0.2:0.1:0.5	0.1:0.1:0.4
2225	0.2:0.1:0.5	0.1:0.1:0.4

2275	0.2:0.1:0.5	0.1:0.1:0.4
2325	0.25:0.25:1	0.2:0.2:0.8
2375	0.2:0.1:0.5	0.1:0.1:0.4
2425	0.3:0.1:0.6	0.2:0.2:0.5
2475	0.1:0.1:0.4	0.1:0.1:0.4

Appendix B: Harmonic current emission of all inverters

Table B-1 Harmonic current emission of all inverters at clean grid voltage at various AC powers

Harm order	Harmonic current (absolute and relative to fundamental) and its phase angle													
	Inverter1			Inverter2			Inverter3			3Φ inverter			Power Router	
	0.6 kW	0.8 kW	1.0 kW	0.6 kW	0.8 kW	1.0 kW	0.7 kW	0.9 kW	1.1 kW	0.9 kW	2 kW	2.5 kW	0.4 kW	0.8 kW
3	0.04A	0.05A	0.05A	0.09A	0.04A	0.04A	0.64A	0.68A	0.76A	0.16A	0.13A	0.16A	0.07A	0.13A
	1.4%	1.3%	1.2%	3.4%	1.1%	0.9%	21.4%	17.6%	15.7%	3.9%	1.4%	1.5%	3.6%	3.5%
	118.1°	120.9°	127.4°	69.0°	40.8°	74.8°	174.5°	174.6°	174.4°	154.8°	-22.6°	159.9°	49.0°	-139.8°
5	0.02A	0.03A	0.03A	0.07	0.04	0.06A	0.35A	0.43A	0.51A	0.13A	0.08A	0.08A	0.06A	0.08A
	0.9%	0.7%	0.6%	2.8%	1.0%	1.2%	11.6%	11.2%	10.5%	2.9%	0.9%	0.7%	3.4%	2.1%
	89.7°	77.0°	69.4°	78.2°	74.6°	84.9°	-173.9°	-174.6°	-175.2°	161.9°	-20.0°	171.2°	7.1°	-159.5°
7	0.02A	0.02A	0.02A	0.03A	0.02A	0.03A	0.05A	0.08A	0.15A	0.08A	0.04A	0.03A	0.03A	0.07A
	0.6%	0.5%	0.4%	1.3%	0.6%	0.6%	1.5%	2.2%	3.0%	1.8%	0.4%	0.3%	1.9%	2.0%
	72.0°	67.4°	78.4°	54.0°	24.2°	73.4°	-77.7°	-141.0°	-157.8°	173.4°	-42.2°	155.5°	-3.6°	168.5°
9	0.02A	0.02A	0.02A	0.02A	0.02A	0.02A	0.02A	0.04A	0.08A	0.06A	0.03A	0.02A	0.01A	0.03A
	0.7%	0.5%	0.4%	0.7%	0.5%	0.4%	0.6%	0.9%	1.6%	1.3%	0.3%	0.2%	0.6%	0.9%
	54.8°	47.9°	42.4°	24.7°	-15.8°	16.6°	84.2°	159.8°	168.8°	-171.6°	-33.3°	159.3°	24.2°	134.6°

Appendix C: Complete model of all inverters

Inverter1
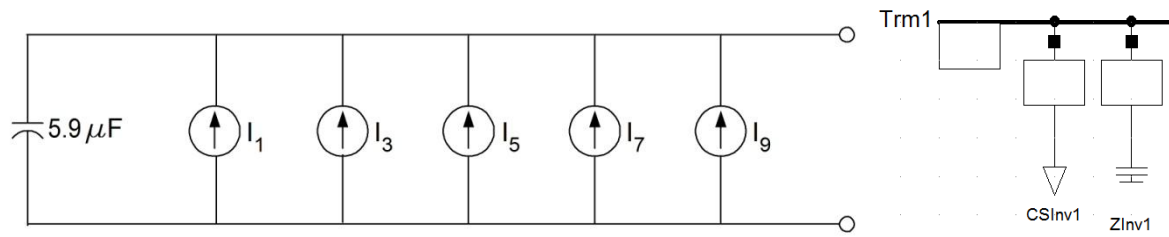
Figure C-1 Complete model of Inverter1 in Simulink and PowerFactory simulation

Inverter2
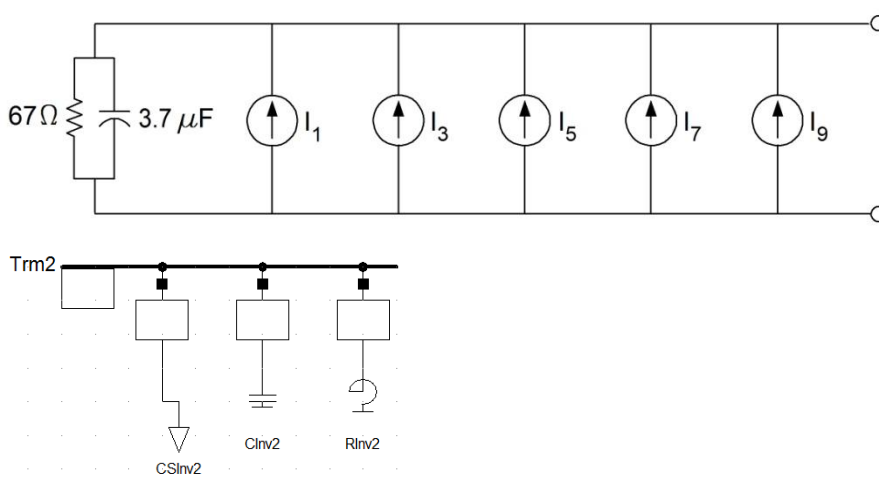
Figure C-2 Complete model of Inverter2 in Simulink and PowerFactory simulation

Inverter3
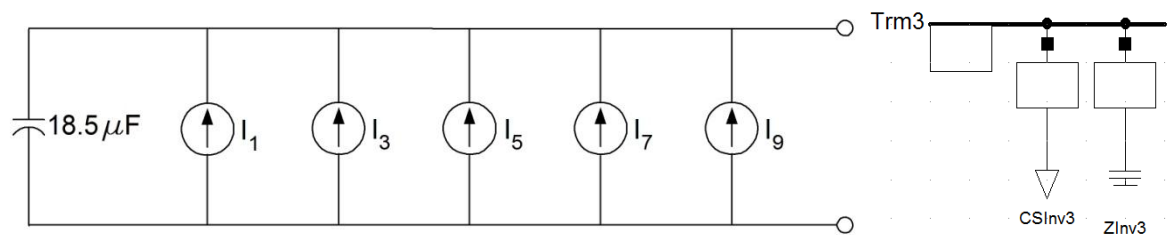
Figure C-3 Complete model of Inverter3 in Simulink and PowerFactory simulation

Three-phase (3Φ) Inverter
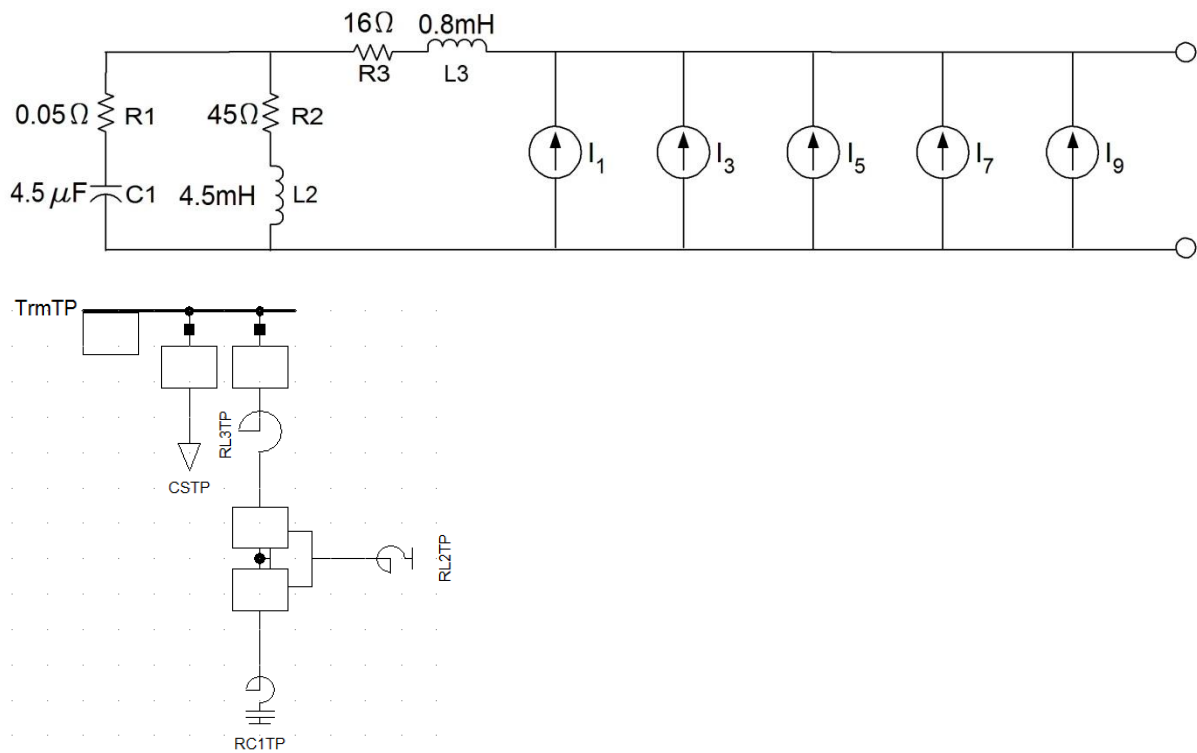
Figure C-4 Complete model of 3Φ Inverter in Simulink and PowerFactory simulation

Power router
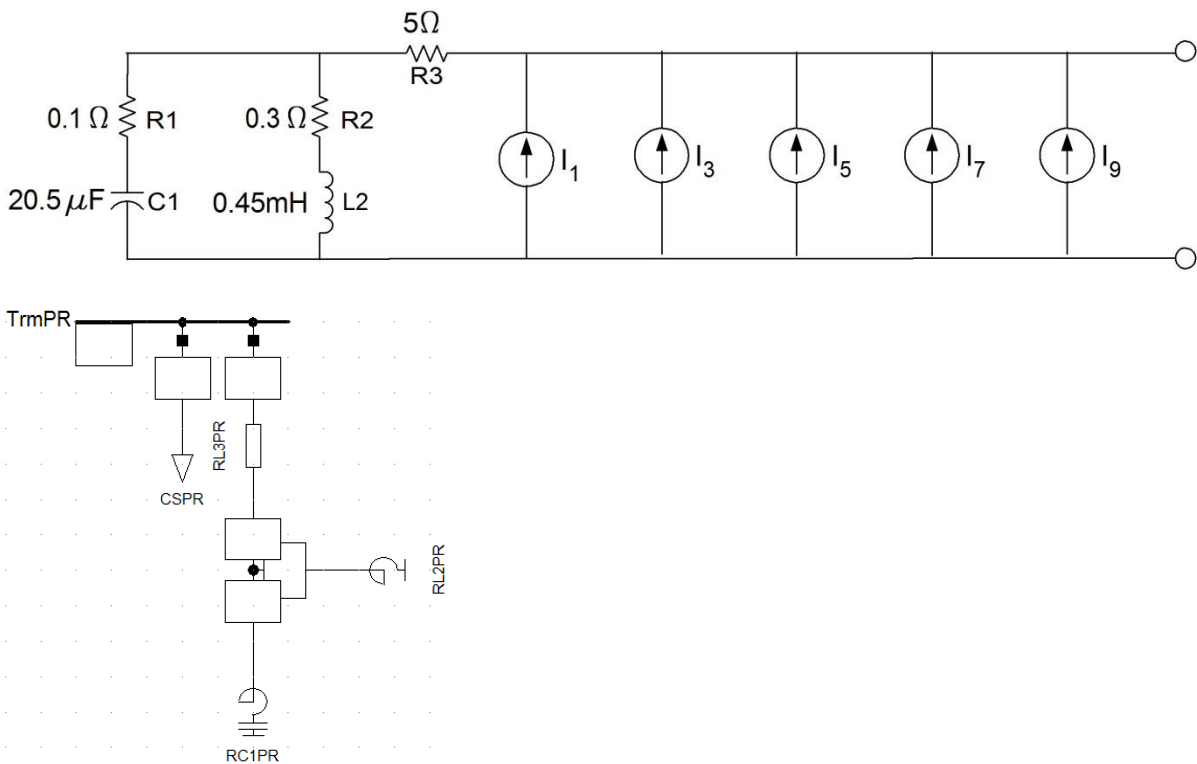
Figure C-5 Complete model of power router in Simulink and PowerFactory simulation

(CS stands for Current Source, TP stands for Three Phase, PR stands for Power Router)

Appendix D: Simulation scheme
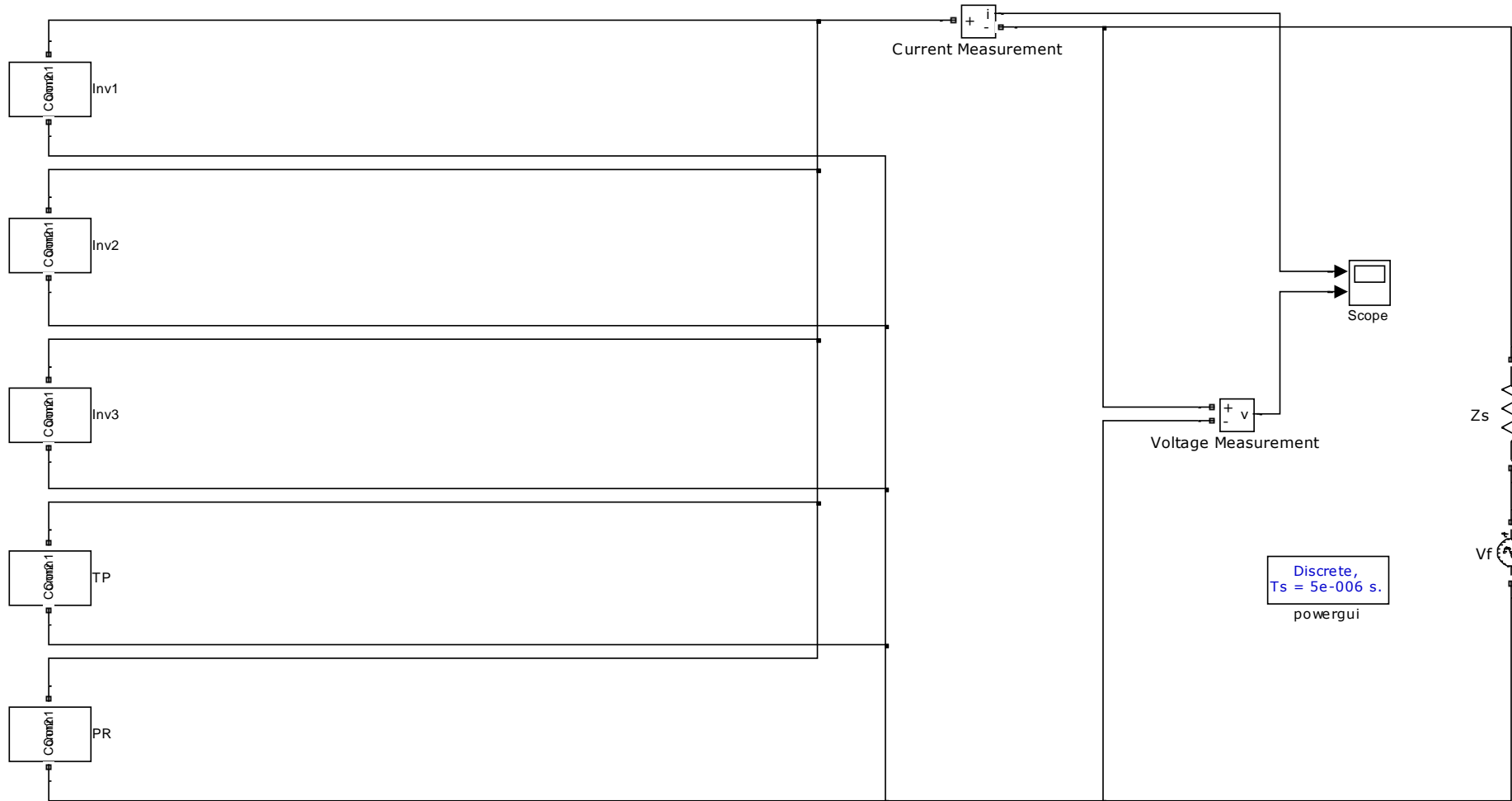
Figure D-1 Simulation scheme in Simulink

(TP stands for Three Phase, PR stands for Power Router, Zf denotes fundamental voltage source, Zs denotes source (and cable) resistance)
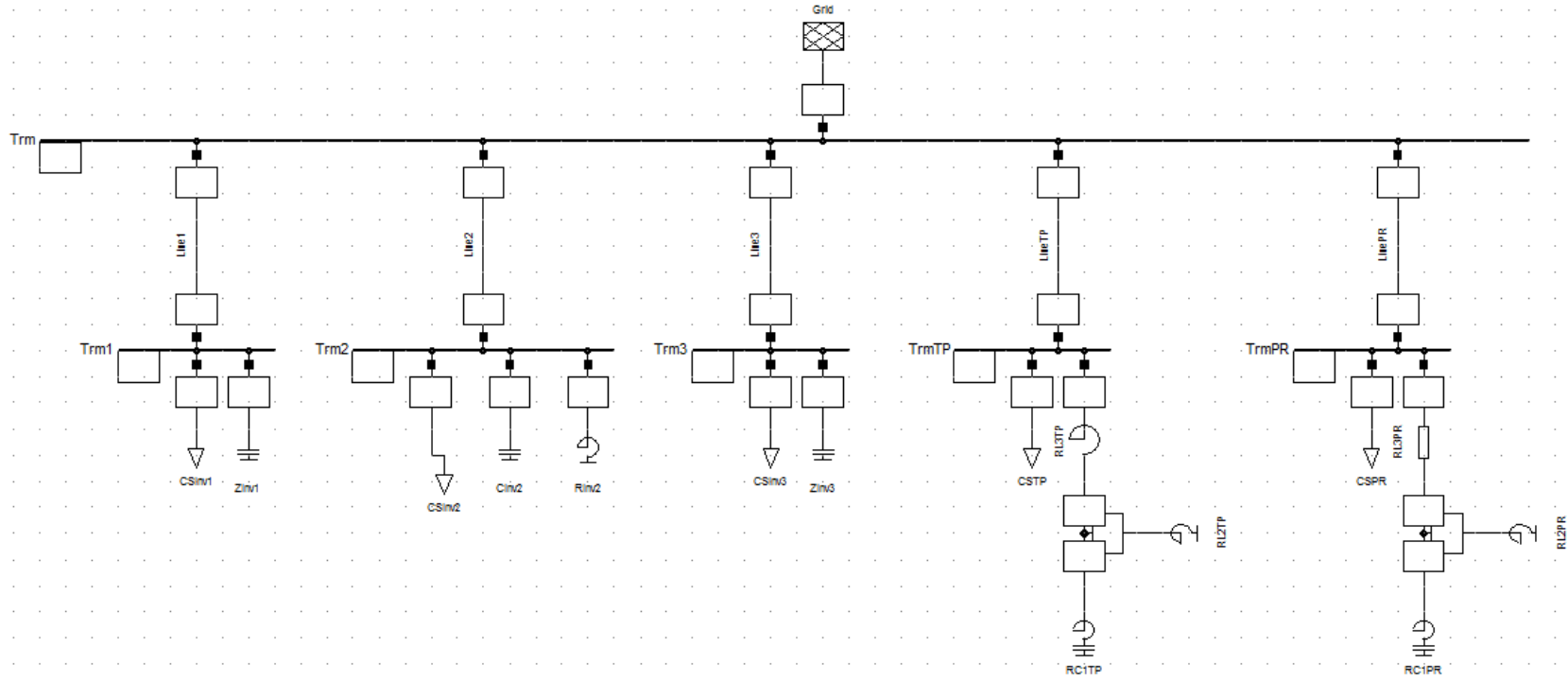
Figure D-2 Simulation scheme in PowerFactory

Appendix E: Aggregation of inverter harmonic currents emissions

Table E-1 Comparison of aggregation of harmonic currents of inverters from measurements, simulation in Simulink, and simulation in PowerFactory

		Fundamental			3rd harmonic			5th harmonic			7th harmonic			9th harmonic		
		Measurement	Simulink	Power Factory	Measurement	Simulink	Power Factory	Measurement	Simulink	Power Factory	Measurement	Simulink	Power Factory	Measurement	Simulink	Power Factory
Inv1+Inv2	Abs (A)	8.95	8.98	8.88	0.12	0.08	0.08	0.08	0.09	0.09	0.06	0.05	0.05	0.04	0.04	0.03
	Rel (%)	100.00	100.00	100.00	1.31	0.90	0.90	0.92	0.99	0.98	0.64	0.55	0.55	0.41	0.43	0.38
	Angle (°)	-3.6	-6.6		82.6	104.2		71.3	79.8		61.2	75.4		18.5	29.5	
Inv1+Inv3	Abs (A)	9.09	9.55	8.96	0.80	0.80	0.78	0.49	0.50	0.48	0.14	0.14	0.13	0.09	0.07	0.06
	Rel (%)	100.00	100.00	100.00	8.75	8.33	8.65	5.42	5.21	5.37	1.52	1.46	1.42	0.96	0.73	0.71
	Angle (°)	-9.2	-19.5		171.4	171.8		182.6	181.7		201.2	195.4		161.6	155.6	
Inv1+TP*	Abs (A)	13.12	13.09	13.06	0.09	0.09	0.08	0.07	0.09	0.06	0.04	0.03	0.02	0.04	0.04	0.02
	Rel (%)	100.00	100.00	100.00	0.70	0.69	0.63	0.57	0.65	0.48	0.31	0.27	0.17	0.28	0.30	0.14
	Angle (°)	2.8	1.6		-14.9	0.0		-10.6	0.3		-23.4	0.0		-28.7	0.0	
TP+PR*	Abs (A)	12.38	12.43	12.32	0.14	0.14	0.16	0.11	0.06	0.08	0.09	0.04	0.06	0.09	0.01	0.01
	Rel (%)	100.00	100.00	100.00	1.10	1.09	1.26	0.88	0.45	0.63	0.77	0.33	0.47	0.74	0.05	0.08
	Angle (°)	2.3	3.3		-63.7	0.0		-58.6	0.0		259.3	198.7		250.0	50.7	
Inv1+PR	Abs (A)	7.92	7.96	7.79	0.12	0.14	0.15	0.07	0.06	0.08	0.08	0.07	0.09	0.07	0.04	0.04

		C1	C2	C3	C4	C5	C6	C7	C8	C9	C10	C11	C12	C13	C14	C15
	Rel (%)	100.00	100.00	100.00	1.54	1.72	1.94	0.89	0.81	1.00	1.07	0.91	1.11	0.86	0.44	0.53
	Angle (°)	-5.3			204.8	198.8		214.9	180.2		191.6	152.7		167.1	100.2	
SP	Abs (A)	13.68	14.08	13.58	0.69	0.79	0.75	0.46	0.49	0.44	0.12	0.13	0.10	0.07	0.06	0.06
	Rel (%)	100.00	100.00	100.00	5.06	5.62	5.55	3.38	3.51	3.19	0.89	0.90	0.72	0.53	0.40	0.41
	Angle (°)	-7.1	-14.2		172.0	168.9		180.4	174.8		218.0	184.0		201.3	142.3	
SP+TP	Abs (A)	22.02	22.57	22.36	0.54	0.66	0.70	0.40	0.42	0.47	0.10	0.10	0.14	0.03	0.03	0.08
	Rel (%)	100.00	100.00	100.00	2.47	2.94	3.16	1.79	1.85	2.07	0.46	0.46	0.61	0.16	0.12	0.38
	Angle (°)	-1.4	-6.0		177.4	171.1		185.1	177.6		236.9	200.4		247.1	137.5	
All	Abs (A)	25.70	26.19	25.88	0.51	0.76	0.84	0.39	0.49	0.51	0.19	0.17	0.10	0.13	0.06	0.06
	Rel (%)	100.00	100.00	100.00	1.99	2.89	3.24	1.53	1.88	1.97	0.73	0.64	0.40	0.52	0.22	0.21
	Angle (°)	-2.7	-6.0		186.2	178.6		195.6	181.2		226.3	187.6		214.3	136.0	

*TP stands for Three Phase, PR stands for Power Router

Appendix F: Aggregation of inverter impedance

Impedance magnitude
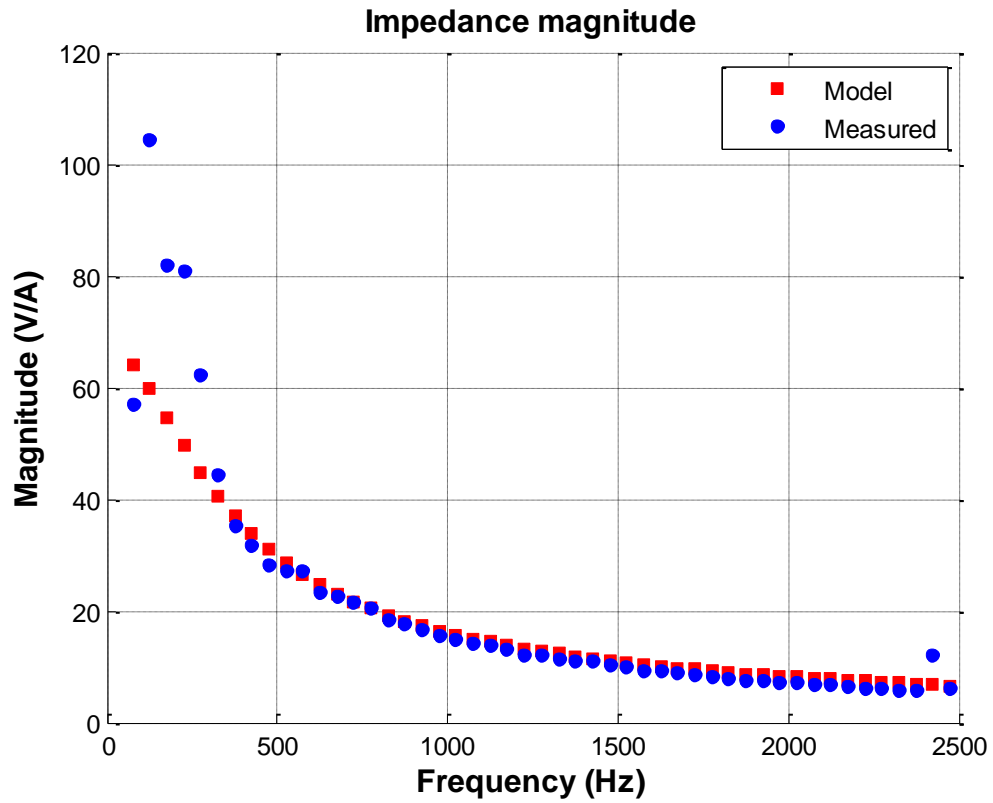
Figure F-1 Impedance magnitude profile of aggregation of Inverter1 and Inverter2

Impedance phase angle
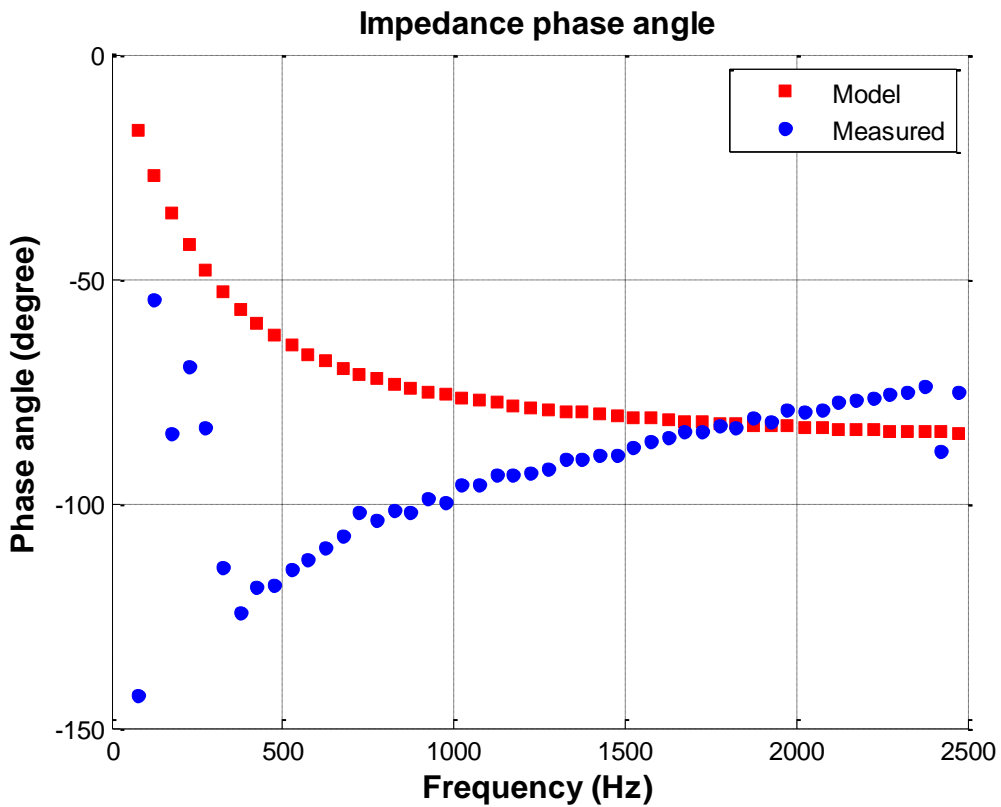
Figure F-2 Impedance phase angle profile of aggregation of Inverter1 and Inverter2

Impedance magnitude
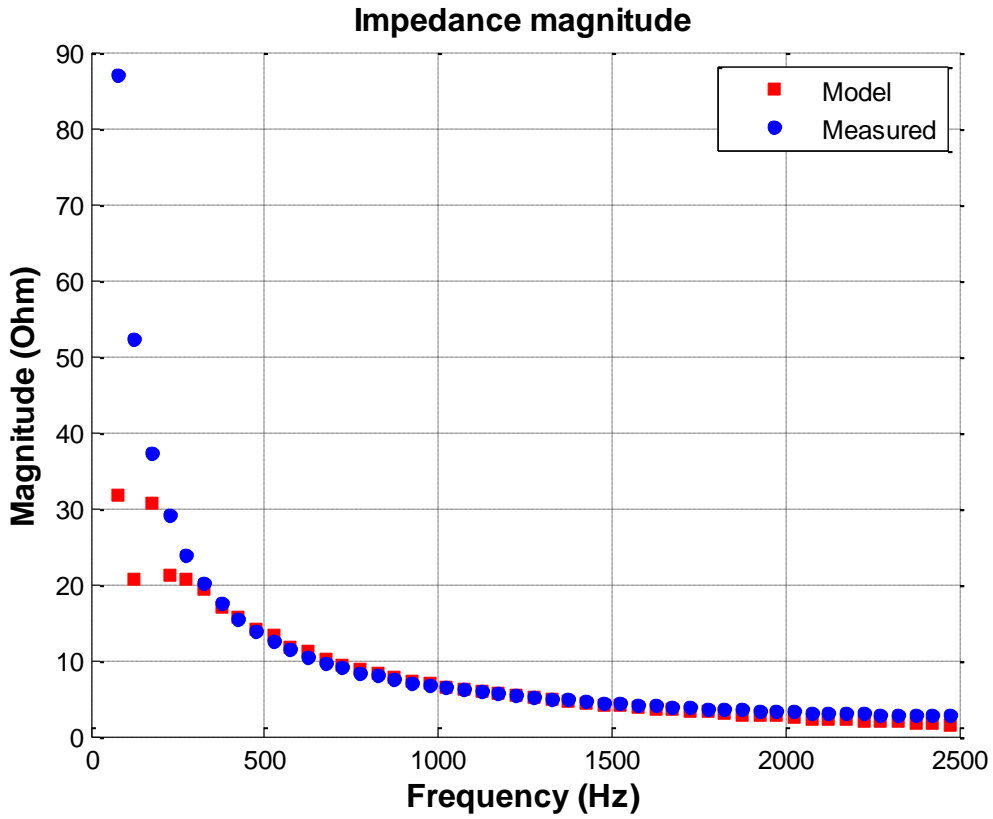
Figure F-3 Impedance magnitude profile of aggregation of Inverter1 and Inverter3

Impedance phase angle
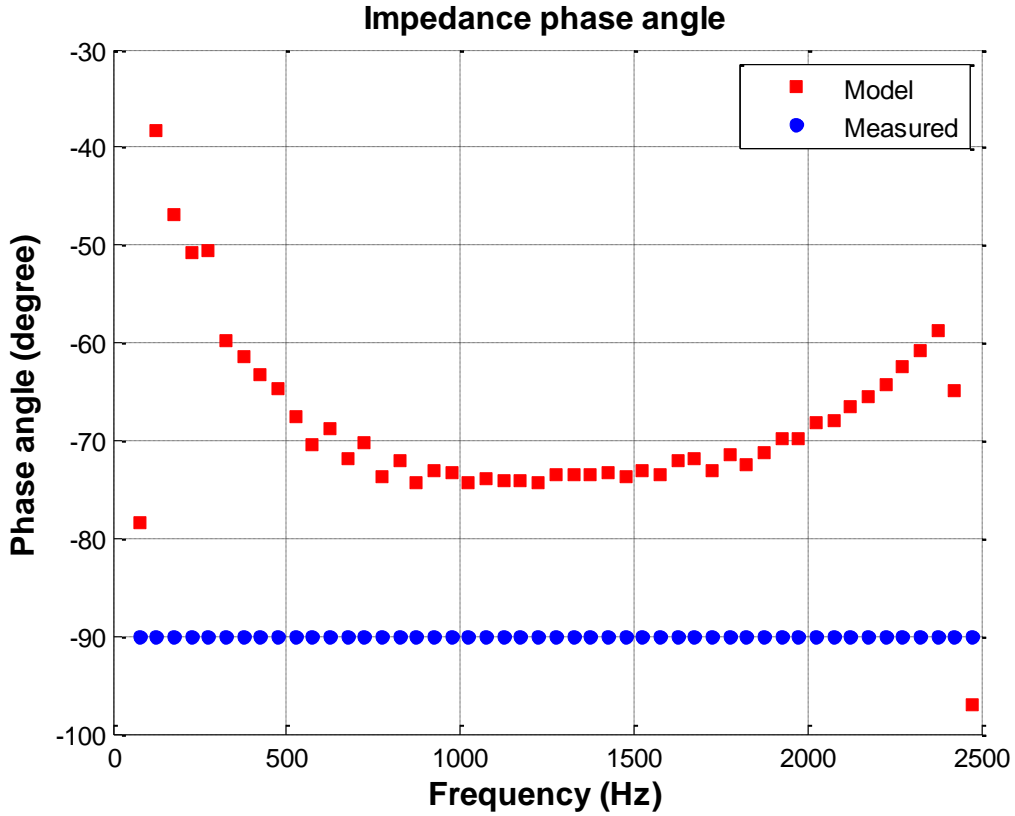
Figure F-4 Impedance phase angle profile of aggregation of Inverter1 and Inverter3
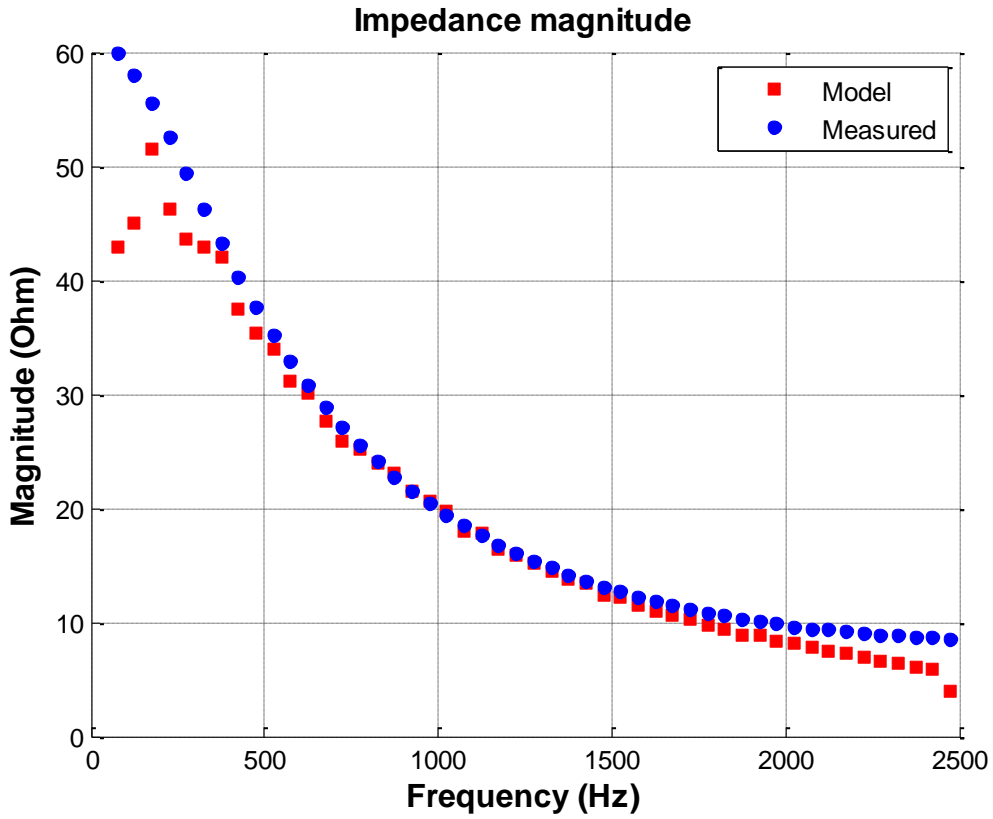
Figure F-5 Impedance magnitude profile of aggregation of Inverter1 and 3Φ inverter
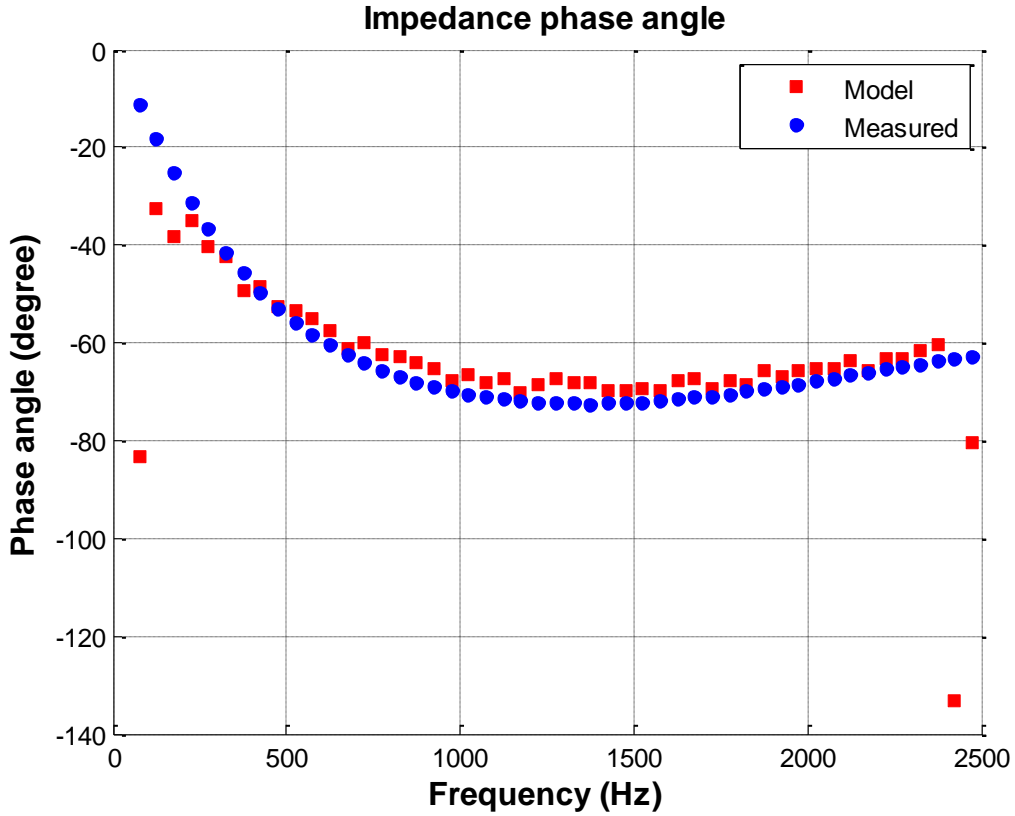
Figure F-6 Impedance phase angle profile of aggregation of Inverter1 and 3Φ inverter
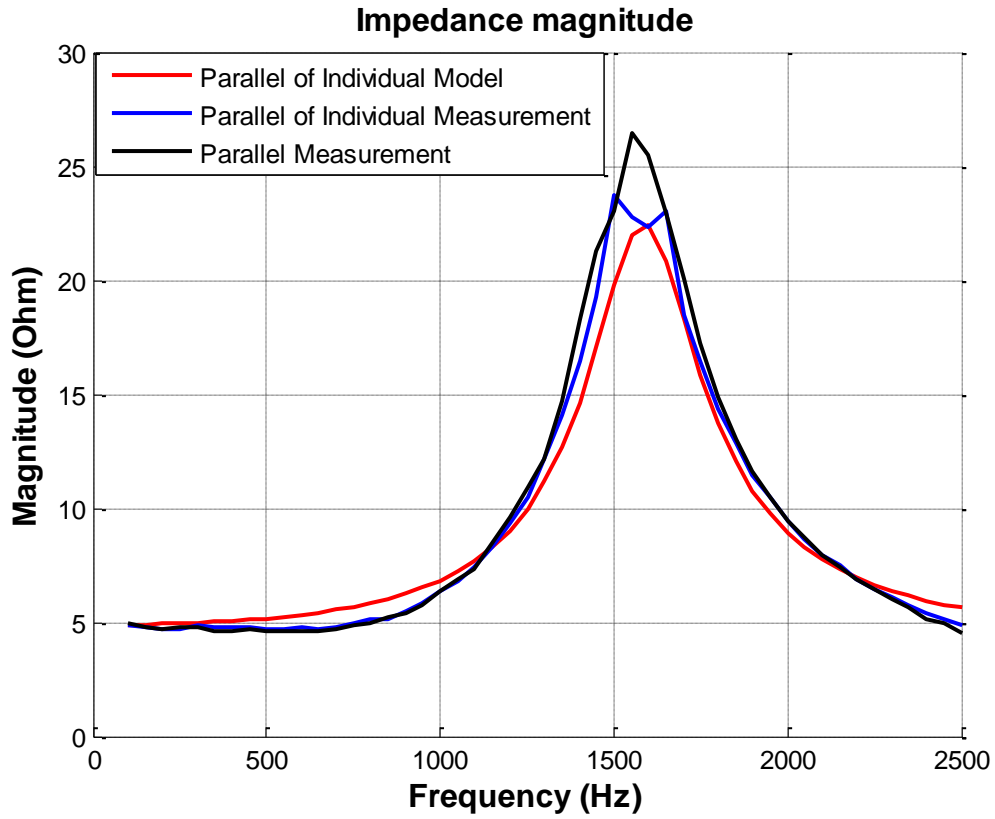
Figure F-7 Impedance magnitude profile of aggregation of 3Φ inverter and power router
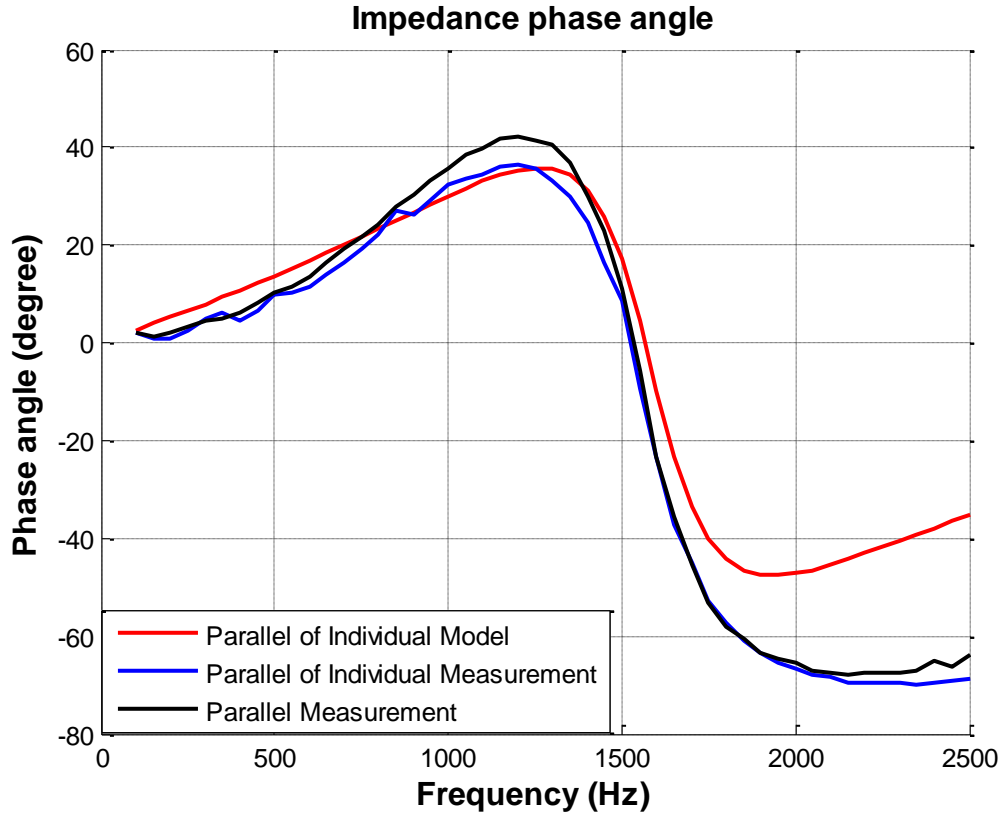
Figure F-8 Impedance phase angle profile of aggregation of 3Φ inverter and power router

Impedance phase angle
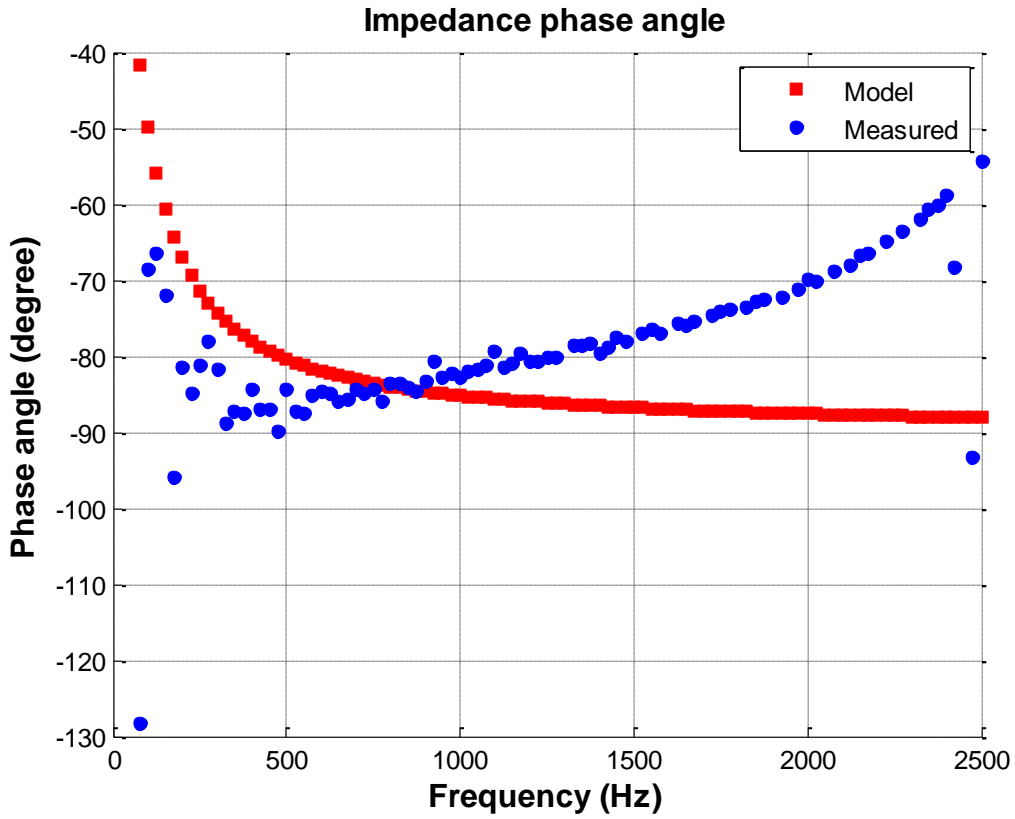
Figure F-9 Impedance phase angle profile of aggregation of Inverter1, Inverter2 and Inverter3

Impedance magnitude
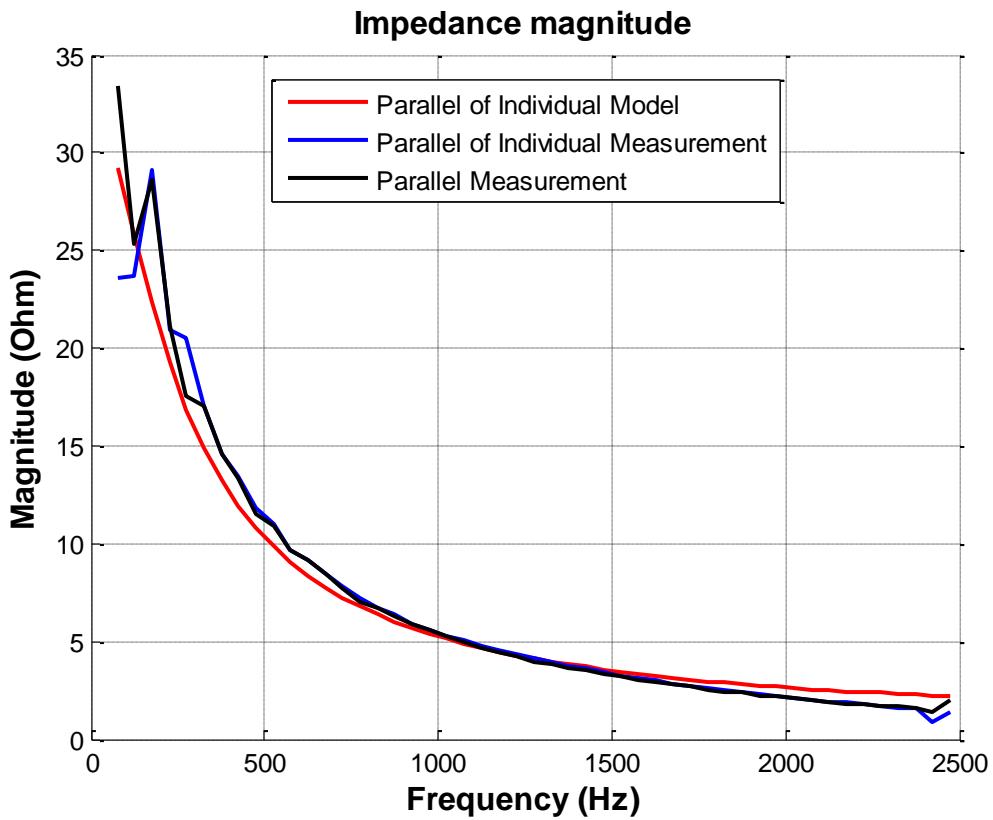
Figure F-10 Impedance magnitude profile of aggregation of Inverter1, Inverter2, Inverter3, and 3Φ inverter
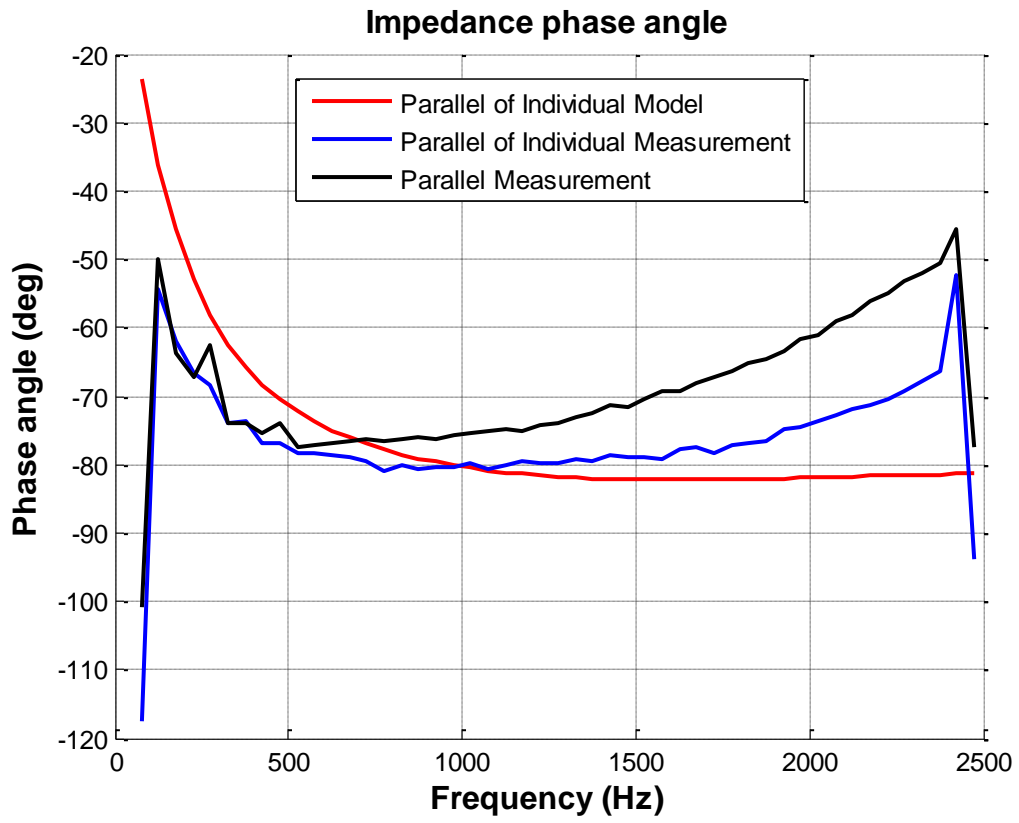
Figure F-11 Impedance phase angle profile of aggregation of Inverter1, Inverter2, Inverter3, and 3Φ inverter

Appendix G: List of Figures

Appendix H: List of Tables

Acknowledgement

I am very grateful to those who assisted me in this work: my supervisor Prof. Dr. ir. Sjef Cobben, Dr. Paulo Ribeiro, and Vladimir Ćuk for their constant support throughout my internship and graduation project and for their contribution to the publication from this study. I am honoured to have worked with a team of high technical knowledge and experience in the field. I would like to thank Prof. ir. Wil Kling and Dr. Ir. Helm Jansen for taking place in my graduation committee and Eloy Maxam Martinez for his help with the laboratory set-up. Last but not least, I would like to thank all fellow students, friends, and family for their company and support during this study.

I give all the credits to God, without whom I would not be able to do a Master study in the first place.

"No good work is done anywhere without aid from the Father of Lights." – C. S. Lewis